Essays on Monetary Transmission and Banking

by

Giorgi Nikolaishvili

A dissertation accepted and approved in partial fulfillment of the
requirements for the degree of
Doctor of Philosophy
in Economics

Dissertation Committee:
Jeremy Piger, Chair
David Evans, Core Member
George Evans, Core Member
Jose Carreno, Core Member
Youchang Wu, Institutional Representative

University of Oregon
Spring 2024

DISSERTATION ABSTRACT

Giorgi Nikolaishvili

Doctor of Philosophy in Economics

Title: Essays on Monetary Transmission and Banking

The commercial banking sector in the United States comprises numerous small, local (community) banks primarily focused on lending to small borrowers in their respective local economies, alongside a smaller group of large, geographically-diversified (non-community) banks that cater to larger borrowers. On average, the lending practices and business models of these two types of banks different substantially. In this dissertation, I analyze the macroeconomic implications of the lending practices of community banks, along with the geographical factors driving their performance dynamics, using a novel method of impulse response function decomposition and existing high-dimensional time-series econometric methodologies, respectively. In brief, I find that the extent of national comovement in community bank performance has increased in recent decades, and that community bank lending plays a significant role in the transmission of monetary policy despite the decline in the presence of community banks relative to that of their noncommunity counterparts.

The second chapter makes a methodological contribution, which informs the analysis of the role of community bank lending in monetary policy transmission in the third chapter. In this chapter, I formulate the concept of a pass-through impulse response function (PT-IRF), which captures the contribution of any given subsystem of a greater dynamical system to the net effect of the propagation of a structural shock. I also describe methods of empirically estimating and performing

inference on PT-IRFs using vector autoregressions and local projections. Finally, I demonstrate the applicability of PT-IRFs by estimating and empirically testing the effect of a monetary policy shock on unemployment through changes in bank lending in a small autoregressive model.

The third chapter examines how heterogeneity in lending practices across community and noncommunity banks influences the transmission of monetary policy to the real economy. Using PT-IRFs, I quantify the contributions of community versus noncommunity bank lending to the dynamic effect of a monetary policy shock on output. My findings show that noncommunity bank lending amplifies the contractionary effects of a monetary tightening in the short run, whereas community bank lending has a stronger amplificatory contribution in the medium run. These results suggest that a continued decline in the relative presence of community banks may lead to a subsequent decline in the persistence of monetary transmission. Furthermore, the adverse impact of a monetary tightening on spending must concentrate more persistently among small businesses and agricultural producers in remote rural areas, since these borrower segments tend to heavily rely on community bank lending as a source of funds.

The fourth chapter studies the comovement in community bank profitability dynamics at three different geographical levels. I use a hierarchical dynamic factor model to extract posterior distributions of national, regional, and state-level latent drivers of quarterly fluctuations in state-average community bank return-on-equity series for all 50 US states. The results show a decrease in the intensity of idiosyncratic performance dynamics since the global financial crisis, along with a near-uniform increase in national comovement. This finding implies an increase

in the exposure of the community banking sector to systemic risk, suggesting a potential increase in fragility during future financial crises.

CURRICULUM VITAE

NAME OF AUTHOR: Giorgi Nikolaishvili

GRADUATE AND UNDERGRADUATE SCHOOLS ATTENDED:

University of Oregon, Eugene, OR, USA
Tufts University, Medford, MA, USA

DEGREES AWARDED:

Doctor of Philosophy, Economics, 2024, University of Oregon
Master of Science, Economics, 2020, University of Oregon
Bachelor of Science, Economics, 2019, Tufts University
Bachelor of Science, Mathematics, 2019, Tufts University

AREAS OF SPECIAL INTEREST:

Macroeconomics
Time Series Econometrics
Financial Economics
Computational Economics

GRANTS, AWARDS AND HONORS:

Emerging Scholar Award, CSBS/FDIC/Federal Reserve, 2023
Graduate Teaching Award, University of Oregon, 2023
Kleinsorge Research Fellowship, University of Oregon, 2023
Best Field Paper Award, University of Oregon, 2022
Graduate Teaching Fellowship, University of Oregon, 2020
Edward G. Daniel Scholarship, University of Oregon, 2020
Graduate Student Fellowship, University of Oregon, 2019
Highest Honors in Thesis, Tufts University, 2019

ACKNOWLEDGEMENTS

I would like to thank all members of my dissertation committee: David Evans, for consistently providing me with insightful feedback and encouraging me to elevate the rigour of my work; George Evans, whose research originally inspired me to attend University of Oregon and study macroeconomics, for numerous helpful conversations; Jose Carreno, for exposing me to new areas of macroeconometrics and making the defense process more enjoyable with his unwavering positivity; Youchang Wu, for his thoughtful comments and fresh outlook on the implications of my work.

Finally, I extend my sincerest gratitude to Jeremy Piger – his exceptional mentorship has been instrumental in the completion of this dissertation and my growth as an economist.

Any remaining errors are my own.

DEDICATION

To Tamara, David, Elene, Andro, and Nikki.

TABLE OF CONTENTS

Chapter Page

Chapter Page

Chapter Page

LIST OF FIGURES

Figure Page

Figure Page

Figure Page

Figure Page

LIST OF TABLES

Table Page

CHAPTER I

INTRODUCTION

The commercial banking sector in the United States is currently composed of approximately 4,500 active banks holding $23T in combined assets. Although the number of commercial banks has been steadily declining over the past few decades, as seen in Figure 1, the U.S. remains an outlier relative to other countries with respect to the size of its banking sector in numbers.

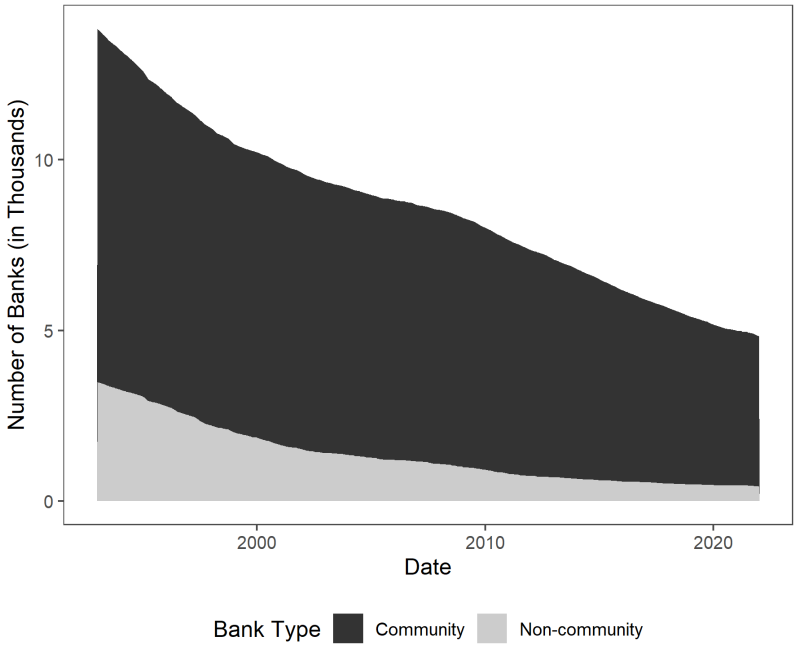

Figure 1. The composition of the total number of Federal Deposit Insurance Corporation (FDIC)-insured commercial banks in the U.S. by bank type. *Source: FDIC Statistics on Depository Institutions.*

As shown above, nearly 90% of all U.S. commercial banks today are classified as *community* banks, which may be informally described as locally owned and operated financial intermediaries that largely focus on serving the needs of

their local credit markets.[1] The remaining *noncommunity* banks tend to be either larger, more geographically diversified, or some combination of both.

Despite the gradual decline in the number of banks, community banks continue to dominate the sector in numbers. On the other hand, the combined share of noncommunity bank assets and net loans has increased noticeably during the same time frame, as illustrated in Figures 2 and 3, respectively. However, the diminished relative presence of community banks does not necessarily indicate their decline – they continue to thrive as "specialists" within their respective local economies.

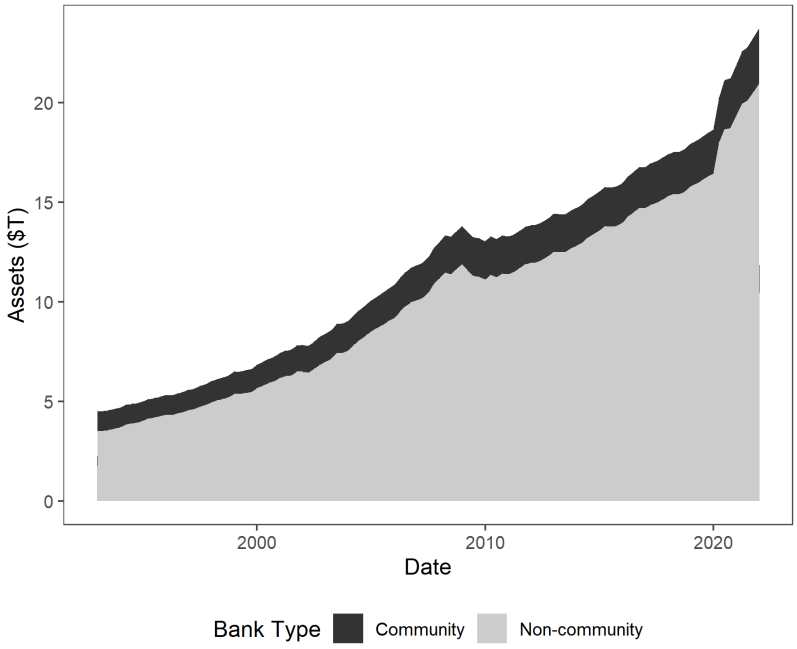

Figure 2. The level and composition of FDIC-insured commercial bank assets in the U.S. over time by bank type. *Source: FDIC Statistics on Depository Institutions.*

[1]The Federal Deposit Insurance Corporation (FDIC) provides a formal definition of a community bank that eliminates all banks that have no loans or core deposits, have foreign assets accounting for $\geq$10% of total assets, and have more than 50% of assets in certain specialty banks, and includes all remaining banks that have total assets of less than $1B, and have total assets over $1B but meet specific criteria such as loan-to-assets >33%, core deposits to assets >50%, fewer than 75 offices, and restricted geographical presence.

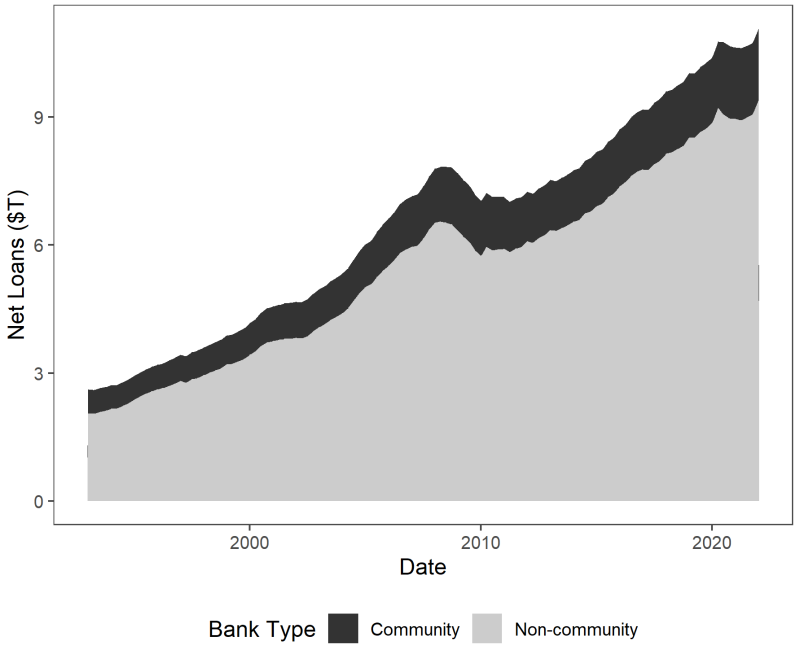

Figure 3. The level and composition of FDIC-insured commercial bank lending in the U.S. over time by bank type. *Source: FDIC Statistics on Depository Institutions.*

Community banks prioritize relationship lending, offering loans that require local knowledge, personalized attention, individual analysis, and ongoing administration. They distinguish themselves from noncommunity banks by building and maintaining personal relationships, and specializing in monitoring local economic conditions. Unlike their competitors, the vast majority of community banks operate within a single state, and most have only one branch, as evidenced by Figures 4 and 5, respectively. Geographic concentration allows community banks to be more agile in their decision making, as opposed to the more rigid centralized organization of noncommunity banks. It also contributes to their ability to gather and process "soft information" on their borrowers and local markets. This enables community banks to more accurately identify creditworthy borrowers,

revealed by their record of achieving greater loan repayment success rates than their noncommunity counterparts (Peirce, Robinson, & Stratmann, 2014).

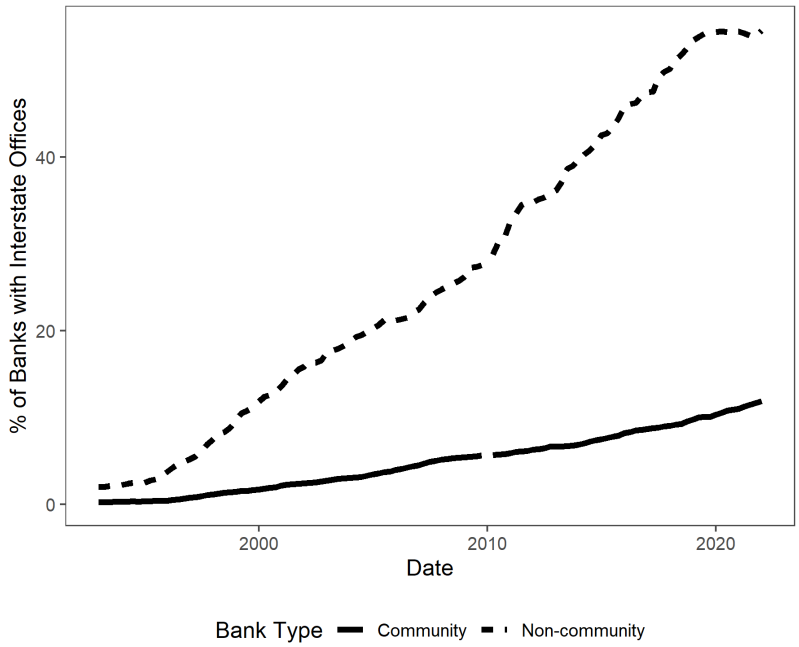

Figure 4. Percentage of FDIC-insured banks with offices across more than one state by bank type. *Source: FDIC Statistics on Depository Institutions.*

For these reasons, community banks play an essential role in the US economy as a critical source of financing for small businesses and agricultural producers, as well as households in remote areas (Hanauer, Lytle, Summers, & Ziadeh, 2021; Lux & Greene, 2015). These borrower segments may otherwise have limited access to credit as a result of information asymmetries that prevent noncommunity banks from issuing loans to their respective borrower segments due to a lack of knowledge and/or confidence. For example, despite issuing only 15% of all bank loans, community banks are responsible for 30% of commercial real estate loans, 36% of small business loans, and 70% of agricultural loans across the U.S. as of 2019. As an additional example, community banks based in rural areas and small

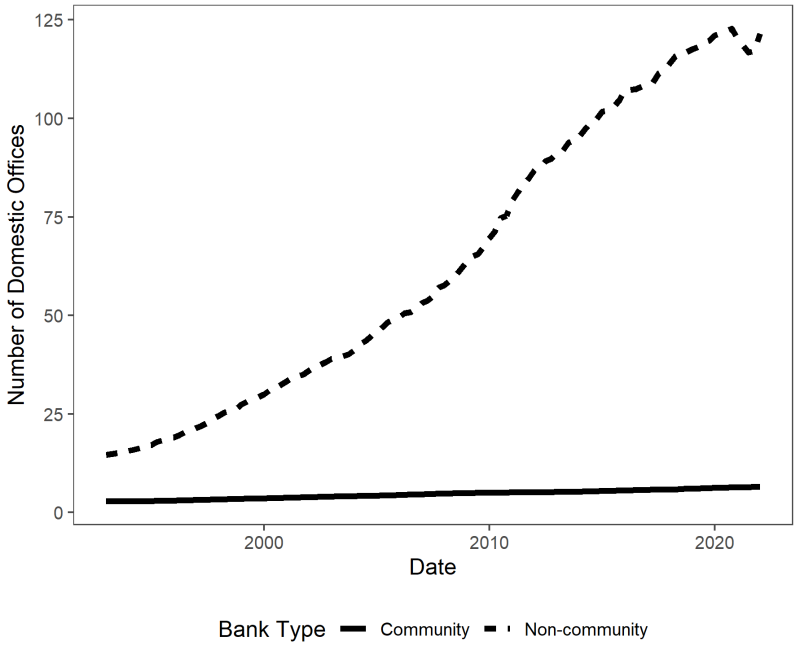

Figure 5. Average number of domestic offices across FDIC-insured banks by bank type. *Source: FDIC Statistics on Depository Institutions.*

metropolitan regions held 67% of all commercial real estate loans in those areas (FDIC, 2020).

Small businesses employ nearly half of the private sector workforce and generate just under half of aggregate economic activity. Banks provide approximately 44% of small business financing, compared to 22% from online lenders and 6% from credit unions. The 36% of total small business loans issued by community banks is double their share of the total of all loans issued by banks. Furthermore, the size of individual loans issued to small businesses differs significantly across community and noncommunity banks. Noncommunity banks tend to originate and hold more loans under $100,000, whereas community banks hold a more significant share of loans between $250,000 and $1M, focusing on larger loans that require greater interaction and analysis to build a relationship between

the bank and the borrower. On the other hand, the majority of loans issued by community banks are for amounts greater than $1M (FDIC, 2020).

By better understanding the nature of the community banking sector, policymakers can develop effective strategies to support these institutions in order to promote stable economic growth. Particularly, the above insights raise the following two questions that I address in this dissertation:

1. To what extent do community bank lending practices contribute to the transmission of monetary policy to real output relative to those of noncommunity banks? As currently understood by the macro-finance literature, changes in interest rates caused by central bank policy affect the supply and demand of bank loans, which in turn affect output by either expanding or contracting firms' and households' access to credit. Given the considerable differences in community versus noncommunity bank business models, there is reason to expect heterogeneity in the extent to which monetary policy affects output via changes in community versus noncommunity bank lending. For instance, since community banks lend primarily to small borrowers while noncommunity banks target larger borrowers, *ceteris paribus* a contraction in community bank credit due to monetary tightening may have a more severe contractionary effect on spending by the former due to a lack of alternative sources of funding. Understanding such transmission heterogeneity is crucial in gauging the role of the composition of the banking sector in the nature of the dynamic effect of monetary policy on output, which is especially pertinent in the case of a consistently-evolving bank sector composition.

2. How have recent changes in the regulatory and macroeconomic landscapes affected the exposure of community banks to systemic risk? In other words, how has community bank interconnectedness evolved in the past few decades? In addition to providing credit to vulnerable borrower segments, community banks have proven themselves to be reliable credit providers during adverse macroeconomic conditions. This has most recently been revealed in the wakes of the global financial crisis and the COVID-19 pandemic (Hassan, Karim, Lawrence, & Risfandy, 2022). Furthermore, there is evidence suggesting that community banks' limited geographical scope generally dampens the transmission of global and remote credit shocks to their respective markets (Petach, Weiler, & Conroy, 2021). However, there is no evidence pointing to the notion that community bank stability and idiosyncrasy has been consistent in the past, or expected to be so in the future. Therefore, it would be valuable to quantify the comovement in community bank performance as a way of gauging their exposure to systemic risk.

To make tackling the first question possible, Chapter II develops a novel empirical methodology called that quasi-decomposes vector autoregression-based impulse response functions, with the purpose of measuring the contributions of the various channels through which a given shock propagates within the specified dynamic model of interest. Chapter III then leverages the method developed in Chapter II to quantify and compare the contributions of community versus noncommunity bank lending to the transmission of monetary policy shocks. I combine macroeconomic and bank-level loan data to estimate a factor-augmented vector autoregression to measure the responses of community versus non-community bank lending to a monetary policy shock, and the subsequent

response of output growth. I find that contractionary monetary policy shocks have a negative effect on output growth via both community and noncommunity bank lending, with the former playing a larger role in the medium run and the latter in the short run.

An examination of the second question is presented in Chapter IV, in which I estimate a Bayesian hierarchical dynamic factor model using a panel of state-level community bank profitability series to gauge the extent to which community bank performance is driven by common vs. idiosyncratic factors at different geographical levels. My current findings show that community bank performance has become significantly more interconnected at the country-level, while also experiencing a decrease in state-level idiosyncrasy since the crisis.

Related Literature. Despite their ubiquity, the interaction of the community banking sector with the macroeconomy has received relatively little attention from researchers and policymakers alike. Particularly, peer-reviewed literature on community banking is presently quite scarcev – the following is a non-exhaustive overview.

Works such as Yeager (2004), Emmons, Gilbert, and Yeager (2004), Meslier, Morgan, Samolyk, and Tarazi (2016), Estes (2014), and Swanson and Zanzalari (2021) pursue a similar interest of identifying the contributions and importance of risk diversification for community banks. Yeager (2004) explores whether decrease in the number of community banks in the US is a result of their preference for geographic diversification as a way of gaining more robustness in the face of local economic shocks. The study finds that community banks withstand local economic shocks well, and therefore geographic diversification must not play a part in driving consolidation in the US community banking sector. Emmons et al. (2004) find that

risk-adjusted return for community banks increases along with their size, which they interpret as evidence of idiosyncratic risk dominating local market risk in the community banking sector. Meslier et al. (2016) find that for small banks, intrastate diversification increases risk-adjusted returns and decreases default risk. Estes (2014) studies the relationship between community bank performance and a variety of portfolio diversification strategies, and finds that diversification may improve risk-adjusted performance. Swanson and Zanzalari (2021) explore the question of whether local labor markets impact bank profitability. Their study finds that an increase in the local market unemployment rate decreases bank profitability, with the additional (counter-intuitive) insight that the impact of local market conditions on profitability is less severe for small banks relative to large banks.

The remaining literature studies evolution of various characteristics of, and causes of heterogeneity within, the community banking sector. DePrince, Ford, and Morris (2011) explore the determinants of interstate heterogeneity in community bank profitability, and find significant relationships between variation in state-average return on assets and each state's economic, demographic, and market structure characteristics. Feng and Zhang (2012) find that relative to large banks, community banks had experienced significantly lower productivity growth and lower levels of returns to scale over the 1997-2006 period. Fang and Yeager (2020) study the ability of community banks to withstand severe and prolonged periods of credit losses. They find that community banks had become less sensitive to such adverse circumstances after the global financial crisis relative to the pre-crisis era. Rice and Rose (2016) find that community banks exposed to the government-

sponsored enterprises Fannie Mae and Freddie Mac saw slower loan growth post-crisis than their unexposed peers.

CHAPTER II

PASS-THROUGH IMPULSE RESPONSE FUNCTIONS

2.1 Introduction

Often in macroeconomics we are interested in studying the dynamic effects of a particular shock on the economy, for which we default to impulse response functions (IRFs) as the tool of choice (Ramey, 2016). Given a dynamical process, an IRF captures the effect of a disturbance on the system over some specified time horizon. Empirical estimates of IRFs allow for the quantification of, and inference on, the effects of various economic shocks of interest on the macroeconomy – two common approaches to estimating IRFs include local projections (Jordà, 2005) and vector autoregressions (J. H. Stock & Watson, 2016). However, despite their ubiquity in the study of shock propagation, IRFs offer little insight into the nature of the channels contributing to the transmission of a shock through a system.

For this reason, Sims and Zha (2006) develop a method of quantifying the contribution of any secondary variable to the dynamic effect of an economic shock on an endogenous variable. Their approach involves holding the secondary "medium" variable constant over a set horizon by simulating a path of its respective structural shock(s) accordingly in the face of a shock of interest. The most prominent example of an application of the Sims-Zha methodology is presented in Bernanke, Gertler, and Watson (1997), in which the authors quantify the contribution of the systematic portion of monetary policy to the effect of oil price shocks on key macroeconomic variables. Other applications can be found in Kilian and Lewis (2011) and Bachmann and Sims (2012), and a recent refinement of the Sims-Zha approach can be found in McKay and Wolf (2023).

In a similar vein, I formulate a new target statistic, to which I henceforth refer as a pass-through impulse response function (PT-IRF), which allows for the quantification of specific transmission channels of a shock within a dynamical system. Given a dynamical system expressed in the form of a VAR, a PT-IRF captures the effect of a structural shock k on an endogenous variable i through some other "medium" variable j, or a set of endogenous variables. Conveniently, PT-IRFs can be estimated using the same information and procedures required to estimate IRFs in the context of VARs, which holds true for inference as well. As explained later in the text, the PT-IRF approach to measuring transmission channels differs fundamentally from Sims-Zha methodology, since the former hinges on the Granger causality of the medium to quantify transmission while the latter relies on keeping the medium fixed over time. In other words, the two approaches interpret the notion of a contribution to dynamic shock propagation differently. However, in terms of the practical comparison between the two methods, it is worth mentioning that PT-IRFs do not require the identification of multiple structural shocks while also offering straight-forward ways of conducting inference.

The VAR case, general formulation, and estimation procedures for PT-IRFs are detailed in Section 2 of this paper. Among other applications, PT-IRFs may be used to estimate, quantify, and conduct inference on various channels of the monetary transmission mechanism. Modern literature on the monetary mechanism has yet to reach an agreement on the roles of various transmission channels with respect to their contributions to the effects of monetary policy. For example, the literature on the credit channel, pioneered by Bernanke and Blinder (1992), remains inconclusive on the existence and nature of the bank lending channel. In Section 3 of this paper, I illustrate the potential of PT-IRFs in this area of research by

estimating the pass-through of monetary policy shocks through bank lending in a low-dimensional macroeconomic VAR. This illustrative application is then further expanded upon in a more sophisticated analysis of monetary transmission via bank lending presented in Chapter III. In the final section, I conclude the paper with a brief discussion of additional potential applications of PT-IRFs.

2.2 Methodology

In this section I define the concept of a PT-IRF starting with the simple case of a linear VAR(1), proceeding to the more general case of a linear VAR(p), and finally generalizing to a stationary Markov process. I also describe how existing methods for estimating VAR IRFs can be used to produce point-estimates and confidence intervals for PT-IRFs.

2.2.1 Linear VAR(1).

Consider the following VAR(1) process:

$$Y_{t+1} = \alpha + AY_t + B\varepsilon_{t+1}\,, \tag{2.1}$$

where $Y_t = (y_{1t}, \ldots, y_{Nt})'$ is a vector of N endogenous variables, $\varepsilon_t = (\varepsilon_{1t}, \ldots, \varepsilon_{Kt})'$ is a vector of K structural shocks, α is an intercept vector, and $A \in \mathbb{R}^{N\times N}$ and $B \in \mathbb{R}^{N\times K}$ are the lag coefficient and contemporaneous impact matrices, respectively. Our goal is to interpret the given linear VAR(1) as a directed weighted graph through which shock impulses travel over time, use this alternative interpretation of a linear VAR(1) to reinterpret the familiar IRF, and finally define the PT-IRF within the given context.

Firstly, notice that the ik-th entry of B represents the contemporaneous effect of the k-th structural shock on the i-th endogenous variable. Refer to Figure 6 for an illustration of the special case of a 3-dimensional VAR(1).

Next, notice that A_{ij} represents the one-period-ahead effect of the j-th variable on the i-th variable. If we think of A as the adjacency matrix in the

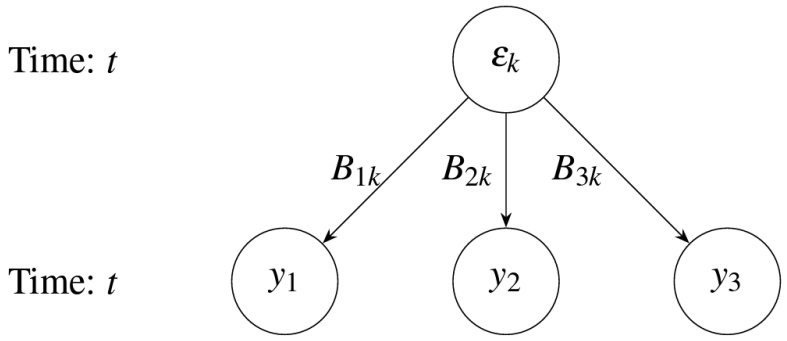

Figure 6. Contemporaneous effects of a structural shock ε_k on a 3-dimensional VAR as a weighted directed graph. ***Note:*** Notice that for each B_{ik}, i indexes the affected variable, while k indexes the shock of origin.

context of a directed weighted graph, where each endogenous variable at a given point in time is a vertex, then A_{ij} may also be interpreted as the intensity of the travel path of a signal from variable j at time t to variable i at time $t + 1$. Once again, for an illustration of the above in the special case of a 3-dimensional VAR(1), refer to Figure 7.

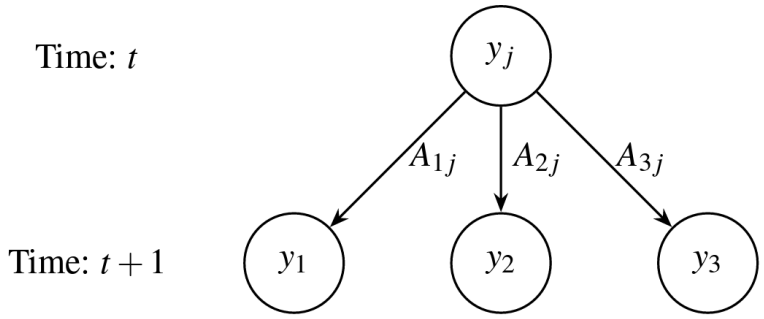

Figure 7. One-period-ahead effects of a change in the variable y_j of a 3-dimensional VAR as a weighted directed graph. ***Note:*** Notice that for each A_{ij}, i indexes the next period's destination variable, while j indexes the variable of origin.

Lastly, we can simply put the above interpretations of B and A together to formulate a VAR(1) as a directed weighted graph, which allows us to trace the propagation of a shock through the system and assess its impact on some variable of interest at a future point in time. Each possible path of a given shock ε_k has a corresponding weight equal to the product of the weights of each of its edges, determined by the contemporaneous impact and lag coefficient matrices. An IRF is simply the sum of the weights of all paths that ultimately reach a destination node corresponding to a variable of interest y_i at a given horizon h. Refer to Figure 13 for an illustration of the one-period-ahead propagation of a shock through a 3-dimensional VAR(1).

A PT-IRF is the sum of weights associated with the subset of the above-mentioned paths that pass at least once through some medium of interest y_j – if a given path never passes through y_j, then it is irrelevant in gauging the role of y_j as a medium for a shock in the system. For example, the one-period-ahead pass-through response of y_i with respect to y_1 as a medium to some shock ε_k in the case illustrated by Figure 13 is equal to $A_{i1}B_{1k}$ – the weight of the only path that allows for the shock to pass through y_1 at least once before reaching its destination. If we were interested in the union of y_1 and y_2 as a medium for ε_k, then the PT-IR would be $A_{i1}B_{1k} + A_{i2}B_{2k}$ – the sum of the weights of the two paths that allow the shock to pass through either y_1 or y_2 at least once before reaching its destination. The same logic can be extended to h-period-ahead impulse responses, with h being strictly greater than 1.

It can be shown that in the case of a VAR(1), the h-period-ahead impulse response (IR) with respect to some vector of shocks $\overline{\varepsilon}$ may be expressed as

$$\mathrm{IR}(h, \overline{\varepsilon}) = A^h \, B \, \overline{\varepsilon} \, . \tag{2.2}$$

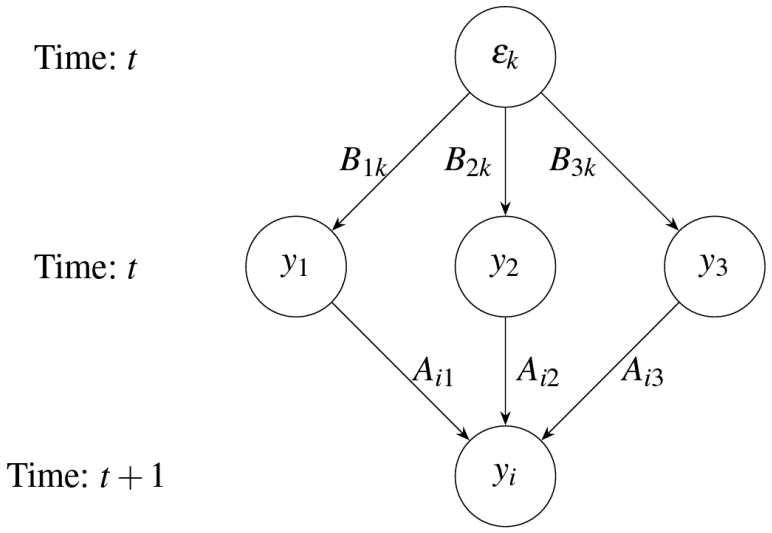

Figure 8. The propagation of an impulse originating at the k-th shock with the i-th variable as its destination, one period ahead. ***Note:*** The one-period-ahead impulse response of y_i with respect to a unit shock to ε_k equals the sum of the weights of all three paths leading to y_{it+1}: $A_{i1}B_{1k} + A_{i2}B_{2k} + A_{i3}B_{3k}$.

It can also be shown that for $h > 0$, the corresponding pass-through impulse response (PT-IR) with pass-through/medium variable y_j is algebraically equivalent to

$$\text{PT-IR}(h, j, \bar{\varepsilon}) \equiv \left(A^h - \widetilde{A}^h\right) B\,\bar{\varepsilon}\,, \tag{2.3}$$

where $\widetilde{A}$ is identical to A across all but the j-th column, which is set equal to the zero vector. In the case that $h = 0$, the PT-IR always equals to zero due to the fact that contemporaneous pass-through of any given shock occurs purely through the impact matrix:

$$\text{PT-IR}(0, j, \bar{\varepsilon}) \equiv 0\,. \tag{2.4}$$

The above equations completely define the PT-IRF in the context of a VAR(1).

2.2.2 Linear VAR(p). Consider the following VAR(p) process:

$$Y_t = \alpha + A(L)Y_t + B\varepsilon_t\,, \tag{2.5}$$

where all familiar objects are defined as before, and $A(L)$ is a lag polynomial of the form

$$A(L) = \sum_{i=1}^{p} A_i L^i\,, \tag{2.6}$$

such that each A_i is a lag coefficient matrix corresponding to Y_{t-i}. Suppose we aim to derive PT-IR($h, j, \overline{\varepsilon}$) for this system. The goal is once again to sum the weights associated only with those paths that originate at the shock of interest, pass through y_j at least once over the given horizon, and end at the response variable of interest h periods ahead.

Suppose we represent a linear VAR(p) in state-space form as a VAR(1) with companion matrix Φ and augmented contemporaneous impact matrix $\Gamma = \begin{bmatrix} B' & \mathbf{0} \end{bmatrix}'$. Then for $h \geq 0$ the corresponding PT-IR with pass-through/medium variable y_j may be expressed as

$$\text{PT-IR}(h, j, \overline{\varepsilon}) \equiv \left(\Phi^h - \widetilde{\Phi}^h\right) \Gamma\, \overline{\varepsilon}\,, \tag{2.7}$$

where $\widetilde{\Phi}$ is the companion matrix of a modified version of the process described in Eq. (2.5) with the i-th lag coefficient matrix restricted to equaling

$$\widetilde{A}_i \equiv \begin{bmatrix} \vec{a}_1 & \dots & \vec{a}_{j-1} & \vec{0} & \vec{a}_{j+1} & \dots & \vec{a}_N \end{bmatrix}\,, \tag{2.8}$$

where $\vec{a}_m$ denotes the m-th column of A_i. Notice that $\widetilde{\Phi}^h \Gamma\, \overline{\varepsilon}$ captures the impulse response of a shock for a restricted version of the given linear VAR(p) in which the Granger causality of the j-th endogenous variable is completely removed (Kilian & Lütkepohl, 2017) – all paths passing through the j-th variable are assigned a weight of zero. Therefore, PT-IR($\cdot$) sums the weights of only those paths that pass

through the j-th variable, which can be interpreted as the impulse response of the system attributable to the Granger-causality of the j-th endogenous variable.

2.2.3 General Formulation. Let $Y_t = (y_{1t}, \ldots, y_{Nt})' \in \mathbb{R}^N$ and $\varepsilon_t = (\varepsilon_{1t}, \ldots, \varepsilon_{Kt})' \in \mathbb{R}^K$ such that Y_t is determined by the stationary Markov process

$$Y_t = G(\varepsilon_t, Y_{t-1}; \theta)\,, \tag{2.9}$$

where $t \in \mathbb{N}^+$ denotes time, $G : \mathbb{R}^K \times \mathbb{R}^N \to \mathbb{R}^N$ is a mapping conditioned on a set of parameters θ, and ε_t is a vector of zero-mean i.i.d. shocks. We may define the h-step impulse response of the given system with respect to some shock vector $\overline{\varepsilon} \in \mathbb{R}^K$ as the following difference between two forecasts $\forall h \in \mathbb{N}$:

$$\mathrm{IR}(t, h, \overline{\varepsilon}) \equiv \mathbb{E}\left[Y_{t+h} \,|\, \varepsilon_t = \overline{\varepsilon},\, Y_{t-1},\, \theta\right] - \mathbb{E}\left[Y_{t+h} \,|\, \varepsilon_t = 0,\, Y_{t-1},\, \theta\right]\,, \tag{2.10}$$

where the conditional expectation operator $\mathbb{E}[\cdot \,|\, \cdot]$ represents the best mean squared error predictor. The pass-through impulse response of the system with respect to the same shock is once again defined as

$$\text{PT-IR}(t, h, j, \overline{\varepsilon}) \equiv \mathrm{IR}(t, h, \overline{\varepsilon}) - \widetilde{\mathrm{IR}}(t, h, j, \overline{\varepsilon})\,, \tag{2.11}$$

where $\widetilde{\mathrm{IR}}$ denotes an object similar to that in Eq. (2.10), but applied to a transformed version of the process expressed in Eq. (2.9) in which the Granger causality of the j-th variable in the system is removed. More specifically, we may define

$$\widetilde{\mathrm{IR}}(t, h, j, \overline{\varepsilon}) \equiv \mathbb{E}\left[\widetilde{Y}_{t+h} \,|\, \varepsilon_t = \overline{\varepsilon},\, Y_{t-1},\, \theta\right] - \mathbb{E}\left[\widetilde{Y}_{t+h} \,|\, \varepsilon_t = 0,\, Y_{t-1},\, \theta\right]\,, \tag{2.12}$$

where $\widetilde{Y}_t \equiv G(\varepsilon_t, \widetilde{I}_j Y_{t-1}; \theta)$, such that $\widetilde{I}_j$ is the identity matrix with the j-th diagonal entry set equal to zero. In other words, $\widetilde{Y}_t$ is generated by the same process as Y_t, but with the influence of the lags of the j-th variable removed from the data generating process (DGP).

Notice that $\widetilde{I}_j$ removes the Granger causality of the j-th variable in the system, thus allowing for $\widetilde{\text{IR}}(\cdot)$ to isolate the impulse response to a shock without accounting for its transmission through y_{jt}. Therefore, subtracting $\widetilde{\text{IR}}(\cdot)$ from $\text{IR}(\cdot)$ yields the impulse response associated with the transmission of a shock through y_{jt}.

2.3 Estimation and Inference

Similarly to an IRF, a PT-IRF may be estimated by first estimating VAR parameters, and then using all relevant parameter estimates from this first step to generate the PT-IRF by a nonlinear mapping. Confidence intervals for a PT-IRF may be obtained by carrying out a simulation procedure of choice to generate IRF distributions (confidence intervals via bootstrapping in the frequentist case, or credible sets via sampling in the Bayesian case) such that an accompanying PT-IRF is generated using the same set of estimated VAR parameters at each step. All statistical properties of IRF estimators simply carry over to the estimation of PT-IRFs, since PT-IRFs are deterministic mappings of VAR parameters. It is also possible to incorporate local projections bootstrap methods in the same manner as Montiel Olea and Plagborg-Møller (2019) and Montiel Olea and Plagborg-Møller (2021) for the purpose of conducting inference on VAR-estimated PT-IRFs.

2.4 Illustrative Application

In this section, I apply PT-IRFs to study monetary transmission. J. Stock and Watson (2001) estimate a simple recursively-identified three-dimensional VAR(4) to generate impulse response functions representing the effect of a one-time monetary policy shock on unemployment. Their model contains quarterly series on US inflation, unemployment, and the federal funds rate over the period of 1960:I-2000:IV. I introduce an additional variable to their model, which I treat as medium of interest for the transmission of monetary policy shocks through the system. I

estimate a PT-IRF to gauge the strength of the bank lending channel (BLC) in the monetary transmission mechanism.

Early literature on the BLC, such as Bernanke and Gertler (1995), define it as the effect of monetary policy on output through changes in the supply of bank loans. In other words, a monetary shock affects bank lending, which subsequently affects output. I add a commercial and industrial (C&I) loan growth rate series to the J. Stock and Watson (2001) VAR as the last variable in the recursive ordering, and use it as a pass-through medium in estimating the PT-IRF of unemployment to a monetary policy shock. The resulting IRF and PT-IRF are presented in Figure 9, which suggests that bank lending acts as a substantial channel for monetary transmission. Furthermore, the shape of the PT-IRF matches the theory behind the BLC – a one-time contractionary policy shock is associated with a temporary rise in unemployment through a decrease in the growth of the supply of bank loans.

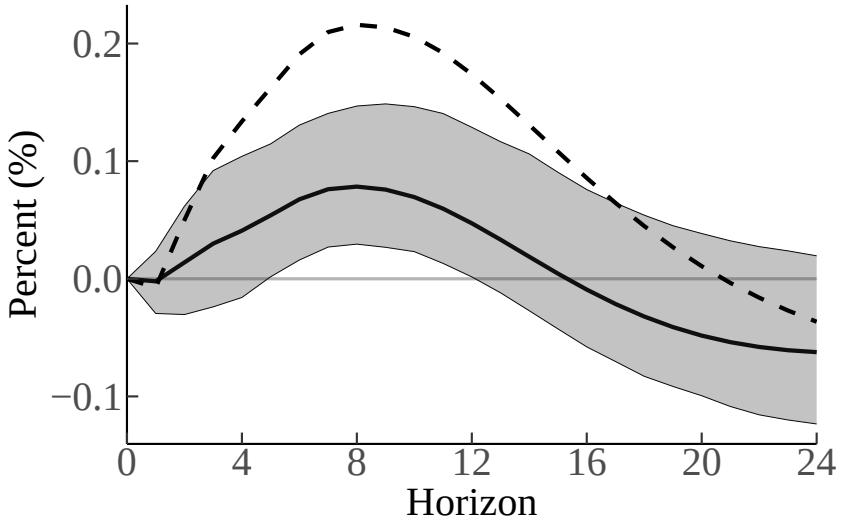

Figure 9. The IRF (dash-dotted line) and PT-IRF (solid line) of unemployment with respect to an interest rate shock, with bank lending as a pass-through medium. Gray bands represent 95% confidence intervals for the PT-IRF.

2.5 Concluding Remarks

PT-IRFs can be a useful tool for measuring the pass-through channels of various economic shocks. Although my application in this paper involves a linear VAR, PT-IRFs can easily be estimated for nonlinear VARs as well. Furthermore, the ability of PT-IRFs to accommodate multiple pass-through media allows for the estimation of multi-dimensional transmission channels – for example, in the case of the BLC, we could have simultaneously included multiple bank loan type series as pass-through media. In the following chapter, I apply PT-IRFs to estimate the transmission of monetary policy to output via community vs. noncommunity bank lending.

CHAPTER III

COMMERCIAL BANK HETEROGENEITY AND THE TRANSMISSION OF MONETARY POLICY THROUGH BANK LENDING

3.1 Introduction

Does bank lending facilitate the transmission of monetary policy? If so, to what extent does it contribute to the impact of monetary policy shocks on output? Since the seminal work by Bernanke and Blinder (1988), there has been much debate regarding these fundamental questions in the monetary policy literature. For instance, Dave, Dressler, and Zhang (2013) and Drechsler, Savov, and Schnabl (2017) show evidence in favor of an active channel of monetary transmission through bank lending in the United States, while Romer and Romer (1990) and Ashcraft (2006) cast doubt upon its current existence at the aggregate level. These studies yield alternative conclusions, but cannot refute each other directly. A primary reason for this discord stems from an absence of consistent methodological frameworks for the measurement of channels of monetary transmission. Moreover, the aggregate role of bank heterogeneity in monetary transmission through bank lending is ambiguous. Considering the ever-evolving composition of the U.S. commercial banking sector, this presents limitations to policy optimization.

In this paper, I employ a flexible reduced-form empirical approach with minimal identification assumptions, leveraging granular panel data to quantify and estimate the nature of aggregate monetary transmission through bank lending. To estimate the effect of bank lending on the transmission of monetary policy shocks, I combine bank-level loan data with a standard set of aggregate macroeconomic series. I use the data to estimate a factor-augmented vector autoregression (FAVAR) with externally identified monetary policy shocks introduced in Bu,

Rogers, and Wu (2021). I then estimate and conduct inference on pass-through impulse response functions (PT-IRFs) – a novel class of IRFs that characterizes the dynamic response of output to monetary policy shocks via bank lending. I categorize the U.S. commercial banking sector into community and noncommunity banks, and examine how variation in their respective lending volumes facilitates the dynamic influence of monetary policy shocks on output. My findings reveal that the transmission of unanticipated monetary policy shocks through bank lending occurs through changes in both community and noncommunity bank lending, such that the latter has a greater effect in the short run, whereas the former drives the persistence of monetary transmission into the medium run.

A key methodological contribution of this paper is the use of PT-IRFs to estimate and quantify monetary policy transmission through bank lending directly. This lending channel of monetary transmission can be described as the effect of monetary policy on output growth via changes in the supply of bank loans, expressed as a two-step causal chain: (1) a change in monetary policy affects the quantity of bank loans, and (2) the change in the quantity of bank loans affects output growth. Previous literature has studied each of these components individually.[1] For example, Dave et al. (2013) analyzes the effect of monetary policy shocks on the quantity of bank loans, while Peek and Rosengren (2000), Peek, Rosengren, and Tootell (2003), Driscoll (2004), and Ashcraft (2006) test whether shocks to bank loan supply impact output. The common practice is to conclude that if either of these relationships is insignificant, then bank lending

[1]My analysis does not separate the contributions of the bank lending and balance sheet channels in the transmission of monetary policy via bank lending. In other words, similar to Dave et al. (2013), I do not distinguish between changes in bank loan supply and demand caused by monetary policy shocks. The identification challenges of separating these two channels is described in Bernanke and Blinder (1992), Bernanke and Gertler (1995), and Kashyap and Stein (2000).

plays no role in the transmission of monetary policy to the real economy. However, separately estimating these relationships cannot directly quantify or test the nature of monetary transmission via bank lending – the shocks to bank lending in this setting are *endogenous* by definition. Therefore, an understanding of the effect of exogenous shocks to lending on output provides limited insight regarding the transmission of monetary shocks to output via lending. I demonstrate that the PT-IRF can estimate impulse responses that *simultaneously* capture both components of the above-mentioned two-step causal chain, allowing for the direct quantification and inference on the dynamic nature of monetary transmission through bank lending.

Another benefit of my empirical approach is that it is effectively agnostic to the different mechanistic views of monetary transmission through bank lending. The last few decades have seen the emergence of a variety of views on the true mechanism underlying the bank lending channel (BLC), which is the elusive supply-side subchannel of the more general lending channel. The conventional formulation argues that the BLC operates through reserve requirements, which create binding liquidity constraints for commercial banks, forcing responses in bank loan supply in the face of monetary policy shocks (Bernanke & Gertler, 1995; Black & Rosen, 2007; den Haan, Sumner, & Yamashiro, 2007; Kashyap & Stein, 1994). An alternative perspective is that the BLC operates through the effect of monetary policy on banks' external finance premia, which either limits or enhances the ability of banks to issue new loans (Disyatat, 2011). A more recent formulation offered by Drechsler et al. (2017) argues that monetary policy affects the supply of bank loans through changes in the quantity of deposits available to commercial banks as a source of funding.

This work contributes to the literature by analyzing the role of bank business model heterogeneity in the monetary transmission mechanism. The U.S. commercial banking sector is remarkably large and diverse, with over 5,000 active banks holding just under $25T in combined assets. Furthermore, banks are heterogeneous across multiple dimensions, such as capitalization, size, asset allocation, and exposure to systemic risk. The BLC literature has attempted to capture the role of heterogeneity in bank behavior by explicitly controlling for some of these dimensions. Kashyap and Stein (1995), Kashyap and Stein (2000), and Kishan and Opiela (2000) find that smaller, less liquid, and less capitalized banks are more sensitive to monetary policy shocks, respectively. Dave et al. (2013) confirms that smaller banks tend to be more sensitive to monetary policy. Bluedorn, Bowdler, and Koch (2017) find that belonging to a bank holding company, and not bank size, is what determines the insensitivity of banks to monetary shocks. Altavilla, Canova, and Ciccarelli (2020) studies banks in the European Union to find that the capital ratio, exposure to domestic sovereign debt, the share of non-performing loans and the stability of the funding structure of a bank contribute to the heterogeneity in monetary pass-through to bank loan supply.

I argue that a key determinant of bank behavior neglected by the above literature is the business model, driven largely by the geographical scope of service provision. The vast majority of banks in the U.S. have historically been community banks, as evidenced by Figure 1. Community bank activity is often limited to local economies, with their business model geared towards relationship-building and the provision of traditional banking services to local firms and households (Nguyen & Barth, 2020) – unlike their geographically-diversified noncommunity counterparts.

The most common approach to controlling for bank heterogeneity in the existing literature is to group them by size. However, such grouping may be problematic due to the equal split between community banks and noncommunity banks in the mid-range of the bank size distribution. There is crucial heterogeneity within this group that remains unaccounted for without partitioning banks according to their business model. Furthermore, as evidenced by Figure 1, the composition of the U.S. banking sector has changed drastically since the early 1990s as a result of consistent consolidation. The evolving composition of the commercial banking sector may have implications for the magnitude and delays in the effects of monetary policy changes. Understanding the role of bank heterogeneity across the business model dimension can be crucial in anticipating changes in the behavior of monetary transmission.

Over the sample period from 1994 to 2019, I find that community bank lending enables contractionary monetary policy shocks to negatively impact output growth. In other words, the pass-through of monetary policy to the real economy through bank lending occurs partially through community bank lending. This finding suggests that bank relationship lending still matters, perhaps even to a greater extent than argued by Fields, Fraser, Berry, and Byers (2006). Moreover, given that community banks lend to small local borrowers (FDIC, 2020), this result may also have distributional implications. Specifically, an unanticipated monetary tightening may have a contractionary effect on output in the medium run via a persistent decline in small business activity caused by limited funding opportunities for such borrowers.

The remainder of this paper is organized as follows. Section 2 presents the empirical approach to estimating the nature of monetary transmission through

bank lending. Section 3 describes the results and their implications. Section 4 concludes the paper.

3.2 Econometric Approach

In this section, I describe the construction of the FAVAR using bank-level loan data, aggregate economic series, and an externally-identified proxy for monetary policy shocks. I also explain how I estimate the model, and use it to generate PT-IRFs in order to gauge the contribution of community, noncommunity, and joint bank lending to the transmission of monetary policy shocks to output growth.

In short, the FAVAR is constructed around a standard monetary VAR with variables capturing quarterly variation in monetary policy, output, inflation, and credit conditions in financial markets. In addition to these aggregate variables, the VAR is augmented with bank lending factors that separately capture comovement in the growth of lending volume of all banks, community banks, and noncommunity banks, respectively. The hierarchical nature of these factors, which are estimated using a large panel of bank lending series, ensures that I isolate latent forces driving group-specific fluctuations in community and noncommunity bank lending behavior. In other words, controlling for comovement across all banks guarantees that the model captures bank type heterogeneity through the group-specific factors. The hierarchical lending factors are estimated using a recursive principal components estimator, beyond which the estimated factors are treated as observables during the estimation of the VAR using least squares. The externally-identified monetary policy shock series is included in the VAR as an endogenous variable without any restrictions on its lag coefficients (similar to the approach taken in Auerbach and Gorodnichenko (2012) to identify news shocks), and its corresponding innovation

is further recursively internally-identified. Finally, PT-IRFs point estimates are generated directly as mappings of the lag coefficient and contemporaneous impact matrix estimates from the previous step. Confidence intervals on the PT-IRFs are obtained using a wild bootstrap (Gonçalves & Kilian, 2004, 2007), such that at each iteration of the bootstrap, the newly-estimated lag coefficients and contemporaneous impact loadings produce a new draw of a PT-IRF of interest. I elaborate on each step in this process in the remainder of this section.

3.2.1 Data. I use a combination of quarterly bank-level loan data, a small set of aggregate macroeconomic series, and externally-identified monetary policy shock series developed by Bu et al. (2021). The sample runs from Q1 of 1995 until Q4 of 2019, constrained by the start of the monetary policy shock series and the beginning of COVID-19. The cleaning procedure for bank loan series, obtained from the FDIC Statistics on Depository Institutions (SDI) database, is described by the following steps:

1. For each FDIC-insured commercial bank that has existed in the U.S. throughout the duration of my sample, I obtain a quarterly series of net loans and leases at the bank level. Net loans and leases equals to loans and lease financing receivables, net of unearned income and the allowance for loan and lease losses. For the remainder of this text, I refer to net loans and leases as "total lending" or simply "lending" interchangeably;

2. I create a balanced panel of bank lending series by discarding data associated with banks with at least one missing observation – in other words, I maintain data only for those banks that have been operational throughout the full sample period;

3. I partition the panel by bank type, yielding two separate sub-panels of bank-level data – one for community bank lending, and another for noncommunity bank lending.

4. Each of the series across the two sub-panels are transformed into growth rates and seasonally adjusted simply by partialling out variation attributable to seasonal dummies in a linear regression model.

The cleaned bank-level data is used to estimate bank lending factors and their loadings in the factor structure of the FAVAR.

The following macroeconomic series, used in the VAR portion of the FAVAR, are obtained from the Federal Reserve Economic Data (FRED) database:

1. **Real Gross Domestic Product** (GDPC1): Baseline proxy for output.

2. **GDP Deflator** (GDPDEF): Baseline proxy for inflation.

3. **Industrial Production** (INDPRO): Alternative proxy for output, often used in monetary VARs with monthly data.

4. **Consumer Price Index** (CPIAUCSL – Consumer Price Index for All Urban Consumers: All Items in U.S. City Average): Alternative proxy for inflation, also frequently used in monthly monetary VARs.

An additional aggregate indicator included in the VAR is the excess bond premium (EBP). The EBP is the average corporate bond spread that is purged from the impact of default compensation. It is one of two components of the credit spread indicator introduced by Gilchrist and Zakrajšek (2012), often referred to as the GZ spread. The EBP is interpreted as an indicator of the capacity of intermediaries to extend loans, or more generally the overall credit supply conditions in the economy.

It aggregates high-quality forward-looking information about the economy – therefore, it improves the reliability and forecasting performance of small-scale VARs (Caldara & Herbst, 2019). Modern monetary VARs often contain the EBP as an endogenous variable to reflect credit market conditions. I follow this convention in the literature due to the desirable properties of the EBP described above. Furthermore, Bu et al. (2021) include the EBP in their monthly VARs with which they test the validity of their monetary policy shock measure – by including the EBP in my model, I am able to more closely replicate their setting.

The final key data series used in this study is the monetary policy shock measure. For the purposes of my analysis, I defer to the Bu-Rogers-Wu (BRW) monetary policy shock measure identified by Bu et al. (2021). I aggregate their provided shock series to the quarterly frequency, as shown in Figure 10. I use the BRW shock instead of others in the literature, such as Romer and Romer (2004), Nakamura and Steinsson (2018), and others mentioned in Ramey (2016), since it is specifically tailored to account for both conventional and unconventional monetary policy over the course of my sample period, which is plagued with a variety of monetary policy regime changes and a long zero lower bound (ZLB) period following the 2007-08 financial crisis.

3.2.2 Model. I estimate a FAVAR that applies a hierarchical factor structure to the bank loan growth rates series in my sample and a shared VAR structure to the corresponding bank lending factors, macroeconomic series, and the monetary policy shock series. The hierarchical factor structure captures factors driving common variation among the growth of bank loans between and across community and noncommunity banks – in other words, it simultaneously contains factors representing common sources of variation among all banks, along with a separate

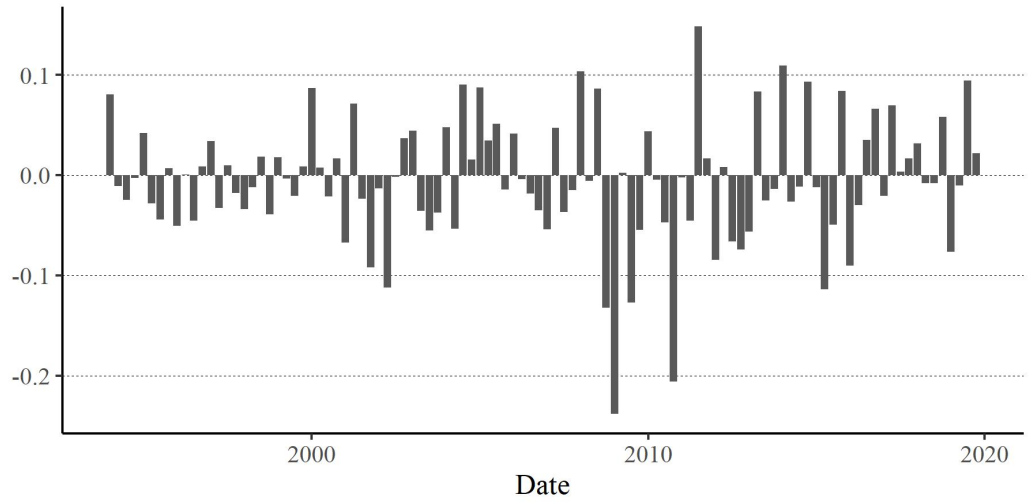

Figure 10. Quarterly BRW shock.

set of factors capturing bank type-specific variation. The VAR yields the dynamic relationship between these bank lending factors, macroeconomic series, and monetary policy. Although the bank lending factors themselves do not have an intuitive interpretation, their impulse responses to various shocks to the observed series in the VAR can be used in conjunction with their corresponding factor loadings to generate bank-specific impulse responses. For example, the FAVAR allows us to estimate bank-specific lending responses to a contractionary monetary policy shock.

The factor structure applied to the loan growth rate series x of each bank i is as follows:

$$x_{it} = \alpha_i + \Gamma_i F_t + \Lambda_i F_t^j + u_{it}\,, \tag{3.1}$$

where t indexes time, $j \in \{\text{community bank}, \text{noncommunity bank}\}$ indexes bank type, F is a vector of lending growth factors common to all banks, F^j is a vector of lending growth factors common only to banks of type j, u is an idiosyncratic disturbance term, α is an intercept coefficient, and Γ and Λ are vectors containing

factor loadings. Note that the factors are unobservable. In words, the growth rate of lending at bank i at time t is assumed to be an affine function of a set of factors representing the comovement in lending across all banks, F_t, a set of factors capturing the comovement in lending across all community or noncommunity banks (depending on the category to which bank i belongs), F_t^j, and an idiosyncratic term capturing dynamics specific to the given bank, u_{it}. Eq. (3.1) can be used to estimate the factor loadings, along with the factors themselves. The hierarchical or multi-level structure of the factors allows me to directly separate common variation across all banks from community and noncommunity bank-specific variation.

The VAR may be expressed as follows:

$$Z_t = \gamma + \Psi(L)Z_{t-1} + Bv_t\,, \tag{3.2}$$

where

$$Z_t \equiv \begin{bmatrix} \text{BRW}_t \\ \log(\text{GDP}_t) \\ \log(\text{GDPD}_t) \\ \text{EBP}_t \\ F_t \\ F_t^{\text{N}} \\ F_t^{\text{C}} \end{bmatrix},$$

such that BRW, GDP, GDPD, CP, and EBP denote the cumulative BRW shock series, gross domestic product, GDP deflator, commodity price index, and excess bond premium, respectively; F^N represents the vector of noncommunity bank lending factors; F^C represents the vector of community bank lending factors; $\Psi(L)$ is a lag matrix polynomial; $v \sim N(0, I)$ is a vector of structural shocks; and B is a

recursively identified contemporanous impact matrix. Refer to Figure 11 for a plot of the cumulative BRW shock.

Figure 11. Quarterly cumulative BRW shock.

Together, Eqs. (3.1) and (3.2) describe the FAVAR in state space form – Eq. (3.1) acts as the transition equation, and Eq. (3.2) as the measurement equation. For completeness, the full model is expressed below:

$$X_t = \alpha + \Gamma F_t + \Lambda^N F_t^N + \Lambda^C F_t^C + u_t\,,\; u_t \sim N(0, \Sigma_u)\,, \tag{3.3}$$

$$Z_t = \gamma + \Psi(L) Z_{t-1} + B v_t\,,\; v_t \sim N(0, I)\,, \tag{3.4}$$

where X_t is the data matrix containing all bank loan growth rate series.

3.2.3 Monetary Policy Surprise Identification. The VAR in Eq. (3.2) includes the monetary policy shock as an endogenous variable. The cumulative BRW shock series is ordered first in the VAR, so that all variables in the system respond contemporaneously to its innovation identified recursively – this is a standard in the VARX literature (Auerbach & Gorodnichenko, 2012; Kilian, 2009). This specification often has zero restrictions imposed on all of the lag coefficients in

the equation for the externally identified shock (Jarociński & Karadi, 2020; Kilian, 2009). In the baseline model, I do not impose these restrictions – however, I show that that an alternatively-specified restricted VAR produces largely the same IRFs and PT-IRFs as the baseline VAR. As an additional robustness test, I estimate the baseline model using industrial production (IP) and the consumer price index (CPI) as proxies for aggregate output and prices, respectively, instead of GDP and the GDP Deflator. Once again, the nature of these additional results qualitatively matches that of the IRFs and PT-IRFs produced using the baseline model.

Alternative approaches in the literature use externally-identified shocks as instruments in VARs or in local projections – this approach is sometimes called a proxy VAR model. Plagborg-Møller and Wolf (2021) show that, under regularity conditions, VARX and proxy VAR modeling approaches yield asymptotically equivalent impulse responses up to a constant scaling factor. For more comparisons of these two methodologies, refer to J. Stock and Watson (2018), Plagborg-Møller and Wolf (2021), Caldara and Herbst (2019), and Paul (2020). I defer to the VARX approach in this paper due to the ease of inference associated with this methodology, particularly in extending it to PT-IRFs.

3.2.4 Factor Estimation. The factors of the described FAVAR are estimated using a principal components approach that combines the hierarchical structure of the Bayesian procedure outlined in L. Jackson, Kose, and Owyang (2015) with the frequentist two-step procedure described in Boivin, Giannoni, and Mihov (2009) (also used by Dave et al. (2013)). Other common approaches to estimating factors in hierarchical models include the Bayesian estimator described in C.-j. Kim and Nelson (1998), which relies on the posterior distribution of the factors developed by Carter and Kohn (1994), and an alternative Bayesian

estimator described in Otrok and Whiteman (1998) (and applied in Kose, Otrok, and Whiteman (2003) and Kose, Otrok, and Whiteman (2008)) which constructs a different method of sampling from the posterior of the factors. The pros and cons of all three of the above estimators are discussed in L. Jackson et al. (2015). The main reason for choosing the principal components approach in this study is due to the size of the bank-level dataset – a key disadvantage of the above-mentioned Bayesian methods preventing me from using them is that they are significantly slower, despite being useful for conducting inference on the factor distributions.

The factor estimation procedure is as follows:

1. Randomly select the same number of community banks as there are noncommunity banks in the sample, and discard the rest. This reduction in the data matrix serves the purpose of estimating the common bank lending factor on an equal number of community and noncommunity banks – otherwise, if the sample is unbalanced, the estimated factor may be capturing group-specific comovement rather than common sources of variation across all banks.

2. Normalize all bank-specific data series by de-meaning and dividing each series by its own standard deviation – this ensures that each series (bank) holds equal weight in the computation of the principal component. For each of the three variable blocks (asset growth rate, change in ROA, and lending growth rate), group the normalized community and noncommunity bank series into a single data block and use it to estimate common bank size, profitability, and lending factors by computing the corresponding first few principal components;

3. For each of the three normalized bank data blocks, partial out the variation attributable to their corresponding common factors from each series by subtracting the factor estimate multiplied by the corresponding coefficient estimates from the series. Once again, separate each normalized data block into community and noncommunity sub-blocks, then use each sub-block to estimate community and noncommunity bank size, profitability, and lending factors by computing the corresponding first few principal components;

4. Normalize all common bank and bank type-specific factors with respect to their corresponding means and standard deviations – this is done to improve the ease of interpretability of bank responses to factor variation;

5. Regress each series in the normalized bank type-specific data blocks associated with each of the three bank variables on their corresponding set of two factors. This final step yields coefficient estimates that represent bank-specific sensitivities to the variation in the relevant bank factors across all series and factors;

6. Repeat steps 2-5 until some form of convergence is achieved in the factor and coefficient estimates, but modify step 1 by partialing out the most recent estimate of the variation attributable to the type-specific factors from each corresponding series.

Figure 12 presents the estimated (1) common, (2) community, and (3) noncommunity bank lending factors. Recall that the first category refers to principal components that load on all standardized bank loan growth series in the sample, while the second and third load only on their respective community and noncommunity bank sub-groups. The set of common bank lending factors

capture common variation in bank loan growth across the set of all banks in the sample, while the community and noncommunity bank lending factors capture the remaining comovement specific to community and noncommunity banks, respectively. Note that the estimation procedure makes sure that the different categories of factors capture orthogonal variation, despite loading on some of the same series. In words – the community and noncommunity bank lending factors are independent of each other, given that all common variation across the set of all banks in the sample is successfully absorbed by the common bank lending factors.

For each of these three categories of bank lending factors – common, community, and noncommunity – I estimate two factors, corresponding to the first two principal components. Table 1 shows the distribution of the joint explanatory power associated only with the common bank lending factors across all community and noncommunity bank loan growth series in my sample. In other words, the table shows the distribution of R^2 coefficients obtained by regressing the individual standardized bank loan growth rate series on the two common bank lending factors. Table 1 also shows the distribution of the joint explanatory power associated with the common and corresponding group-specific bank lending factors across all community and noncommunity banks. In this table, I shows the distribution of R^2 coefficients obtained by regressing each of the standardized (non)community bank loan series on the common and (non)community bank lending factors. According to the results presented in these tables, the group-specific lending factors approximately double the explanatory power of the factor structure of the FAVAR, as captured by the R^2 coefficient – therefore, their inclusion is warranted. Despite the inclusion of all of the lending factors in the factor structure, it seems that bank lending is largely idiosyncratic at the bank-level – this matches the results in Dave

et al. (2013). Regardless, the factors can help identify common responses in lending behavior among U.S. commercial banks to monetary policy shocks.

The interpretation of the time variation in the factor estimates is not the focus of the paper – rather, the factors are used for the purposes of dimension reduction. However, a few items of note include the following: (1) In Figure 12a, the first principle component captures a gradual decline in bank loan growth after the 2008 recession, followed by a slow recovery. The second principle component captures a similar post-crisis dip that recovers much quicker. (2) A comparison between the community bank factors in Figure 12b with the noncommunity bank factors in Figure 12c shows a much sharper response to the crisis by noncommunity banks, as evidenced by outlying drop in the second principle component in 2008, and the temporary decline in the first principle component post-2008. The comovement among community banks is more difficult to interpret once the common bank lending factors are partialed out, however, as evidenced by the community bank lending factors.

Bank Type	**10%**	**25%**	**50%**	**75%**	**90%**
Community	0.04	0.07	0.12	0.22	0.31
	(0.007)	(0.021)	(0.064)	(0.125)	(0.228)
Noncommunity	0.02	0.05	0.09	0.16	0.27
	(0.005)	(0.017)	(0.047)	(0.098)	(0.171)

Table 1. R^2 percentiles obtained by regressing individual bank loan growth series on the common bank lending factors, along with their corresponding type-specific factors. In parentheses, I show the R^2 percentiles associated with regressing only on the common factors.

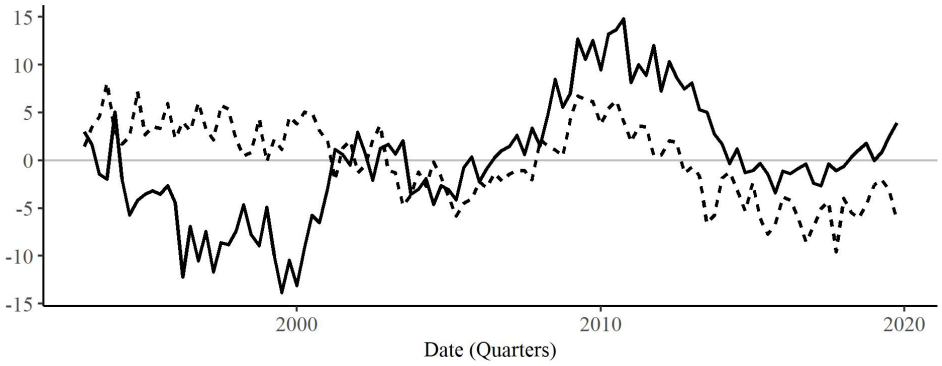

(a) Common bank loan growth factors.

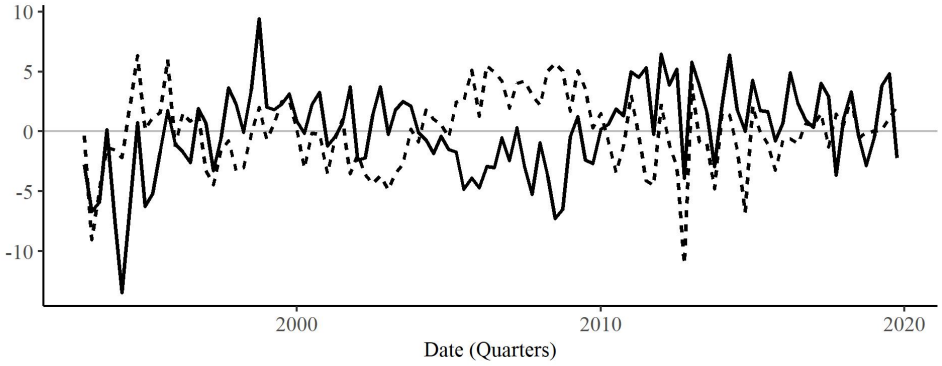

(b) Community bank loan growth factors.

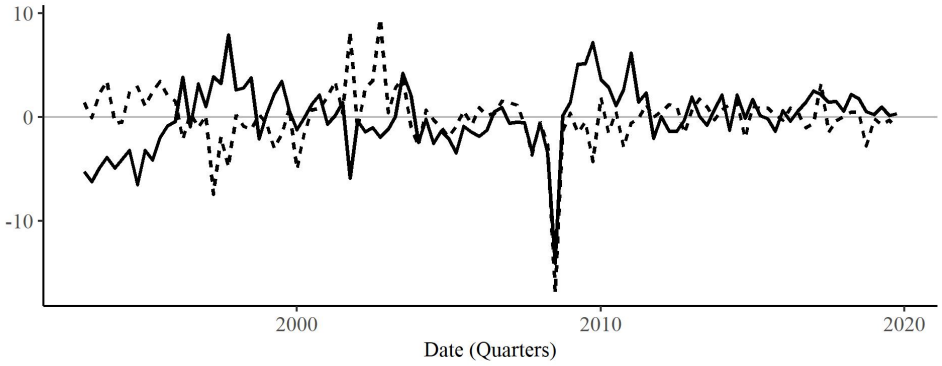

(c) Noncommunity bank loan growth factors.

Figure 12. Bank lending factor timeplots. The solid and dashed lines represented the first and second principal components of their corresponding panels of bank loan growth rate series, respectively.

3.2.5 VAR Estimation. The estimated factors are treated as observable series, and included in the transition equation of the FAVAR, which is essentially a VAR. The parameters of the VAR are estimated using least squares. The VAR estimates are then used to construct IRFs and PT-IRFs with bootstrapped confidence intervals. The recursive identification scheme used to obtain the IRFs and PT-IRFs is a simple recursive ordering of the shocks, with the BRW policy shock ordered first so that it can potentially affect all variables in the system contemporaneously. Practically, in my application, this scheme is exploited only for the identification of monetary policy innovations – my analysis does not rely on the clean identification of the remaining "structural" shocks in v_t.

Specifying and estimating VARs in levels has become common practice in the literature – recent examples include Bu et al. (2021); Görtz, Tsoukalas, and Zanetti (2022), among many others. This deviates from the past common practice of differencing and/or otherwise transforming seemingly integrated variables to achieve stationarity before estimating the VAR. However, VARs expressed in levels produced unbiased estimates of smooth functions of the model parameters. More importantly, Gospodinov, Herrera, and Pesavento (2013) show that structural IR estimators based on the levels specification have consistently and significantly lower MSE than those based on pretested models. For these reasons, I choose to specify my base model in levels. However, it is worth noting that the the results obtained using this specification are robust to transformations of the macroeconomic indicators to growth rates, with the latter specification having wider confidence intervals and more persistent impulse responses. The growth rate specification results are available upon request.

3.2.6 PT-IRF Illustration. In this section, I once again briefly explain the intuition behind PT-IRFs in a simple setting that emulates the context of this study. Consider the following VAR(1) process:

$$\begin{bmatrix} Y_{t+1} \\ N_{t+1} \\ C_{t+1} \end{bmatrix} = \begin{bmatrix} \phi_{YY} & \phi_{YN} & \phi_{YC} \\ \phi_{NY} & \phi_{NN} & \phi_{NC} \\ \phi_{CY} & \phi_{CN} & \phi_{CC} \end{bmatrix} \begin{bmatrix} Y_t \\ N_t \\ C_t \end{bmatrix} + \begin{bmatrix} b_Y \\ b_N \\ b_C \end{bmatrix} m_{t+1} \tag{3.5}$$

where Y, N, and C denote output, noncommunity bank lending, and community bank lending as the endogenous variables of the system, respectively, and m denotes a monetary policy shock. We may represent the dynamics of the system dictated by the above VAR(1) as a directed weighted graph – this representation can be used to motivate IRFs, and naturally extend them to PT-IRFs.

Notice that ϕ_{ij} represents the one-period-ahead impact of a change in the j-th variable on the i-th variable. In the context of a directed weighted graph, we may think of each endogenous variable at a given point in time as a vertex, and ϕ_{ij} as the intensity of the travel path of a signal from variable j at time t to variable i at time $t+1$. Also notice that b_i represents the contemporaneous impact of a change in m on variable i. Therefore, we may think of the set of all b_i as composing an adjacency matrix in the context of a directed weighted graph that determines the intensity of arrival of a signal through the monetary policy shock for all endogenous variables in the system. A visual representation of this mapping of the given VAR(1) to a graph is presented in Figure 13 – a monetary shock that arrives at time t must first pass through all of the variables in the system before reaching a given destination at time $t+1$.

Suppose we are interested in gauging the one-period-ahead effect of a monetary policy shock on output. Figure 13 shows us that there are three distinct

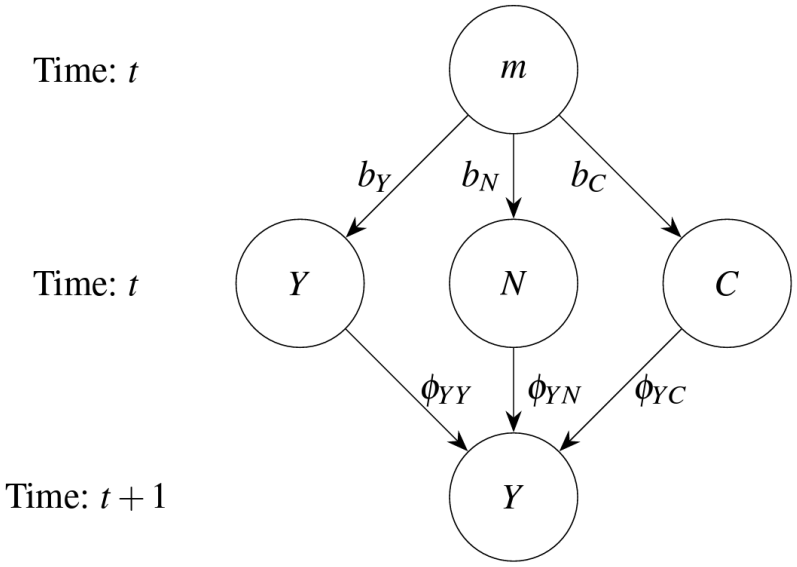

Figure 13. A graph-based illustration of the propagation of an impulse originating at m with destination Y one period ahead in the system determined by Eq. (3.5).

paths through which m ultimately affects Y – (i) a path through Y; (ii) a path through noncommunity bank lending, N; (iii) a path through community bank lending, C. The contribution of each path to the overall effect of m_t on Y_{t+1} is the product of the weights of its corresponding edges: (i) $\phi_{YY}b_Y$; (ii) $\phi_{YN}b_N$; and (iii) $\phi_{YC}b_C$, respectively. Summing these contributions, or path weights, yields the one-period-ahead response of Y with respect to an impulse from m:

$$\frac{\delta Y_{t+1}}{\delta m_t} = \frac{\delta Y_{t+1}}{\delta Y_t}\frac{\delta Y_t}{m_t} + \frac{\delta Y_{t+1}}{\delta N_t}\frac{\delta N_t}{m_t} + \frac{\delta Y_{t+1}}{\delta N_t}\frac{\delta N_t}{m_t} = \phi_{YY}b_Y + \phi_{YN}b_N + \phi_{YC}b_C\,. \tag{3.6}$$

Extending this framework for gauging the effects of an impulse in a VAR(1) to longer horizons gives us an IRF.

Now, suppose instead that we are interested in gauging the one-period-ahead contribution of community bank lending to the transmission of a monetary policy shock to output. Clearly, two of the three paths shown in Figure 13 – the

ones passing through Y and N – are irrelevant to community bank lending, and do not reflect its influence on the transmission of m. Therefore, we may subtract the contributions/weights of these paths from the overall impulse response expressed in Eq. (3.6) to obtain the contribution of C to the one-period-ahead effect of m on Y: $\phi_{YC}b_C$ – the weight of the only path passing through C. Extending this framework to longer horizons is precisely a PT-IRF that conditions on community bank lending as a medium of transmission for monetary policy shocks to output.

3.2.7 PT-IRF Application. The FAVAR can be used to generate PT-IRFs that allow for the assessment of the effect of a contractionary monetary policy shock on output growth via its transmission through bank lending. Specifically, once the VAR specified in Eq. (3.4) is estimated, I use the PT-IRF approach to estimate the dynamic response of the GDP to a positive shock to the BRW series, while conditioning on different combinations of the bank lending factors in F_t, F_t^C, and F_t^N as media for the transmission of the shock.

Let us represent the linear VAR(p) expressed in Eq. (3.4) as a VAR(1) with companion matrix Φ and augmented contemporaneous impact matrix $\Gamma = \begin{bmatrix} B' & \mathbf{0} \end{bmatrix}'$:

$$Z_t = \theta + \Phi Z_{t-1} + \Gamma v_t \,. \tag{3.7}$$

Then for $h \geq 0$ the corresponding PT-IR to a monetary policy shock $\overline{v}$ with pass-through medium variable z_j (the j-th component of vector Z – let us suppose this is one of the bank lending factors) may be expressed as

$$\text{PT-IR}(h, j, \overline{\varepsilon}) \equiv \left(\Phi^h - \widetilde{\Phi}^h\right) \Gamma \, \overline{v} \,, \tag{3.8}$$

where $\widetilde{\Phi}$ is the companion matrix of a modified version of the process described in Eq. (3.4) with the i-th lag coefficient matrix restricted to equaling

$$\widetilde{\Psi}_i \equiv \begin{bmatrix} \vec{a}_1 & \dots & \vec{a}_{j-1} & \vec{0} & \vec{a}_{j+1} & \dots & \vec{a}_N \end{bmatrix}, \tag{3.9}$$

where $\vec{a}_m$ denotes the m-th column of Ψ_i. Notice that $\widetilde{\Phi}^h \Gamma \overline{\varepsilon}$ captures the impulse response to the shock for a restricted version of the given linear VAR(p) in which the Granger causality of the j-th endogenous variable is completely removed (Kilian & Lütkepohl, 2017) – all paths passing through the j-th variable are assigned a weight of zero. Therefore, PT-IR($\cdot$) sums the weights of only those paths that pass through the j-th variable, which can be interpreted as the impulse response of the system attributable to the Granger-causality of the j-th endogenous variable.

The above framework can be extended to allow for multiple pass-through media. In the next section, I present the pass-through impulse responses of the GDP to a contractionary monetary policy shock separately via (1) all bank lending factors, (2) only common and community bank lending factors, as well as (3) only common and noncommunity bank lending factors. We may interpret the first PT-IRF described above as measuring the combined transmission of monetary policy to output via (all) bank lending. The second and third PT-IRFs may be interpreted as measuring the transmission of monetary policy to output separately via community and noncommunity bank lending, respectively.

It is also possible to easily conduct inference on differences between PT-IRFs with different media. Suppose that for some dependent variable i, we would like to compare PT-IR$(h, i, j, \overline{\varepsilon})$ to PT-IR$(h, i, j', \overline{\varepsilon})$ to assess whether j plays a bigger role in the transmission of the shock $\overline{\varepsilon}$ to i than does j'. We can define a new object ΔPT-IR$(h, i, j, j', \overline{\varepsilon}) \equiv$ PT-IR$(h, i, j, \overline{\varepsilon}) -$ PT-IR$(h, i, j', \overline{\varepsilon})$, which is also a nonlinear mapping of the reduced form parameters of the state equation of the FAVAR. We

can then estimate confidence intervals for the ΔPT-IR object the same way as we do for IRFs and PT-IRFs, using the wild bootstrap, for a given level of statistical significance. If for a range of h the confidence intervals of this object is above 0, that implies j plays a greater role in the transmission of shock $\overline{\varepsilon}$ to variable i than does j'. I apply ΔPT-IR by comparing the transmission of monetary policy shocks to output via community versus noncommunity bank lending.

3.3 Results

The baseline FAVAR produces the following key results: **(i)** Output responds negatively to a contractionary monetary policy shock through the set of all bank lending factors as the medium of transmission – this confirms the traditional understanding of the role of bank lending in the monetary transmission mechanism; **(ii)** Output responds negatively to a contractionary monetary policy shock through the set of factors that load on *community* bank lending series – this demonstrates that community banks contribute to the overall transmission of monetary policy through bank lending; **(iii)** Output responds negatively to a contractionary monetary policy shock through the set factors that load on *noncommunity* bank lending – less surprisingly, this evidences the significance of noncommunity bank lending in monetary transmission; **(iv)** Finally, conducting inference on the difference between the monetary PT-IRs conditional on community versus noncommunity bank lending shows evidence of community bank lending having a greater (in magnitude) effect in the short run, whereas noncommunity bank lending plays a more significant role in monetary transmission in the medium run.

These results are echoed by the alternative model, which uses IP and CPI as proxies for output and inflation instead of GDP and the GDP Deflator.

Furthermore, both models confirm that unexpected monetary policy shocks are identified correctly – macroeconomic indicators respond as expected (mimicking the monthly VAR results in Bu et al. (2021)), and the distribution of individual bank loan responses lies mostly below zero for the entire 10-year post-shock period. I begin by discussing the aggregate and bank-level impulse responses in the following two subsections, after which I return to the discussion of PT-IRFs and evidence of heterogeneous pass-through via community versus noncommunity bank lending.

3.3.1 Aggregate IRFs. Figure 14 shows the dynamic responses of all variables in the VAR as a result of a one standard deviation shock to the cumulative BRW series. The BRW series itself quite rapidly converges back to zero, whereas the GDP and the deflator respond with a delay – the former remains significantly below zero for a period of approximately five years post-shock, whereas the latter persists for the entire 10-year period of examination. The EBP also behaves in the expected manner, as documented in Bu et al. (2021). The responses of the individual factors are uninformative – however, it is worth noting that they all converge back to zero with time. The shapes and directions of these impulse responses are closely matched by those of the model with zero restrictions, presented in Figure A.5, as well as the models with alternative measures of macroeconomic variables and monetary policy shock, presented in Figures A.11 and **??**, respectively. Furthermore, these impulse responses are statistically significant at comparable horizons.

3.3.2 Bank-Level Loan IRFs. Figure 15 shows the effects of a one standard deviation contractionary monetary policy shock on individual bank lending separately for community and noncommunity banks. The two impulse response distribution plots imply that, on average, both community and

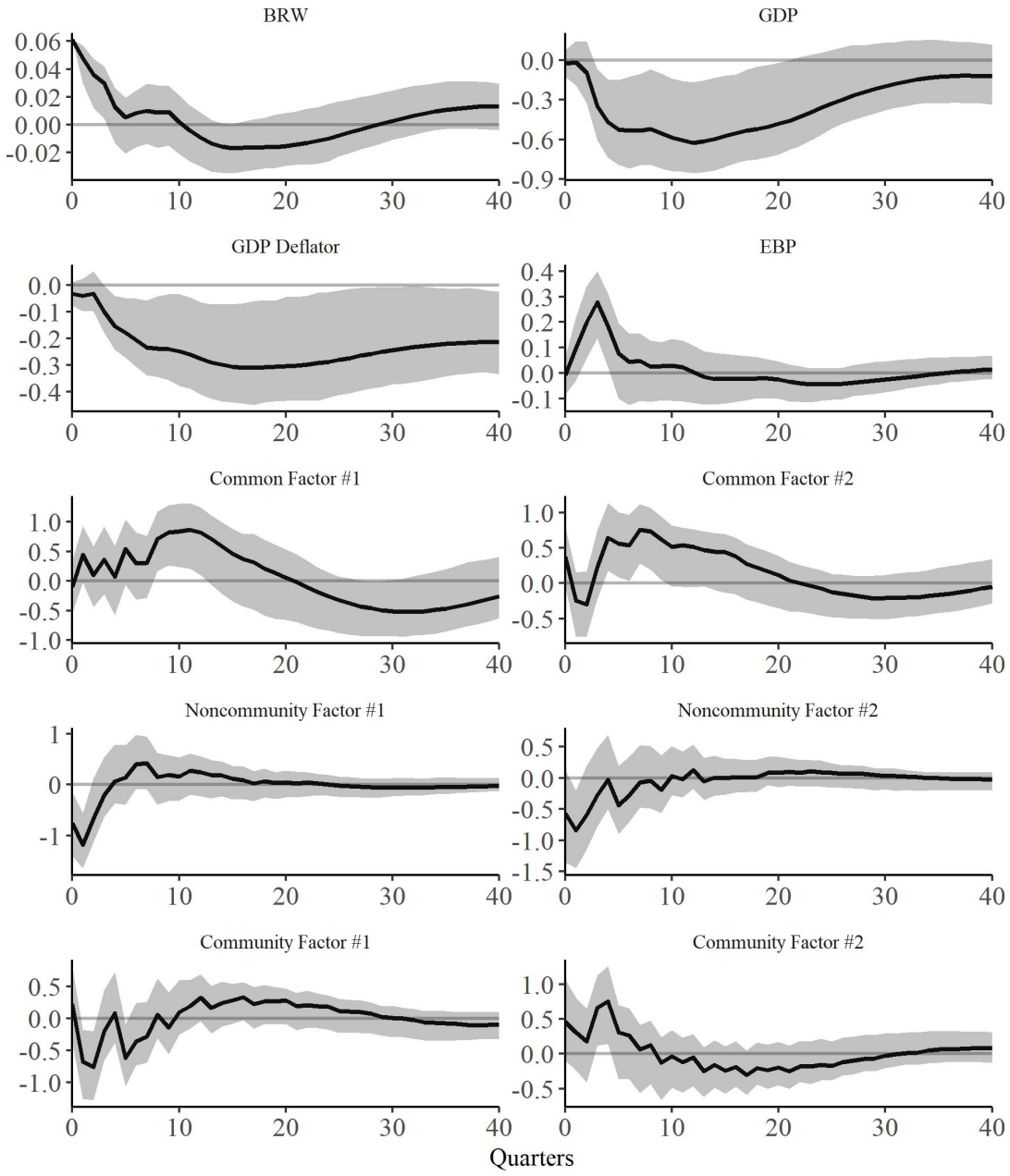

Figure 14. Impulse responses of all variables in the VAR to a one standard deviation positive (contractionary) monetary policy shock via bank lending. Solid black lines represent point estimates. Gray bands represent 90% confidence intervals generated using the wild bootstrap with 1,000 runs.

noncommunity banks tighten lending over the course of a 10-year horizon as a result of a contractionary shock, although the median of both groups converges back to its original level by the end of the period. In the first two years after the shock however, the distribution of responses for both groups centers at approximately zero, with minor positive deviations. This type of delay in loan volume contraction may potentially be caused by the rate of loan commitment draw-downs outpacing the slowdown in loan issuance in some of the banks, as described in Ivashina and Scharfstein (2010).

The same behavior can be seen in the bank-level loan impulse responses generated using the model with alternative measures of output and inflation, presented in Figure A.12, as well as the specification with an alternative policy shock series, presented in Figure A.18. The VAR with zero restrictions yields similar delayed declines in loan volume across both community and noncommunity banks, but without convergence back to a zero-centered distribution for the former group, as shown in Figure A.6. Overall, the distributions of these responses across all three models further confirm that the monetary policy shock is correctly identified, since a delayed contraction in bank lending is precisely what has been documented in a wide range of existing studies in the literature (Drechsler et al., 2017; Kashyap, Rajan, & Stein, 2002; Kashyap & Stein, 1994, 1995, 2000).

3.3.3 PT-IRFs. Figure 16 shows plots of the PT-IRFs associated with the pass-through of a one standard deviation contractionary monetary policy shocks to GDP via combined, community, and noncommunity bank lending. Figures A.2, A.3, and A.4 each present PT-IRFs conditioned on combined, community, and noncommunity bank lending, respectively, for all endogenous variables in the model. The same figure for the zero-restricted VAR is presented in Figures A.8,

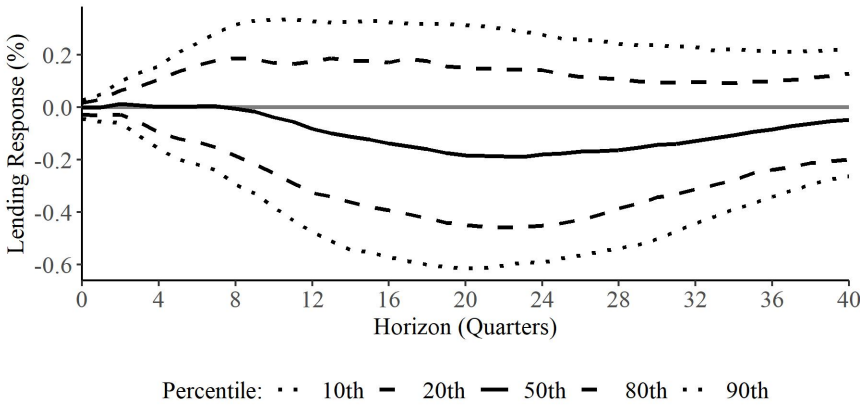

(a) Distribution of community bank lending volume responses

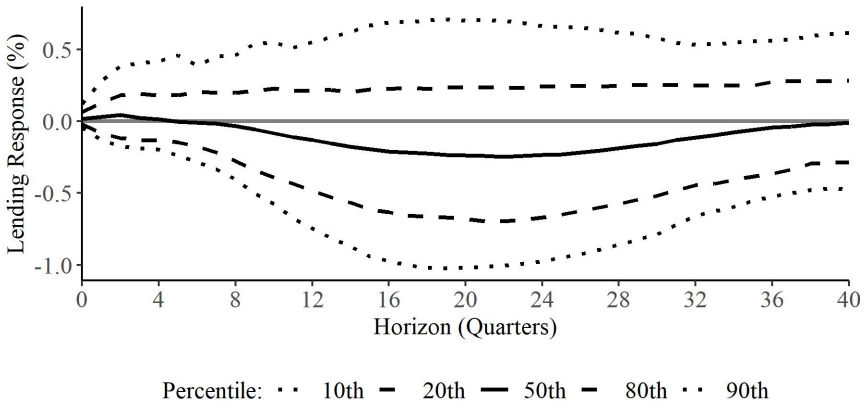

(b) Distribution of noncommunity bank lending volume responses

Figure 15. Bank-specific responses in loan quantity (cumulative loan growth rate) to a one standard deviation positive (contractionary) monetary policy shock.

A.9, and A.10. Equivalent displays for the model with alternative measures of macroeconomic indicators and monetary policy shocks are presented in Figures A.14, A.15, and A.16 and Figures A.20, A.21, and A.22, respectively.

The PT-IRF presented in Figure 16a is conditioned on all bank lending factors in the model as media of transmission. I interpret this object as capturing the transmission of monetary policy through bank lending of all types. It shows that a monetary tightening has a negative expected effect on output that persists for at least six years, although only approximately the first four years are significant with 90% confidence. The same kind of behavior is displayed by the equivalent PT-IRF generated using the alternative model specification, presented in Figure A.14.

Figure 16b is conditioned only on factors that load on the community bank lending series – the common and community bank lending factors – as media of transmission for the contractionary monetary shock. I interpret this object as capturing the overall transmission of monetary policy through community bank lending. It shows that a monetary tightening has a negative, delayed expected effect on output that persists quite strongly before beginning to converge back to zero at around the fifth year. For this PT-IRF, the effect is statistically significant as far as the fifth year after the shock. The same kind of behavior is displayed by the equivalent PT-IRF generated using the alternative model specification, presented in Figure A.15.

Finally, Figure 16c is conditioned on factors that load on the noncommunity bank lending series – the common and noncommunity bank lending factors – as media of transmission for the contractionary monetary shock. This object captures the transmission of monetary policy via noncommunity bank lending. The shape

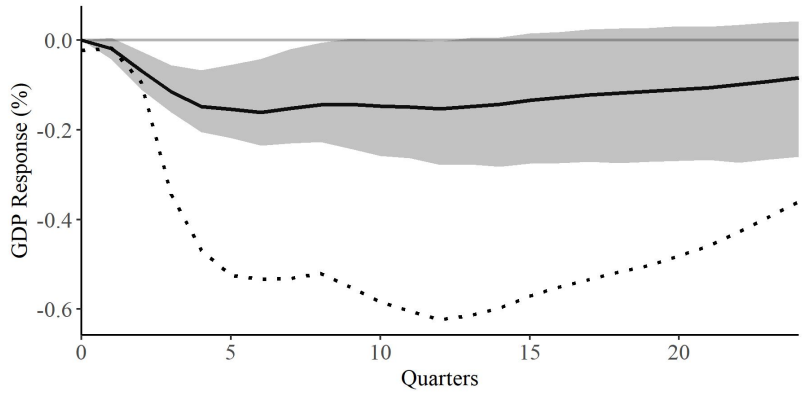

(a) **Medium:** Combined bank lending

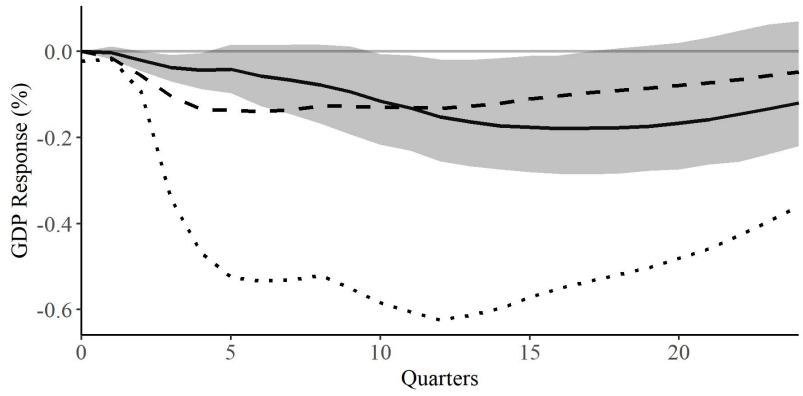

(b) **Medium:** Community bank lending

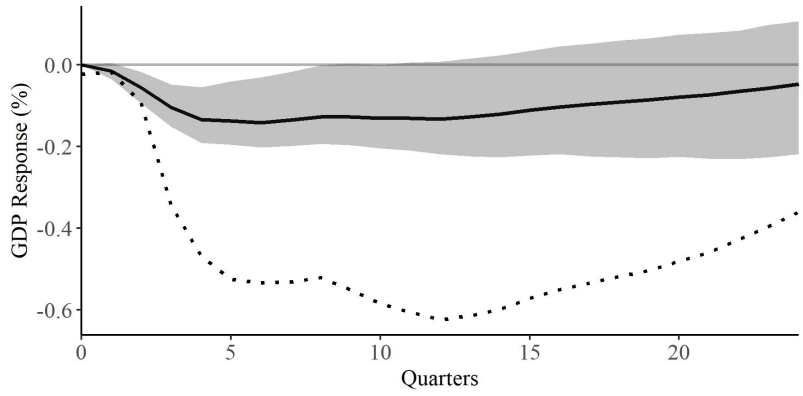

(c) **Medium:** Noncommunity bank lending

Figure 16. PT-IRs of GDP to a one standard deviation positive (contractionary) monetary policy shock via bank lending. Solid black lines represent point estimates. Gray bands represent 90% confidence intervals generated using the wild bootstrap with 1,000 runs. The dotted lines represent the net effect of the monetary shock on GDP. The dashed line in Fig 10b represents the point estimates of noncommunity bank lending PT-IRs, included for easy comparison.

and magnitude of this PT-IRF match that of the combined bank lending PT-IRF quite closely. However, its confidence interval crosses zero at a faster rate, and covers a larger portion above zero by the end of the six-year horizon – implying less persistence in the response compared to the combined PT-IRF. As with the previous PT-IRFs, this behavior is matched by the equivalent PT-IRF generated using the alternative model, presented in Figure A.16.

These PT-IRFs suggest that community bank lending plays a larger role in the transmission of monetary policy in the medium run, and noncommunity bank lending operates more strongly in the short run. As discussed in the methodology section on PT-IRFs, this hypothesis can be tested more directly using inference on ΔPT-IR objects. I present the results of that analysis in the next subsection.

3.3.4 Heterogeneity in Monetary Transmission. Recall that it is possible to conduct inference on differences between PT-IRFs with different media. Let $J = \{F, F^C\}$ represent the set of common and community bank lending factors, which I use to estimate PT-IR$(h, GDP, J, \bar{\varepsilon})$ – the transmission of monetary policy to output via *community* bank lending. On the other hand, let $J' = \{F, F^{NC}\}$ represent the set of common and noncommunity bank lending factors, which I use to estimate PT-IR$(h, GDP, J', \bar{\varepsilon})$ – the transmission of monetary policy to output via *noncommunity* bank lending. I define a new object

$$\Delta\text{PT-IR}(h, i, J, J', \bar{\varepsilon}) \equiv \text{PT-IR}(h, i, J, \bar{\varepsilon}) - \text{PT-IR}(h, i, J', \bar{\varepsilon}), \tag{3.10}$$

which captures the difference between the two PT-IRFs. I obtain point estimates and confidence intervals for ΔPT-IR using the wild bootstrap, for a 90% level of statistical significance. The resulting ΔPT-IRs are presented in Figure 17 for both the baseline and alternative model specifications.

Across both models, I find that the estimated ΔPT-IR is above zero in the short run, and below zero in the medium run. Considering that both PT-IRFs being compared are shown to be negative in the specified time frame, this implies that the magnitude of monetary transmission via noncommunity bank lending is greater than through community bank lending in the short run, while the opposite is true in the medium run. The short run results are statistically significant with 90% confidence across all model specifications. Refer to the final rows of Figures A.1, A.13, A.7, and A.19 for an alternative formulation of this test, where PT-IRFs that condition on only the group-specific lending factors are compared – the results match the ones presented in this section.

3.4 Conclusion

I use a factor-augmented vector autoregression (FAVAR) with bank lending factors and externally identified monetary policy shocks to estimate pass-through impulse response functions (PT-IRFs), which characterize the dynamic response of output growth to monetary policy shocks via changes in community, noncommunity, and combined bank lending. For robustness, I carry out the analysis using three alternative model specifications – a baseline model, a model with exclusion restrictions enforce the exogeneity of the monetary policy shock series, and an additional model which uses alternative proxies for output and inflation. I find that across all of these model specifications, there is evidence of the following outcomes as a response to a contractionary monetary policy shock: (i) negative short and medium run monetary transmission via joint bank lending; (ii) negative short run transmission via noncommunity bank lending; (iii) negative medium run transmission via community bank lending. Direct inference on the difference between monetary transmission via community versus noncommunity

bank lending also shows evidence of heterogeneity in the short run, with some evidence of heterogeneity in the medium run.

These results suggest that monetary transmission via bank lending occurs mainly through resulting changes in noncommunity bank lending in the short run, while changes in community bank lending drive the persistence of the response of output to monetary shocks into the medium run. Therefore, the evolving

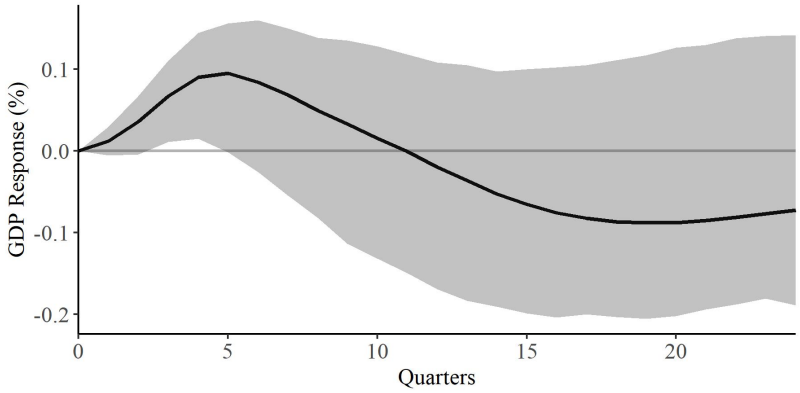

(a) Baseline model

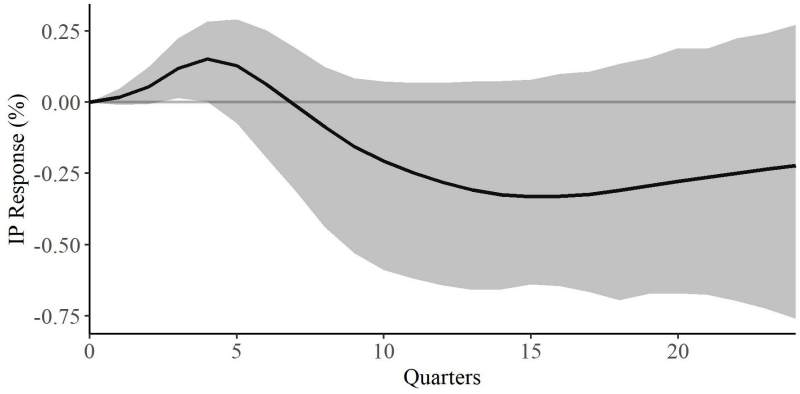

(b) Alternative model

Figure 17. Differences between the PT-IRs of (a) GDP and (b) IP, conditional on community versus noncommunity bank lending factors as the media for transmission, with respect to a one standard deviation positive (contractionary) monetary policy shock via bank lending. Solid black lines represent point estimates. Gray bands represent 90% confidence intervals generated using the wild bootstrap with 1,000 runs.

composition of the U.S. commercial banking sector may have implications for the magnitude and delays in the effects of monetary policy changes. Understanding the role of bank heterogeneity across the business model dimension can be crucial in anticipating changes in the behavior of monetary transmission. This study provides a step in that direction.

CHAPTER IV

THE EVOLUTION OF COMMUNITY BANK INTERCONNECTEDNESS

4.1 Introduction

The total market share of community banks in the US banking sector has experienced a steady decline over the past few decades. Despite the gradual drop in size, mainly due to consolidation, community banks support economic growth and stability through the provision of loans to small local borrowers. For example, community banks have historically played a significant role in providing services to rural communities – as of June, 2020, community bank branches held approximately 2/3 of total rural deposits in the US (Hanauer et al., 2021). Furthermore, community banks are major credit providers to agricultural and commercial borrowers in their respective local markets (Lux & Greene, 2015). Community banks have also proven themselves to be reliable credit providers during adverse macroeconomic conditions – most recently during the global financial crisis and the COVID-19 pandemic (Hassan et al., 2022). And unlike their larger geographically-diversified counterparts, there is evidence that community banks' specialization in local markets limits the transmission of global and remote credit shocks to their respective markets (Petach et al., 2021).

After the global financial crisis, the focus of researchers and policymakers on the interconnectedness of large banks formed the consensus that the potential exposure of community banks to common risk factors does not present a threat to the financial system (U.S. Treasury Department, 2017). Policymakers targeted large banks as the main contributors to the housing bubble, market crash, and the subsequent recession. For this reason, post-crisis regulatory reforms, most notably the Dodd-Frank Wall Street Reform and Consumer Protection Act, were

largely aimed at constraining the involvement of large banks in risky activities. A key focus of these regulatory changes was the alleviation of the extent of interconnectedness and exposure to systemic risk among large banks (Yellen, 2013). A further revelation of the belief that community banks cannot contribute to systemic risk manifested in the exemption of community bank holding companies from certain regulatory capital requirements. In fact, post-crisis sentiment on the supposed adverse effects of Dodd-Frank on the competitiveness of community banks led to the de-regulation of the community banking sector through the Economic Growth, Regulatory Relief, and Consumer Protection Act (EGRRCPA), passed by Congress in 2018 (Kress & Turk, 2020). I aim to fill a gap in the academic and policy literature by investigating the notion that community banks lack exposure to systemic risk.

In this study I find that state-level community bank performance in the United States has been co-moving less idiosyncratically at the state level and more similarly at the national level since the global financial crisis, relative to the pre-crisis era. This development implies a fundamental and arguably undesirable deviation of the community banking sector from its traditional role in the US financial system. Stronger national comovement of community bank performance is consistent with greater national interconnectedness of community banks, as well as a potential increase in common exposure to macrofinancial shocks.[1] In other words, the relative decrease in (state-level) idiosyncrasy may result in a future financial crisis having a more intensely adverse and uniform effect on the community

[1]Stronger national comovement may also be evidence of a persistent post-crisis increase in the magnitude of macrofinancial shocks. Despite this likely being true for the intra-crisis period, existing indicators of financial market volatility, such as the Chicago Board Options Exchange Volatility Index (CBOE VIX), point to a reversion to pre-crisis shock magnitudes after the end of the crisis.

banking sector. This is precisely the small bank equivalent to the concept of "too-big-to-fail", aptly named "too-many-to-fail" – an increase in the exposure of many small banks to the same sources of risk may lead to their mass failure in the event of a large adverse shock, with devastating effects on the financial system. This effectively bridges the gap between the risk profiles of community banks and large banks, thus shrinking the risk diversification opportunity choice set of depositors. These changes may be a result of either the various post-crisis regulatory policy changes in the banking sector, a push toward more nationally and/or globally diversified asset portfolio allocations by the community banks themselves, or perhaps some deeper structural change caused directly by the financial crisis.

My findings contribute to our understanding of the manner in which the US community banking sector has been evolving in recent decades, as well as the trajectory it may adopt for the near future. Once again, I identify an increase in the extent to which community bank performance co-moves across the country, along with a decrease in the extent of state-level idiosyncrasy. I obtain this insight by capturing dynamic and cross-sectional co-variation across a balanced panel of state-average community bank return-on-equity (ROE) series using a hierarchical dynamic factor model (HDFM), estimated using a Bayesian approach. A careful analysis of national and regional variance decompositions of the country- and region-level factors across pre-crisis, intra-crisis, and post-crisis subsamples shows a near-uniform decrease in state idiosyncrasy for both intra- and post-crisis subsamples relative to the pre-crisis subsample, and a near-uniform increase in national comovement for both intra- and post-crisis subsamples relative to the pre-crisis subsample.

The remainder of this paper is structured as follows: Section 2 is a review of the existing literature on systemic risk in the banking sector, community banks, and HDFMs; Section 3 describes the data and the structure of the HDFM; Section 4 presents and analyzes the results; Section 5 provides an interpretation of the results along with a discussion of their implications.

4.2 Related Literature

In this section I review the existing literature associated with the domain and methodology of this study. I partition the literature into groups of studies on the following topics: (1) the causes and effects of the interconnectedness of banks, as well as the nature of systemic risk associated with such interconnectedness; (2) the application of hierarchical dynamic factor modeling in macroeconomics. This study contributes to all of the above strands of literature in the analysis of community bank interconnectedness using hierarchical dynamic factor modeling.

4.2.1 Bank Interconnectedness and Systemic Risk. The level of bank interconnectedness can be used to gauge the presence of systemic risk in the banking system. Systemic risk may arise due to exposure to common factors – for example, Caccioli, Shrestha, Moore, and Farmer (2014) find that overlapping portfolios of financial institutions may lead to contagion. For a comprehensive coverage of literature on systemic risk, some of which touches on the manifestation of systemic risk in banking systems, refer to M. Jackson and Pernoud (2021). Interdependencies among financial institutions may also amplify and create channels for local shocks to propagate within the entire financial system (Eisenberg & Noe, 2001). For example, Elsadek Mahmoudi (2021) shows how a local credit shock induced by hurricane Katrina has affected real and credit markets in distant regions in the United States. More notably, Acemoglu, Ozdaglar, and Tahbaz-

salehi (2015) generalizes the results of Eisenberg and Noe (2001) to find that while a densely connected network of financial institutions likely supports financial stability, it may also lead to more severe propagation of large shocks. Similarly, Gai, Haldane, and Kapadia (2011) find that greater complexity and concentration in a financial network make such systems more fragile to shocks.

I contribute to this line of literature by identifying the dynamic interconnectedness of a large set of small banks across multiple geographical levels using a reduced form approach with minimal structural assumptions. Dynamic interconnectedness is measured by observing the extent of dynamic comovement among a set of bank-specific or aggregated financial bank data using variance decompositions of a given set of series – the greater the variance contribution of a dynamic factor at a certain geographical level (country, region, state, etc.), then the greater the dynamic comovement, and therefore the greater the interconnectedness among banks at that geographical level. Relative to existing methods of measuring bank interconnectedness, my approach is arguably more flexible and intuitive due to its atheoretical dimension-reducing nature, while also capturing complex dynamic relationships with clear policy implications. Kapinos, Kishor, and Ma (2020) develop a measure of the dynamic interlinkages among a small set of bank holding corporations using a similar approach. They use a dynamic factor model with time-varying parameters and stochastic volatility in the style of Del Negro and Otrok (2011) to decompose a balanced panel dataset of the return-on-assets (ROA) and net chargeoffs (NCO) series of 86 US bank holding companies as a linear combination of a common factor and a unit-specific idiosyncratic disturbance terms. Unlike this study, Kapinos et al. (2020) do not account for potential geographical factor hierarchies.

4.2.2 Hierarchical Dynamic Factor Models.

Dynamic factor models (DFMs) have been in use as a method of atheoretically capturing business cycle dynamics since Sargent and Sims (1977). DFMs allow to capture the comovement of a large set of series by modeling the underlying data-generating process (DGP) as being driven by a vector of common autoregressive latent factors. Refer to Doz and Fuleky (2020) for an overview of fundamental DFM estimation approaches, and to J. H. Stock and Watson (2016) for an excellent survey of the use of DFMs in macroeconomics. A discussion of DFM identification is presented in Bai and Wang (2012). Multi-level/hierarchical dynamic factor models (HDFMs) are a type of DFM that partitions series into groups across multiple levels, and assigns a latent dynamic factor to each group. Moench, Ng, and Potter (2013) presents a general description of an HDFM. Kose et al. (2003) applies an HDFM to a large panel of country-level data to estimate world, region, and country-specific factors representing business cycle fluctuations. Kose et al. (2008) similary applies an HDFM to G-7 country series to estimate common and country-specific business cycle factors.

4.3 Model

In the following two subsections I describe the data used in the study, along with the specification of the HDFM applied to the data, respectively. For details on the estimation of the HDFM, refer to Appendix B.

4.3.1 Data.

The dataset used in this study is a balanced panel of 50 series, with each representing the state-average community bank return on equity (ROE) of a state in the United States. Each series has 115 observations, running from Q4 of 1992 up to Q2 of 2021. The series are constructed using raw bank-level quarterly call report data provided publicly by the Statistics on Depository Institutions (SDI)

database maintained by the Federal Deposit Insurance Corporation (FDIC). The following procedure is carried out to generate the final state-level dataset used in this study, in the given order:

1. Select net income and equity variables for each quarter;

2. Generate a new ROE variable defined as

$$\text{ROE} = \frac{\text{Net income}}{\text{Equity}};$$

3. Filter for community banks (SDI database contains a binary categorization variable that classifies each observation as belonging to a community bank when true);

4. Match the community banks by each quarter with corresponding geographical variables – particularly, each community bank must be assigned to a US state and the corresponding FDIC supervisory region under which the given state falls (the following 6 regional FDIC offices oversee the entirety of the United States: Atlanta, Chicago, Dallas, Kansas City, New York, San Francisco);

5. Group ROE by state for each quarter, and compute state-average ROE;

6. Combine quarterly data into a single dataset containing a balanced panel of 50 state-average community bank ROE series;

7. Seasonally adjust each series with seasonal-trend (STL) decomposition using locally estimated scatter plot smoothing (LOESS) (Cleveland, Cleveland, McRae, & Terpenning, 1990).[2] Refer to Fig. 18 for randomly-selected timeplots comparing raw and seasonally-adjusted state-average ROE series.

[2]Effectively, the average deviation from the full-sample average of the quarter corresponding to each observation is subtracted from the observed value.

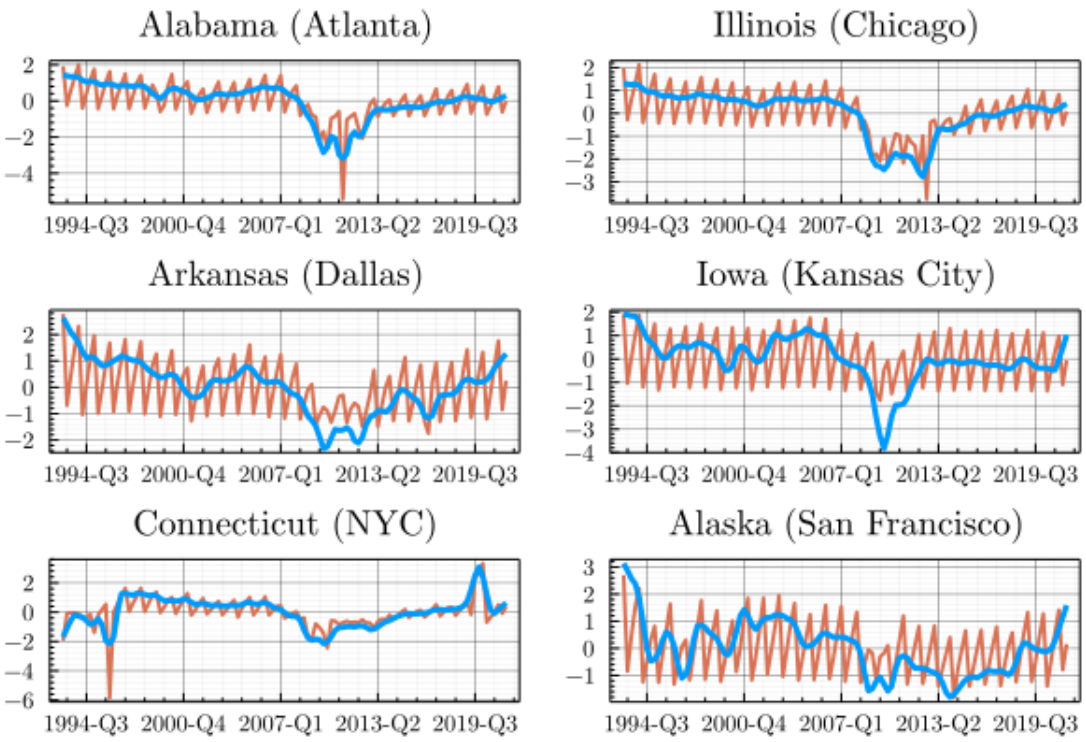

Figure 18. This graph presents a timeplot of normalized level state-average ROE series for one state in each FDIC supervisory region (in orange), along with its seasonally adjusted equivalent (in blue). The supervisory region corresponding to each state is written in parentheses next to their respective subplot labels.

Note that the number of community banks implicitly contained in the final dataset does not stay constant over time – some banks do not survive over the course of the entire sample period, while others are established after the initial sample period. Therefore, the variation in the finalized series is partially driven by young, failing, and ultimately-consolidated community banks. Alternatively, I could have constructed the final state-level dataset by initially filtering out such banks from the raw bank-level data, but this would have yielded a biased picture of actual performance of the community banking of each state at each given point in time. Refer to Fig. 19 for timeplots of the total number of US community banks, and the number of community banks by state over the sample period.

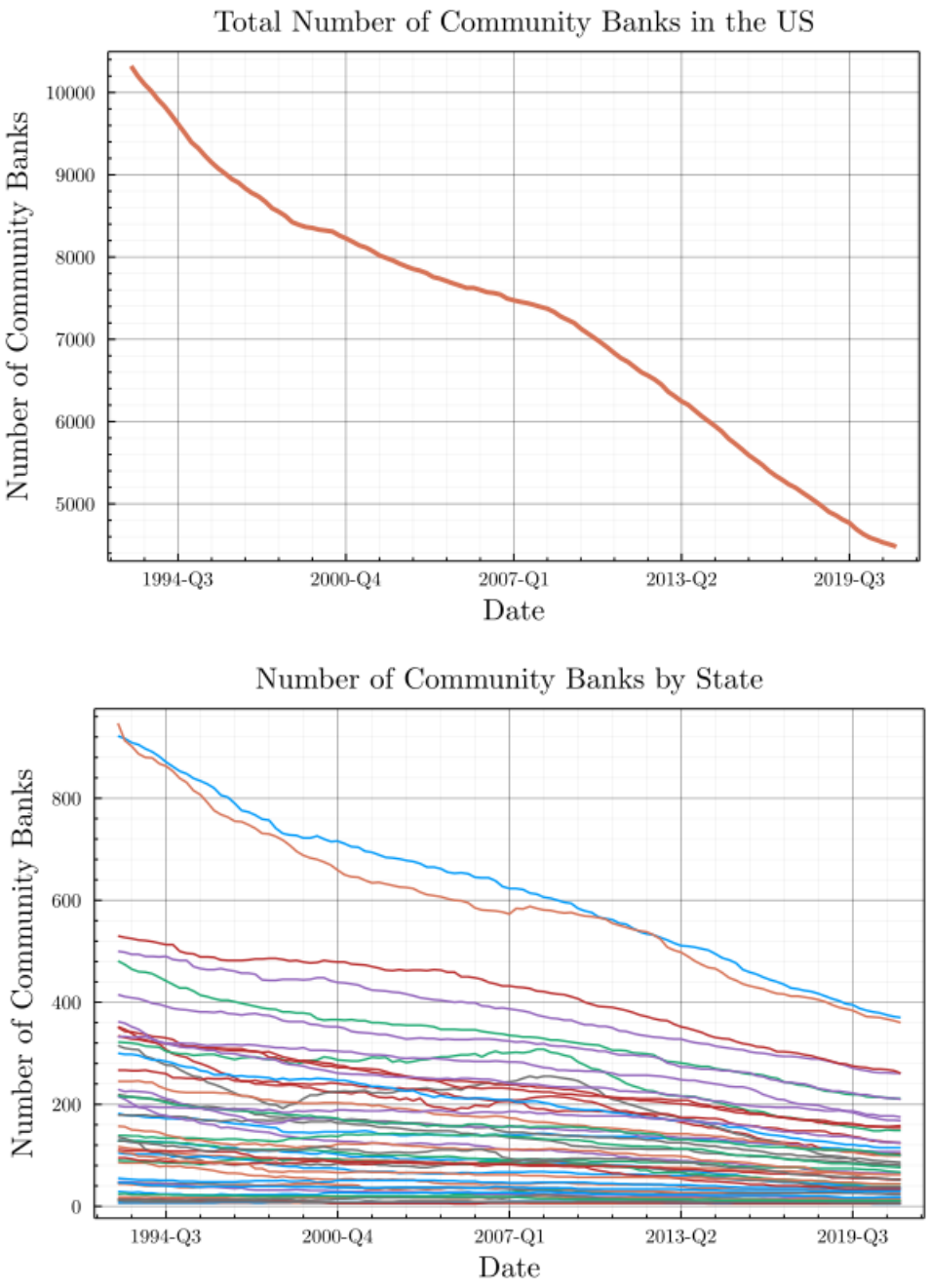

Figure 19. The top plot in this figure represents the total number of community banks in the US over the full sample period. The bottom plot represents the total number of community banks by state over time (each series represents one of 50 US states).

4.3.2 HDFM. The i-th series in the dataset, expressed as y_i for $i \in \{1, \ldots, I\}$ with $I = 50$, is treated as being generated by an affine combination of a country-wide factor, f^{US}, and a corresponding region-wide factor, f^{r_i}, in the following manner:

$$y_{it} = \beta_{0i} + \beta_{1i} f_t^{US} + \beta_{2i} f_t^{r_i} + \varepsilon_{it}\,, \tag{4.1}$$

where $\beta^i = (\beta_{0i}, \beta_{1i}, \beta_{2i})$ are coefficient hyperparameters, and ε_i is the idiosyncratic disturbance process specific to the i-th state. Notice that the country-wide factor, f^{US}, applies to all series. There exist a total of $R = 6$ FDIC supervisory regions, f^r, such that state i belongs to only one corresponding region $r_i \in \{1, \ldots, R\}$.

All latent factors and idiosyncratic disturbance terms are modeled as following autoregressive processes. The country factor may be expressed as the following order-p autoregressive process:

$$f_t^{US} = \psi_1^{US} f_{t-1}^{US} + \ldots + \psi_p^{US} f_{t-p}^{US} + v_t^{US}\,, \tag{4.2}$$

where $\psi^{US} = (\psi_1^{US}, \ldots, \psi_p^{US})$ are lag coefficient hyperparameters, and $v_t^{US} \in i.i.d.N(0, \sigma_{US}^2)$ is an innovation term. The r-ith regional factor may similarly be expressed as the following order-q autoregressive process:

$$f_t^r = \psi_1^r f_{t-1}^r + \ldots + \psi_q^r f_{t-q}^r + v_t^r\,, \tag{4.3}$$

where $\psi^r = (\psi_1^r, \ldots, \psi_q^r)$ are lag coefficient hyperparameters, and $v_t^r \in i.i.d.N(0, \sigma_r^2)$ is an innovation term. Lastly, the state-specific idiosyncratic disturbances may also be expressed as the following order-k autoregressive process:

$$\varepsilon_{it} = \phi_1^i \varepsilon_{it-1} + \ldots + \phi_k^i \varepsilon_{it-k} + u_t^i\,, \tag{4.4}$$

where $\phi^i = (\phi_1^i, \ldots, \phi_k^i)$ are lag coefficient hyperparameters, and $u_t^i \in i.i.d.N(0, \sigma_i^2)$ is an innovation term.

The above-specified model has the following restrictions. Firstly, it is assumed that $\sigma^2_{US} = \sigma^2_r = 1$. This restriction allows us to simultaneously identify the magnitude of the factors and their β coefficients in Eq. (4.1), both of which are otherwise unidentified. Secondly, it is assumed that $\beta_{11} > 0$, which enforces a positive relationship between the country factor and the first series in dataset. This assumption is necessary to identify the direction of f^{US}, which may otherwise be mirrored along with the β_{1i} coefficients to yield an identical unconditional distribution. In addition, it is assumed that $\beta_{2i} > 0$ for the first i in each level-2 state region groups for the same reason of identifying the direction of the regional factors. Lastly, it is assumed that $p = q = k = 3$ – in other words, all latent factors and idiosyncratic disturbance processes have the same lag order of 3.[3] This completes the specification of the HDFM assumed to be generating the state-average ROE series.

To be able to apply the Kim-Nelson estimator, we must express the given HDFM in state-space form. Let $\beta_0 = \begin{bmatrix} \beta_{01} & \beta_{02} & \dots & \beta_{0I} \end{bmatrix}'$ be an $I \times 1$ matrix containing the intercept terms of all series in the dataset. Also, let $\beta_1 = \begin{bmatrix} \beta_{11} & \beta_{12} & \dots & \beta_{1I} \end{bmatrix}'$ be an $I \times 1$ matrix containing the national factor loadings of all series in the dataset. Let $\mathbf{R}$ be an $I \times R$ matrix containing the regional factor loadings of all series in the dataset, such that $\mathbf{R}_{ij} = 0$ if the j-th regional factor does not correspond to state i, and $\mathbf{R}_{ij} = \beta_{i2}$ otherwise. Lastly, we define the vector $S_t \equiv \begin{bmatrix} f^{US}_t & f^1_t & \dots & f^R_t & \varepsilon_{1t} & \dots & \varepsilon_{It} \end{bmatrix}$ of length $L = 1 + R + I$. Given these objects,

[3] The lag specification of the model is chosen to be parsimonious, while also including enough parameters to account for complex dynamics in quarterly data. While it is possible to test for the optimal number of lags for each of the latent processes using model selection criteria, I have chosen to instead default to the standard approach taken in the literature of simply setting the lag orders of each of the latent processes equal to the same reasonable lag order given the frequency of the data. As examples of this, refer to Kose et al. (2003), Kose et al. (2008), and other HDFM studies mentioned in the literature review section.

we may express the measurement equation of the state-space form of the HDFM as

$$\begin{bmatrix} y_{1t} \\ y_{2t} \\ \vdots \\ y_{It} \end{bmatrix} = \begin{bmatrix} \beta_0 & \beta_1 & \mathbf{R} & I & \mathbf{0}_{(1+Lp)\times(1+Lp)} \end{bmatrix} \begin{bmatrix} 1 \\ S_t \\ S_{t-1} \\ \vdots \\ S_{t-p} \end{bmatrix} . \tag{4.5}$$

If we denote the state vector as β_t, then we may express the state equation as

$$\beta_t = F\,\beta_{t-1} + w_t\,, \tag{4.6}$$

where F is a companion matrix and w_t contains i.i.d. disturbance terms. The second moment matrix of w_t may be expressed as the following $(1 + Lp) \times (1 + Lp)$ matrix:

$$E(w_t w_t') = Q = \begin{bmatrix} 0 & 0 & 0 & \dots & 0 \\ \vdots & I_{1+R} & 0 & \vdots & \vdots \\ \vdots & \mathbf{0}_{(1+R)\times(1+R)} & \Sigma & \vdots & \vdots \\ \vdots & \dots & \mathbf{0}_{((L-1)p)\times((L-1)p)} & \vdots & \vdots \end{bmatrix} , \tag{4.7}$$

where

$$\Sigma = \begin{bmatrix} \sigma_1^2 & 0 & 0 & \dots & 0 \\ 0 & \sigma_2^2 & 0 & \dots & 0 \\ \vdots & & & \ddots & 0 \\ 0 & & \dots & & \sigma_I^2 \end{bmatrix} . \tag{4.8}$$

4.4 Results

In this section I present and describe the quantitative results obtained by estimating the HDFM. I first present the unconditional posterior distributions of all latent dynamic factors. Then I analyze relevant subsample variance decompositions of all observable series with respect to the national factor and idiosyncratic

disturbance estimates, and follow up with a similar analysis of the variance contributions of each of the regional factors toward series in their respective regions. I find that the dynamics of the national factor, as evidence by the plot of the unconditional posterior distribution of the national factor, seem to accurately match the major historical developments in the banking sector over the course of the last four decades. And although the regional factor estimates are more difficult to decipher, they too seem to show plausible changes over the same time period. I also show using full-sample variance decompositions that over the entire sample period, regional factors have had very limited contributions to the variation in state-average community bank ROE – the majority of the variation in all series is attributable either to state-specific idiosyncrasy or the national factor. Most importantly, comparisons of variance decompositions of pre-, intra-, and post-global financial crisis subsamples demonstrate that the role of the national factor in driving state-average community bank ROE dynamics has grown since the crisis, while the extent state-specific idiosyncrasy has fallen.

4.4.1 Factor Estimates. Let us observe the nature of the estimated US national latent dynamic factor. Refer to Fig. 20 for a plot of the posterior distribution of the national factor. Firstly, it is worth noting that the confidence bands around the median of the distribution remain relatively tight throughout the full sample period, which implies that the national factor is estimated with precision. More intuitively, we may say that given the priors and the accuracy of the data, the national factor is unlikely to "look" significantly different from the median of the posterior distribution presented in Fig. 20. Secondly, notice that the path of the median seems to accurately match the 21st century developments in the US banking sector. Starting at around the year 2007 the factor begins to drop,

and reaches a trough a few years later, after which it begins to trend upward quite monotonously until the present time.

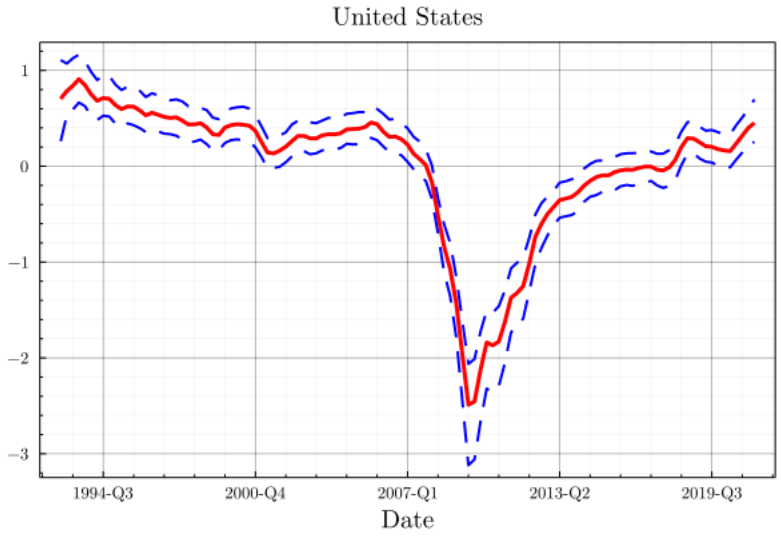

Figure 20. This graph presents a timeplot of the estimated unconditional distribution of the US national latent dynamic factor over the full sample period. The solid red line represents the median of the distribution at each given point in time, while the dashed blue lines represent the 5th and 95th percentiles of the distribution – in other words, the dashed blue lines represent 90% confidence bands around the median.

Furthermore, although the direction of the variation in the latent factors has no clear meaning without knowledge of the directions of the factor loadings, in the given case the interpretation is both clear and consistent since the factor loadings on the national factor with respect to each of the state-average ROE series overwhelmingly have posterior distributions situated convincingly above zero, with *all* of their point estimates and posterior medians being strictly positive. Therefore, a drop in the national factor may directly be interpreted as a nation-wide downward force on the state-average profitability of community banks across the United States. This implies that the behavior of the median of the posterior distribution of the national factor matches the downfall of the US banking sector

during the global financial crisis, and the subsequent post-crisis nation-wide recovery. Furthermore, the relatively small pre-crisis variation of the factor above its mean also reflects uneventfulness of the period and the consistently favorable conditions in the banking sector during the Great Moderation.

Unlike the national factor, interpreting the posterior distributions of the regional factors presented in Fig. B.1 is more challenging due to the difficulty of identifying FDIC's supervisory region-specific historical events and policy changes in the community banking sector. However, we may still make some stylistic observations regarding the behavior of these posterior distributions. For example, a quality shared by all of the regional factors is the presence of either a sharp "uptick" or "downtick" during the crisis period. Once again, the direction of these changes is not very informative – even with the posterior distributions of these factor loadings it is difficult to make a clear observation about the effects of the factors. Unlike those of the national factor, the regional factor loadings seem to be more inconsistent in their directions across states. Another notable property of the posterior distributions is that they are wider than that of the national factor – this implies less precision, likely caused by the smaller set of data used to estimate the regional factors.

4.4.2 Full Sample Variance Decompositions. Variance decomposition plots allows us to gauge the extent to which the national and regional factors drive the variation in each of their corresponding state-average ROE series. In Fig. 21, I present a full-sample variance decomposition for all 50 states, from which we may draw a number of conclusion regarding the significance of the roles played by the latent dynamic factors. Firstly, it is apparent that the national factor is a major contributor to the state-average ROE variation for a considerable

portion of the states. Secondly, many of the state-average ROE series vary quite idiosyncratically. Thirdly, the regional factors seem to play a minor role in contributing to the variation in all of the states' respective series. Lastly, there is noticeable heterogeneity in the roles of the national factor and state-specific idiosyncrasies across the set of all states – in other words, the majority of the variation in some states may confidently be attributed to the national factor, while the variation in others is overwhelmingly idiosyncratic. Therefore, it is difficult to make qualitative statements regarding the magnitude of the role of the national factor – some states co-move with the rest of the country to significantly lesser degree than others across the full sample period.

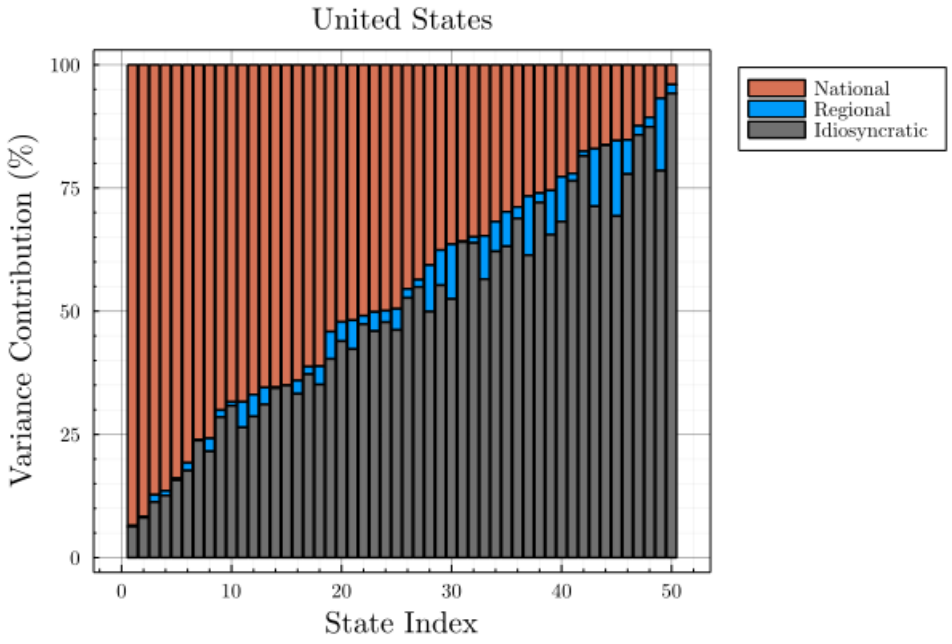

Figure 21. This graph presents the variance decomposition of each of the state-average ROE series in the dataset with respect to the three non-intercept independent variables: (1) the national factor, (2) a corresponding regional factor, and (3) the corresponding state-specific idiosyncratic disturbance process. In other words, the graph shows the percentage of the total variance of each observable series that may be attributed to each of its possible contributing drivers. The state index orders states by their national factor contribution in decreasing order.

A similar graph is presented in Fig. B.2, which groups full-sample variance decompositions of each of the state-average ROE series by region. Such grouping allows us to better observe any potential group-specific heterogeneity in full-sample variance contributions by the national and regional factors, as well as state-specific idiosyncrasies. Note that although the HDFM does not explicitly account for such level-2 (regional) variance decomposition dependencies, it also makes no restrictions that may prevent the emergence of such patterns. I make the following observations about the regionally-grouped full-sample variance decompositions presented in Fig. B.2: Firstly, there seem to be no clear group-based tendencies in the variation contribution of the national factor, although some regions (e.g. Dallas) seem to have lower average national factor contributions, while others (e.g. Chicago) seem to have consistently higher average national factor contributions. Secondly, the NYC region seems to have consistently grater contributions to its state-average ROE series from its respective regional factor than do the rest. Lastly, there exist no apparent regional group-based patterns in the variation contributions of the state-specific idiosyncratic processes. Therefore, I conclude that there are no notable and/or accountable region-specific tendencies in the full-sample variance decompositions across the six FDIC supervisory regions.

4.4.3 Subsample Variance Decompositions. Figs. B.3-B.8 present the pre-, intra-, and post-global financial crisis variance contributions of the Atlanta, Chicago, Dallas, Kansas City, New York City, and San Francisco region factors, respectively, to each of their corresponding state-average community bank ROE series. The contribution of the corresponding regional factors for the majority of the states in the Atlanta, Kansas City, and New York City, and San Francisco regions sees a decrease post-crisis relative to the pre-crisis period. The same cannot

be said for the rest of the regions, however, which seem to have no other noticeable temporal patterns. Another noteworthy insight from these subsample regional variance decompositions is that the New York City factor seems to influence its corresponding states more strongly throughout the full sample period than any of the other regional factors. Furthermore, it is the only region in which the intra-crisis variance contribution of the regional factor is noticeably greater for most of the related states than its pre- and post-crisis contribution. These properties perhaps reflect the notably strong presence and influence of large financial institutions in the region relative to others.

I present the most striking results of this study in Figs. 22 and 23. I begin by accounting for the results shown in Fig. 22, which compares the contribution of the national factor to the variation in all 50 state-average ROE series across the pre-, intra-, and post-global financial crisis subsamples. The first plot in Fig. 22 compares the pre-crisis and crisis periods, with the former lasting until Q4 of 2006, and the latter starting at Q1 of 2007 and lasting until Q4 of 2009. It is clear that the variance contribution of the national factor saw a significant near-uniform increase during the crisis, relative to the pre-crisis period. Only 2 of the 50 states show a decrease in the variance contribution of the national factor. This result implies that state-average community bank ROE series co-moved more strongly at the national level during the approximate time interval associated with the global financial crisis up until that point since the beginning of the sample period. The second plot in Fig. 22 compares the pre-crisis and post-crisis periods, with the latter starting at Q1 of 2010 and lasting until the end of the sample period at Q2 of 2021. Once again, the variance contribution of the national factor seems to have seen a significant near-uniform increase after the crisis, relative

to the pre-crisis period. Only 3 of the 50 states show a decrease in the variance contribution of the national factor after the crisis. This result implies that state-average community bank ROE series co-moved more strongly at the national level since the approximate end of the global financial crisis period than it did before its approximate beginning. In summary, the results presented in Fig. 22 demonstrate that the extent of national comovement among the state-average community bank ROEs has increased nearly uniformly since the start of the global financial crisis.

Next I describe the results shown in Fig. 23, which compares the contribution of the state-specific idiosyncratic disturbance processes to the variation in all 50 of their corresponding state-average ROE series across the pre-, intra-, and post-global financial crisis subsamples. The first plot in Fig. 23 compares the pre-crisis and crisis periods. It is apparent that the variance contribution of the state-specific idiosyncratic processes saw a significant near-uniform decrease during the crisis, relative to the pre-crisis period. Only 4 of the 50 states show an increase in state-specific idiosyncrasy. This result implies that state-average community bank ROE series varied more idiosyncratically during the global financial crisis up until its occurrence since the beginning of the sample period. The second plot in Fig. 23 compares the pre-crisis and post-crisis periods. Once again, the variance contribution of the state-specific idiosyncratic processes saw a significant near-uniform decrease after the end of the crisis, relative to the pre-crisis period. Only 5 of the 50 states show a increase in state-specific idiosyncrasy. This result implies that state-average community bank ROE series varied more idiosyncratically since the end of the global financial crisis period than it did before its beginning. In summary, the results presented in Fig. 23 demonstrate that the extent of state-specific dynamic idiosyncrasy among the state-average community bank ROEs

has decreased nearly uniformly since the start of the global financial crisis. Notice that this result does not deliver the same information as that given by Fig. 22, but rather complements it – the latter does not consider the potential changes in regional comovement, while the former accounts for changes in the sum of national and regional comovement.

In Fig. 20 it is apparent that much of the variation in the national factor is contained in the post-crisis subsample is contained between the very beginning of said subsample and Q1 of 2013. This may leave the reader questioning whether the shown increase in the variance contribution of the national factor is attributable solely to this period of high national factor volatility, after which it returns to its pre-crisis contribution level. However, it is also true that the state-average ROE series generally show the same type of behavior – most of them exhibit a considerable drop during the crisis period, followed by a slow convergence back to their pre-crisis levels. The significant determinant of the source of the post-crisis increase in variance contribution is the *relative* behaviors of the national factor and the state-average ROE series. To dispel such doubts, I repeat the same variance decomposition analysis by defining the post-crisis period as beginning in Q1 of 2013, and present the results in Figs. B.9 and B.10. Although to a lesser extent, this alternative analysis yields the same type of results as the original analysis. This implies that the ratio of post- and pre-crisis average volatility of innovations to the national factor is consistently greater than that of the majority of state-specific disturbance processes. In other words, the increased national comovement of state-average community bank ROEs seems to be a persistent phenomenon.

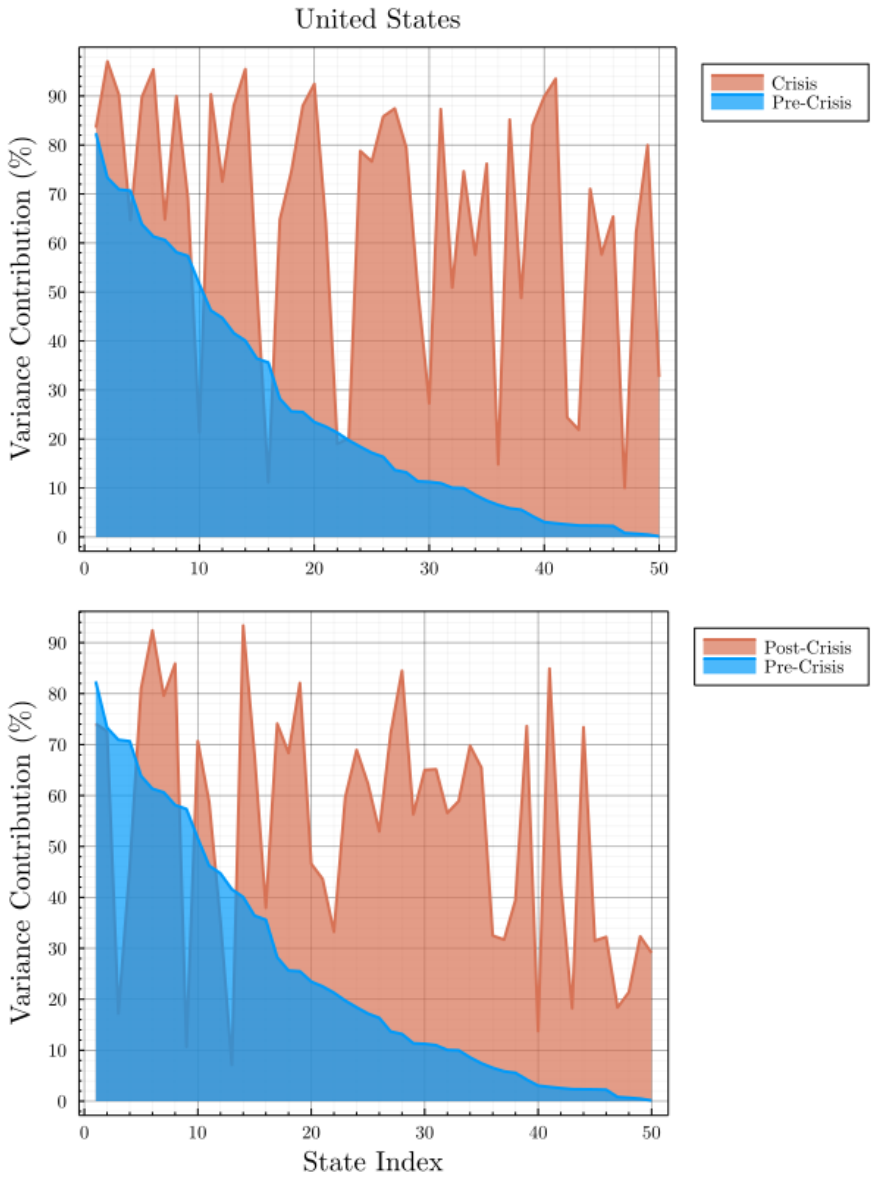

Figure 22. This graph plots the percent variance contribution made by the US national factor toward each of the state-average ROE series in the dataset. The first facet compares the variance contributions made by the national factor during the pre- vs. intra-crisis periods, while the second facet compares that of pre- vs. post-crisis periods. The state index orders states by their pre-crisis national factor contribution in decreasing order.

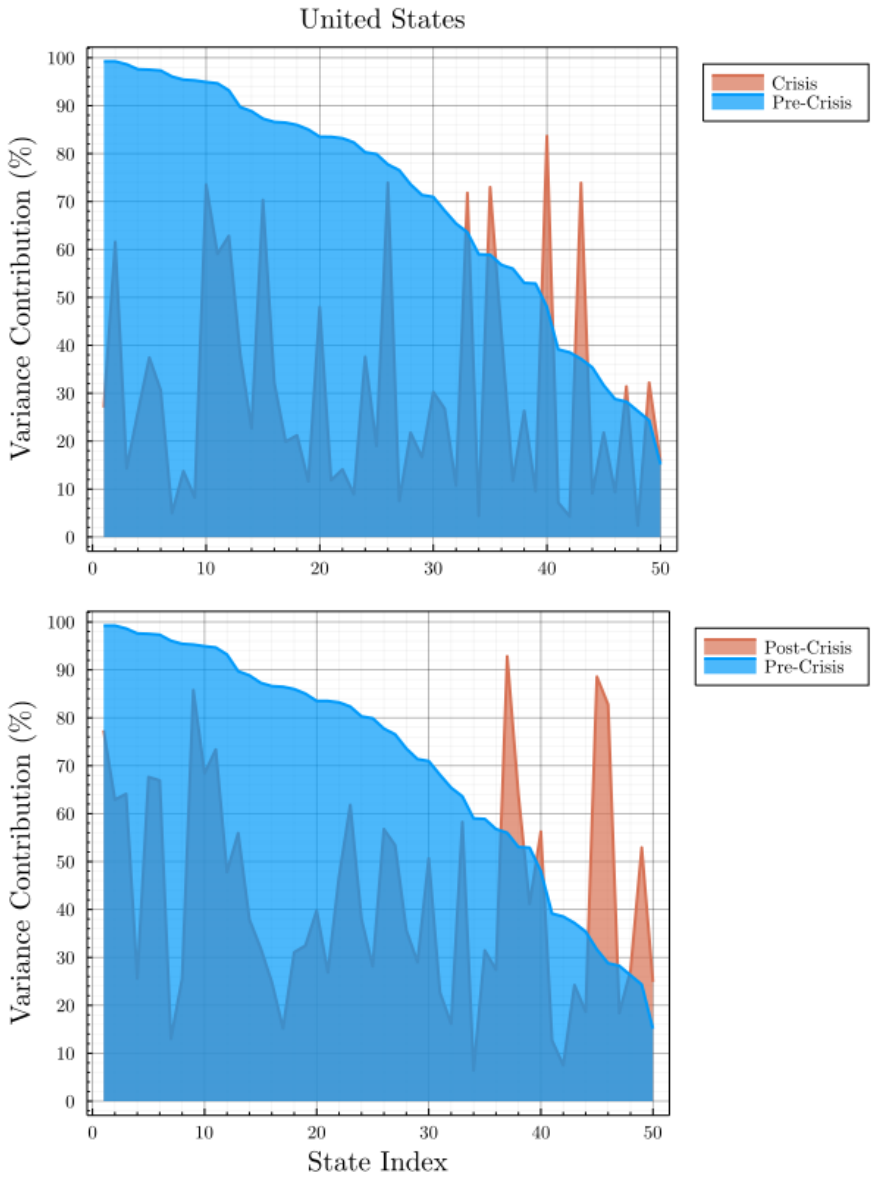

Figure 23. This graph plots the percent variance contribution made toward each of the state-average ROE series in the dataset by their respective idiosyncratic disturbance processes. The first facet compares the variance contributions during the pre- vs. intra-crisis periods, while the second facet compares that of pre- vs. post-crisis periods. The state index orders states by their pre-crisis national factor contribution in decreasing order.

4.5 Conclusion

In this study I estimate a multi-level/hierarchical dynamic factor model using a balanced panel of 50 state-average community bank return-on-equity series to measure national and region-level comovement, as well as state-specific idiosyncrasy, in community bank profitability at the state level. My analysis shows historical evidence of the following: (1) strong country-level dynamic comovement in community bank profitability in the United States; (2) weak regional comovement in community bank profitability; (3) significant state-specific idiosyncratic dynamics to community bank profitability; (4) the extent of national comovement has increased almost uniformly across all states since the global financial crisis, while the extent of state-specific idiosyncrasy has decreased. These empirical findings may be interpreted as showing an increase in the interconnectedness of community banks across the United States since the crisis, which implies an intensification in their exposure to common macrofinancial shocks. The increased interconnectedness implies greater systemic risk, which in turn increases the likelihood of bank contagion, thus leading to greater negative effects on community banks in the United States in the event of another financial crisis. Based on the historical role of the community banking sector as a group of locally-specialized financial intermediates intended to be less sensitive to adverse macroeconomic shocks (as opposed to large banks), these results seem to shed light on an undesirable trajectory of the evolution of the sector.

An alternative interpretation of the increase in national comovement and decrease in the state-specific idiosyncrasy of community bank profitability, as evidenced by Figs. 22 and 23, respectively, is an increase in the underlying country-level volatility of the banking sector rather than its interconnectedness. I offer a

non-rigorous explanation of why this interpretation is likely invalid through a brief discussion in the introductory section of this paper, but I reiterate it here. The underlying volatilities (the magnitudes of structural shocks) of the US banking sector are believed to have increased during the crisis, but reverted back to their normal levels after the end of the crisis (Duffie, 2018; H. Kim, Batten, & Ryu, 2020; Sykes, 2018). Furthermore, it is unlikely that the community banking sector underwent a drastically different experience relative to the rest of the banking sector around this time period. For this reason, the increase in comovement is most probably the result of an increase in the structural interconnectedness of community banks across the country. In future works I plan to further explore the validity of this alternative interpretation more rigorously by performing a similar analysis with time-varying parameters (utilizing the approach developed by Del Negro and Otrok (2011)). This method of analysis will allow me to check whether the increased national comovement is the result of a relative increase in the national factor loadings or an increase in its innovation volatility, where the former confirms my original interpretation and the former is evidence of the alternative interpretation.

The increased interconnectedness of the US community banking sector may be the result of a variety of changes that occurred during and immediately after the global financial crisis. Although this study points toward the emergence of this phenomenon, it does little to identify the mechanisms that led to such a development. One likely possibility is the increased interconnectedness being caused by the convergence in the asset portfolio allocations of community banks in an effort to diversify idiosyncratic risk. I believe that testing this hypothesis is a

fruitful avenue for future studies, among other reasonable hypotheses as to why the community banking sector in the US has become more interconnected.

APPENDIX A

CHAPTER III APPENDIX

A.1 Baseline Model IRFs & PT-IRFs

The baseline model is expressed as

$$X_t = \alpha + \Gamma F_t + \Lambda^N F_t^N + \Lambda^C F_t^C + u_t \,,\; u_t \sim N(0, \Sigma_u) \,,$$

$$Z_t = \gamma + \Psi(L) Z_{t-1} + B v_t \,,\; v_t \sim N(0, I) \,,$$

where X_t is the data matrix containing all bank loan growth rate series and

$$Z_t \equiv \begin{bmatrix} \text{BRW}_t \\ \log(\text{GDP}_t) \\ \log(\text{GDPD}_t) \\ \text{EBP}_t \\ F_t \\ F_t^{\text{N}} \\ F_t^{\text{C}} \end{bmatrix} ,$$

such that BRW, GDP, GDPD, and EBP denote the *cumulative* BRW shock series, gross domestic product, GDP deflator, and excess bond premium, respectively; F^N represents the vector of noncommunity bank lending factors; F^C represents the vector of community bank lending factors; $\Psi(L)$ is a lag matrix polynomial; $v \sim N(0, I)$ is a vector of structural shocks; and B is a recursively identified contemporanous impact matrix.

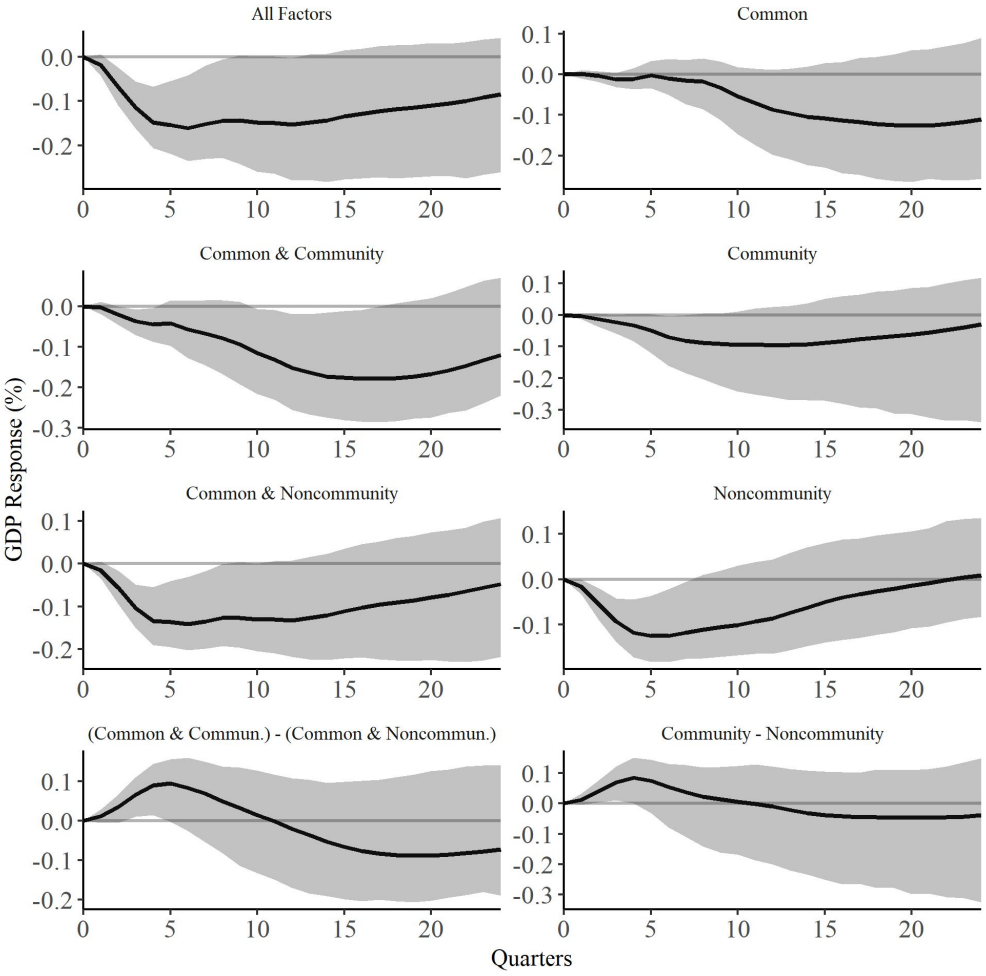

Figure A.1. PT-IRs of GDP in response to a one standard deviation positive (contractionary) monetary policy shock via all relevant combinations of bank lending factors. Solid black lines represent point estimates. Gray bands represent 90% confidence intervals generated using the wild bootstrap with 1,000 runs.

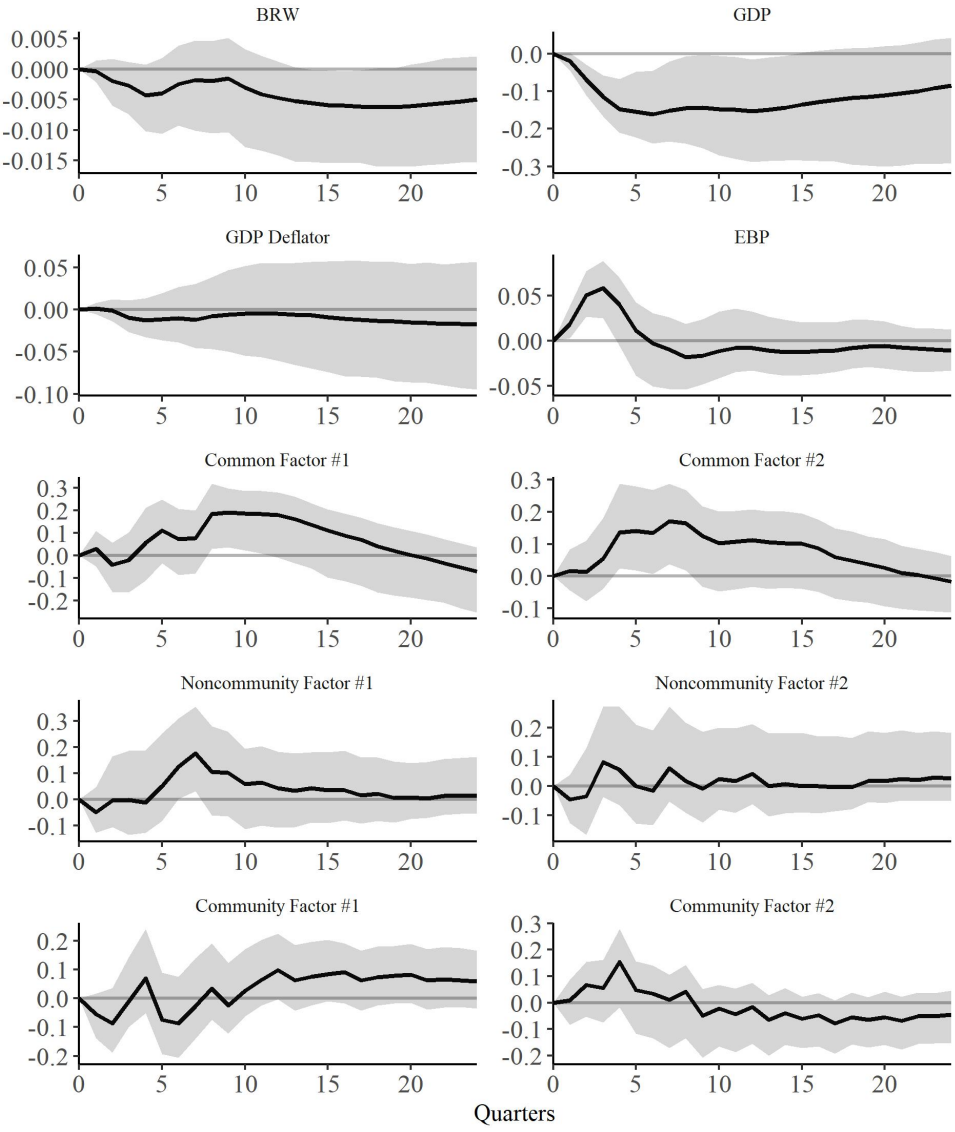

Figure A.2. PT-IRs of all variables in the VAR to a one standard deviation positive (contractionary) monetary policy shock via all bank lending factors. Solid black lines represent point estimates. Gray bands represent 90% confidence intervals generated using the wild bootstrap with 1,000 runs.

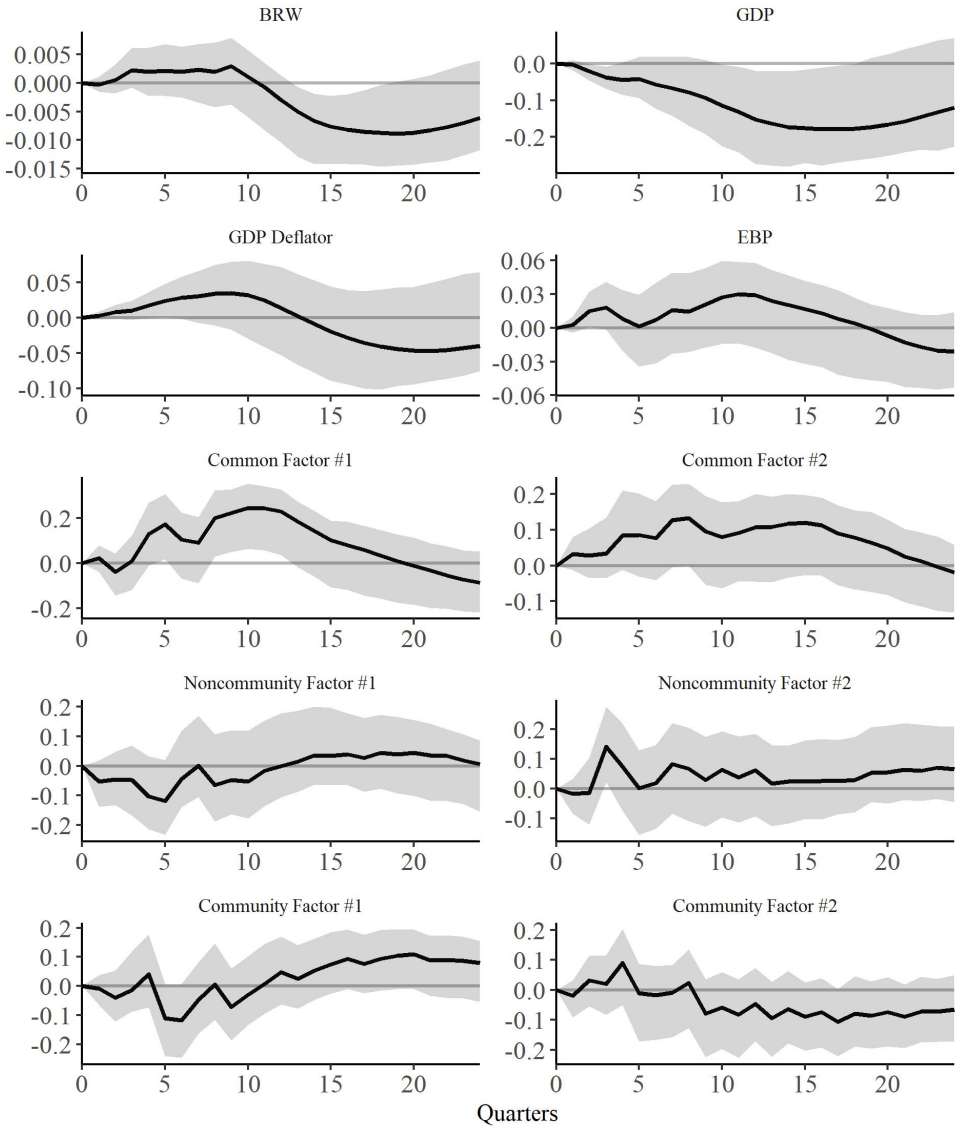

Figure A.3. PT-IRs of all variables in the VAR to a one standard deviation positive (contractionary) monetary policy shock via common and community bank lending factors. Solid black lines represent point estimates. Gray bands represent 90% confidence intervals generated using the wild bootstrap with 1,000 runs.

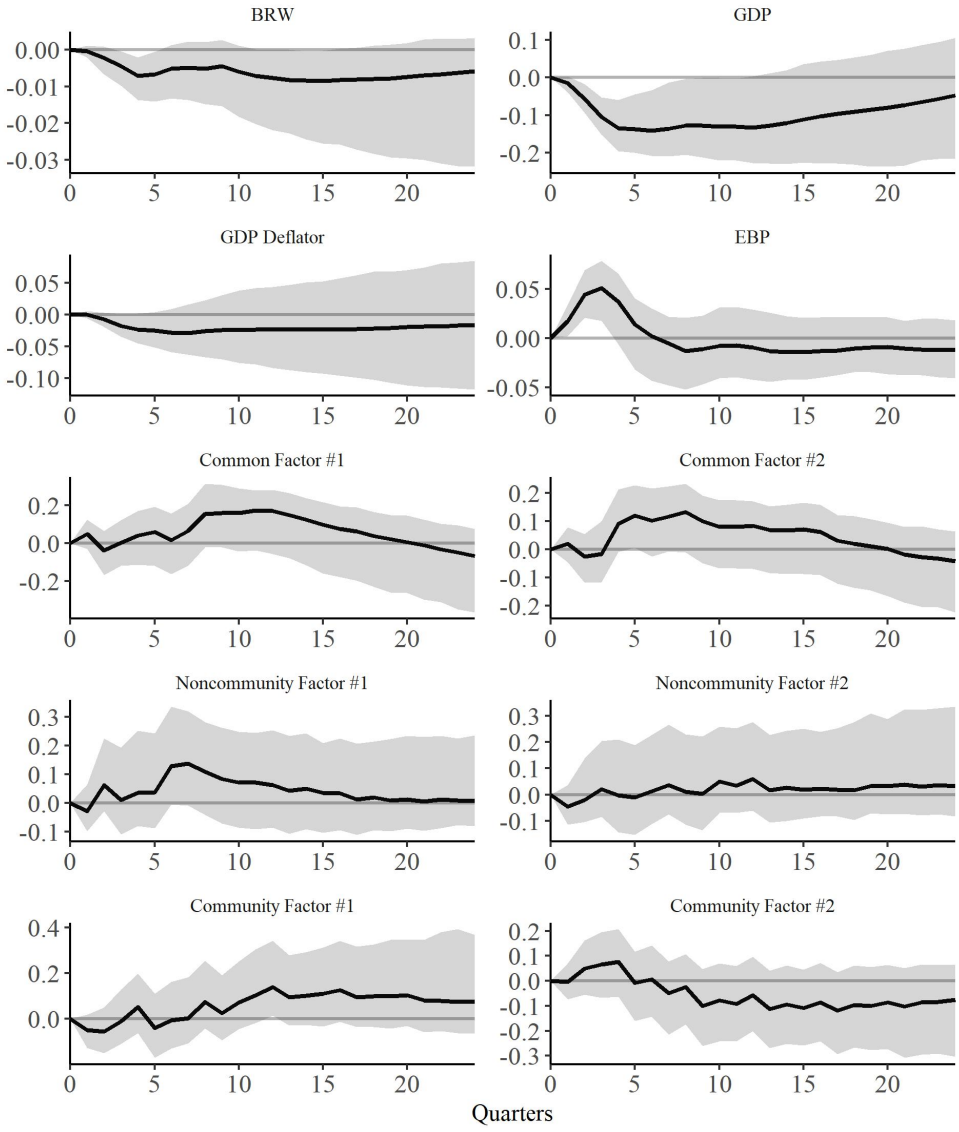

Figure A.4. PT-IRs of all variables in the VAR to a one standard deviation positive (contractionary) monetary policy shock via common and noncommunity bank lending factors. Solid black lines represent point estimates. Gray bands represent 90% confidence intervals generated using the wild bootstrap with 1,000 runs.

A.2 Robustness: Policy Shock Exogeneity Restriction

The alternative model is expressed as

$$X_t = \alpha + \Gamma F_t + \Lambda^N F_t^N + \Lambda^C F_t^C + u_t \,,\; u_t \sim N(0, \Sigma_u) \,,$$

$$Z_t = \gamma + \Psi(L) Z_{t-1} + B v_t \,,\; v_t \sim N(0, I) \,,$$

where X_t is the data matrix containing all bank loan growth rate series and

$$Z_t \equiv \begin{bmatrix} \text{BRW}_t \\ \log(\text{GDP}_t) \\ \log(\text{GDPD}_t) \\ \text{EBP}_t \\ F_t \\ F_t^{\text{N}} \\ F_t^{\text{C}} \end{bmatrix} ,$$

such that BRW, GDP, GDPD, and EBP denote the *raw* (non-cumulative) BRW shock series, gross domestic product, GDP deflator, and excess bond premium, respectively; F^N represents the vector of noncommunity bank lending factors; F^C represents the vector of community bank lending factors; $\Psi(L)$ is a lag matrix polynomial; $v \sim N(0, I)$ is a vector of structural shocks; and B is a recursively identified contemporanous impact matrix.

This alternative specification deviates from the baseline model in that the lag coefficients of all variables in the equation for the monetary policy shock series are restricted to zero.

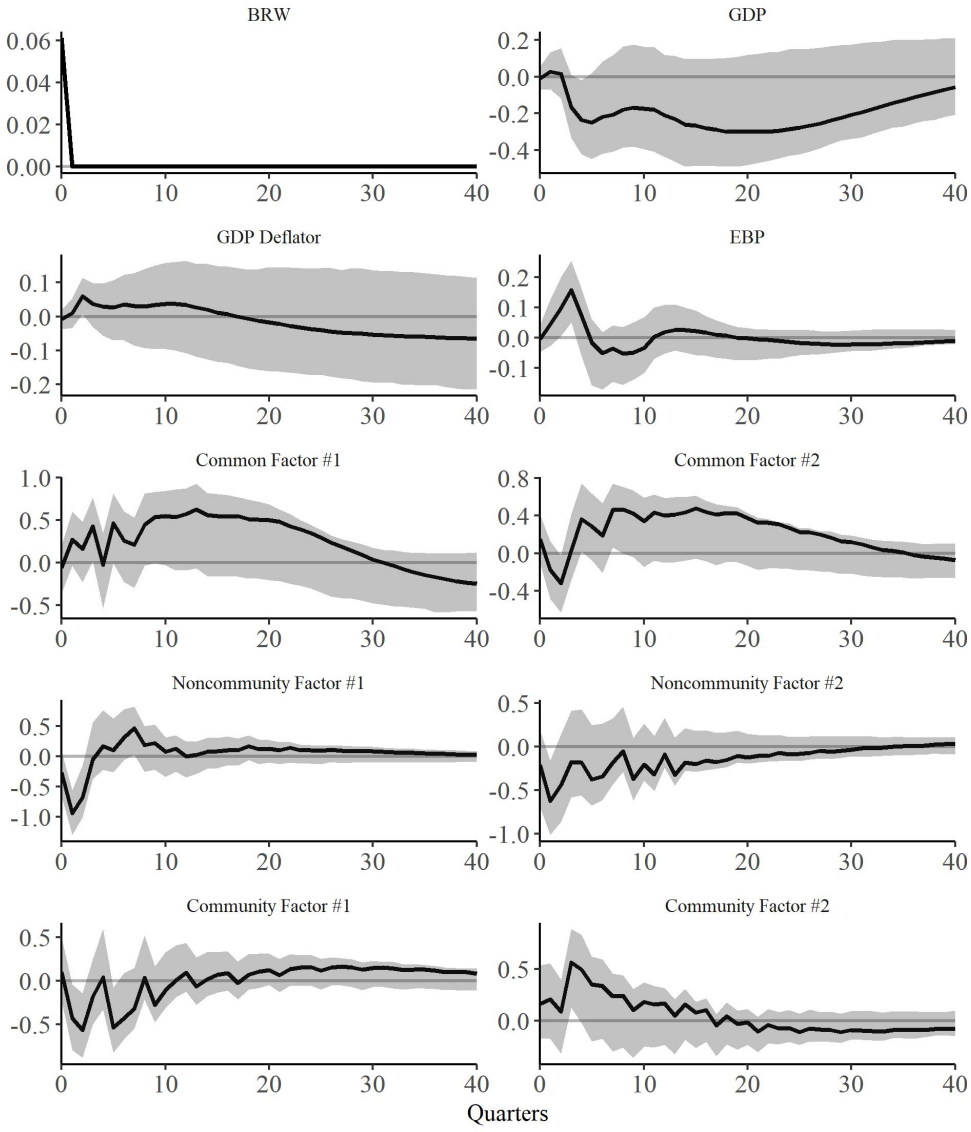

Figure A.5. Impulse responses of all variables in the VAR to a one standard deviation positive (contractionary) monetary policy shock via bank lending. Solid black lines represent point estimates. Gray bands represent 90% confidence intervals generated using the wild bootstrap with 1,000 runs.

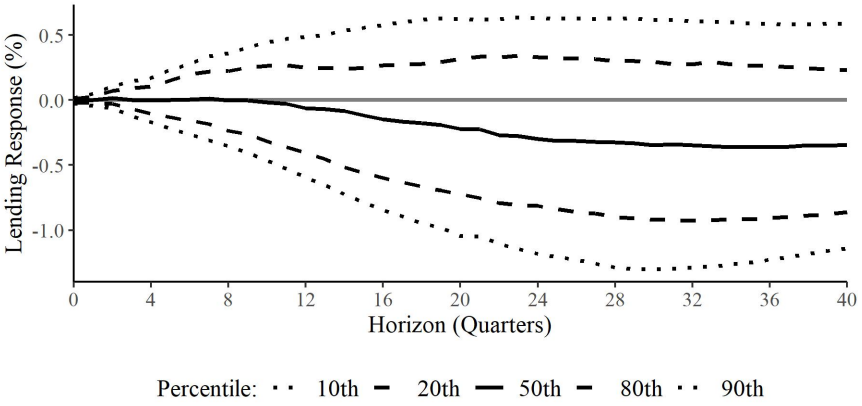

(a) Distribution of community bank lending volume responses

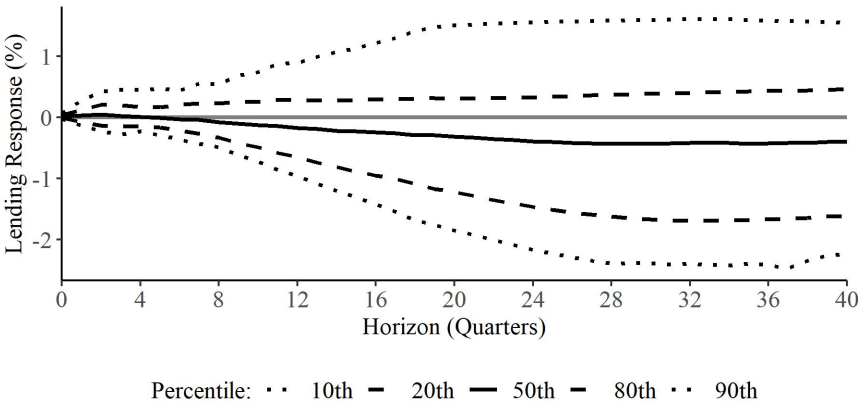

(b) Distribution of noncommunity bank lending volume responses

Figure A.6. Bank-specific responses in loan quantity to a one standard deviation positive (contractionary) monetary policy shock.

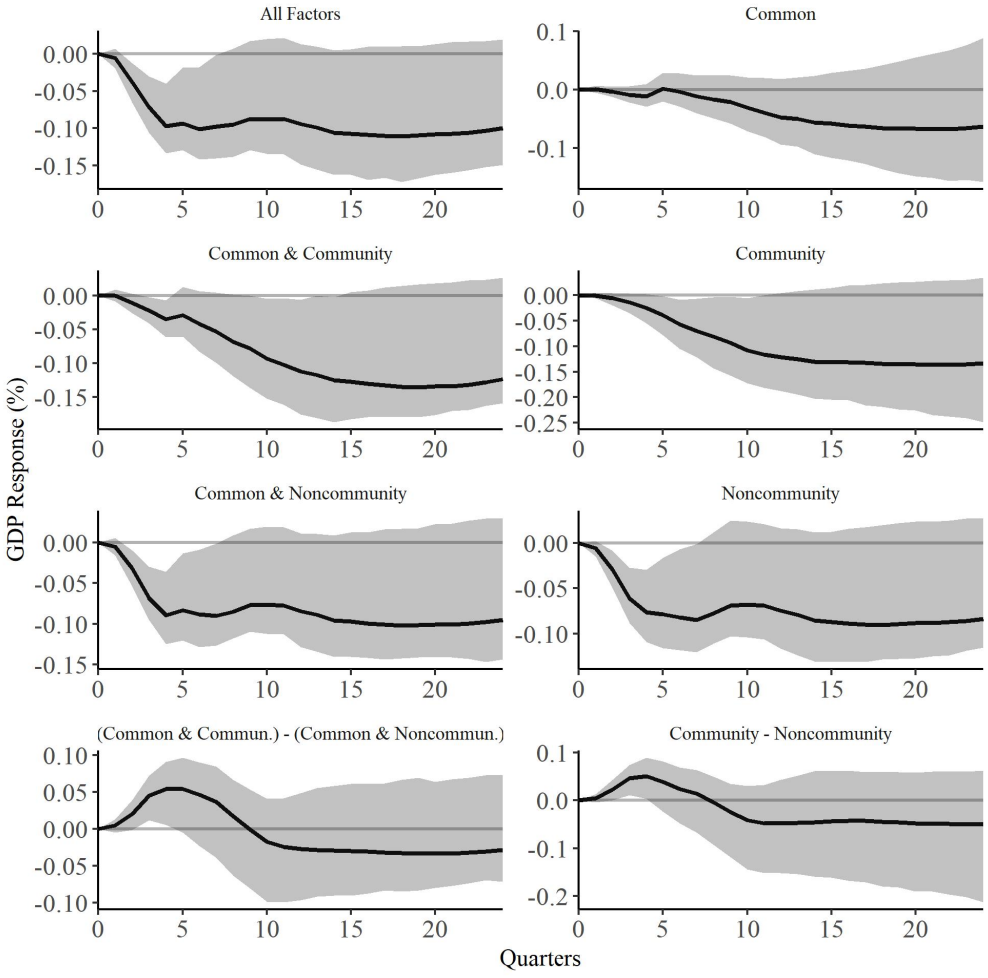

Figure A.7. PT-IRs of IP in response to a one standard deviation positive (contractionary) monetary policy shock via all relevant combinations of bank lending factors. Solid black lines represent point estimates. Gray bands represent 90% confidence intervals generated using the wild bootstrap with 1,000 runs.

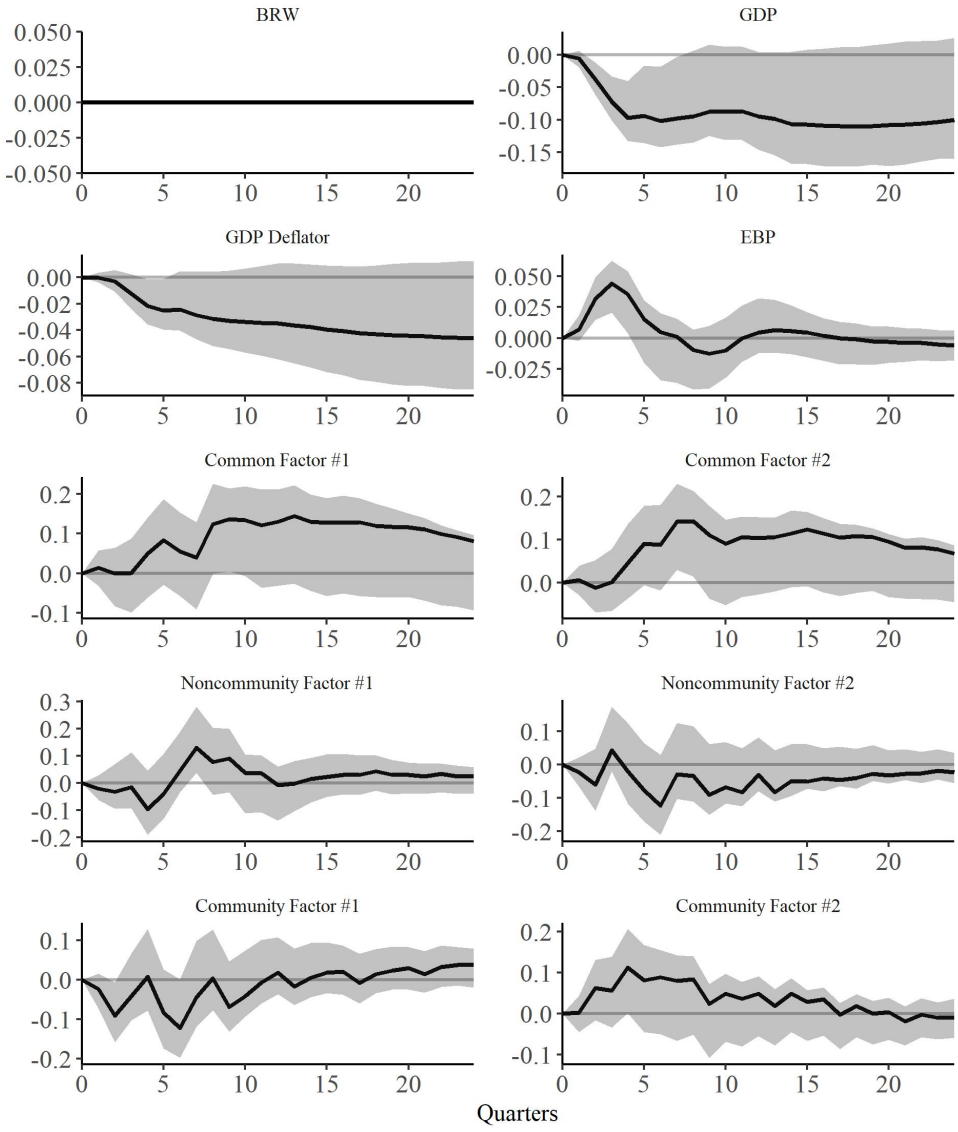

Figure A.8. PT-IRs of all variables in the VAR to a one standard deviation positive (contractionary) monetary policy shock via all bank lending factors. Solid black lines represent point estimates. Gray bands represent 90% confidence intervals generated using the wild bootstrap with 1,000 runs.

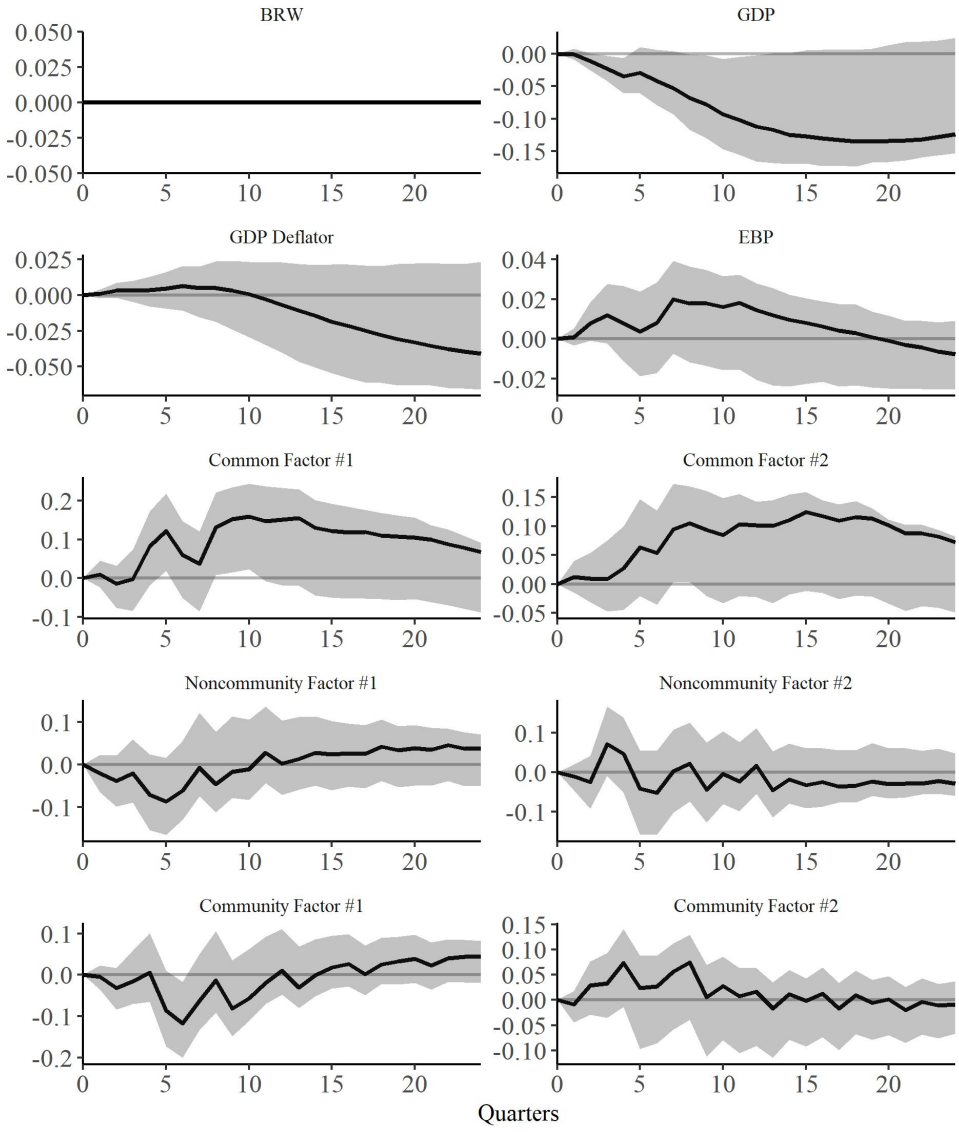

Figure A.9. PT-IRs of all variables in the VAR to a one standard deviation positive (contractionary) monetary policy shock via common and community bank lending factors. Solid black lines represent point estimates. Gray bands represent 90% confidence intervals generated using the wild bootstrap with 1,000 runs.

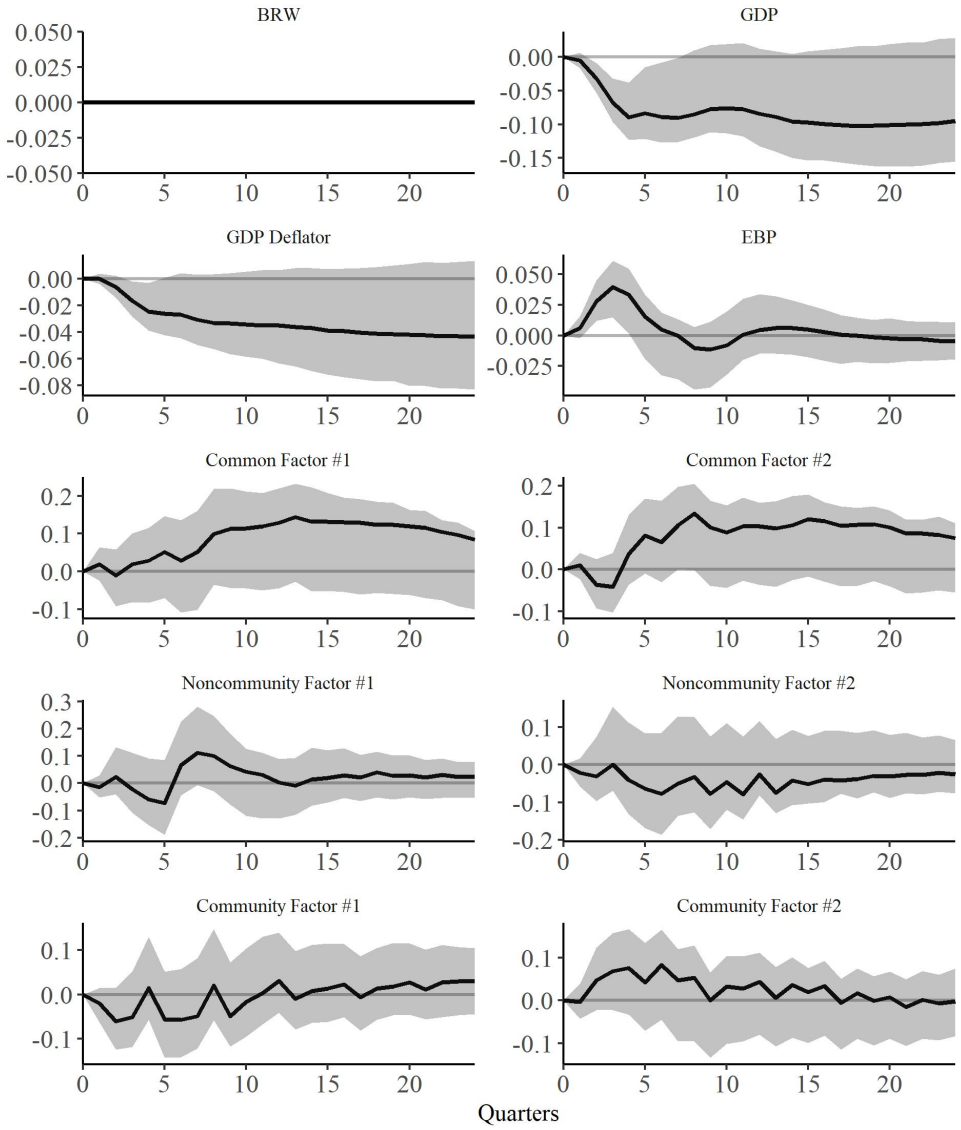

Figure A.10. PT-IRs of all variables in the VAR to a one standard deviation positive (contractionary) monetary policy shock via common and noncommunity bank lending factors. Solid black lines represent point estimates. Gray bands represent 90% confidence intervals generated using the wild bootstrap with 1,000 runs.

A.3 Robustness: Alternative Variables

The alternative model is expressed as

$$X_t = \alpha + \Gamma F_t + \Lambda^N F_t^N + \Lambda^C F_t^C + u_t \,,\; u_t \sim N(0, \Sigma_u) \,,$$

$$Z_t = \gamma + \Psi(L) Z_{t-1} + B v_t \,,\; v_t \sim N(0, I) \,,$$

where X_t is the data matrix containing all bank loan growth rate series and

$$Z_t \equiv \begin{bmatrix} \text{BRW}_t \\ \log(\text{IP}_t) \\ \log(\text{CPI}_t) \\ \text{EBP}_t \\ F_t \\ F_t^{\text{N}} \\ F_t^{\text{C}} \end{bmatrix} ,$$

such that BRW, IP, CPI, and EBP denote the *cumulative* BRW shock series, industrial production, consumer price index, and excess bond premium, respectively; F^N represents the vector of noncommunity bank lending factors; F^C represents the vector of community bank lending factors; $\Psi(L)$ is a lag matrix polynomial; $v \sim N(0, I)$ is a vector of structural shocks; and B is a recursively identified contemporanous impact matrix.

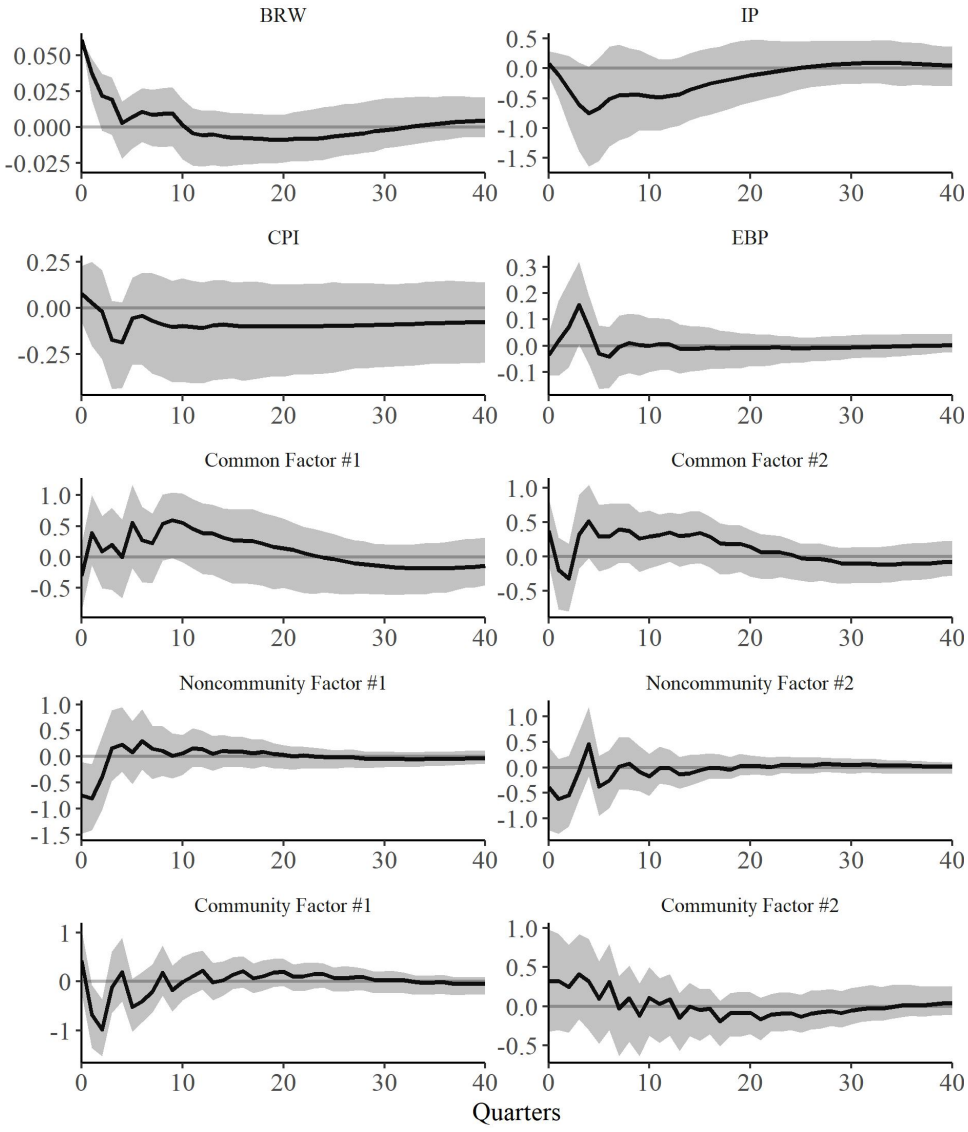

Figure A.11. Impulse responses of all variables in the VAR to a one standard deviation positive (contractionary) monetary policy shock via bank lending. Solid black lines represent point estimates. Gray bands represent 90% confidence intervals generated using the wild bootstrap with 1,000 runs.

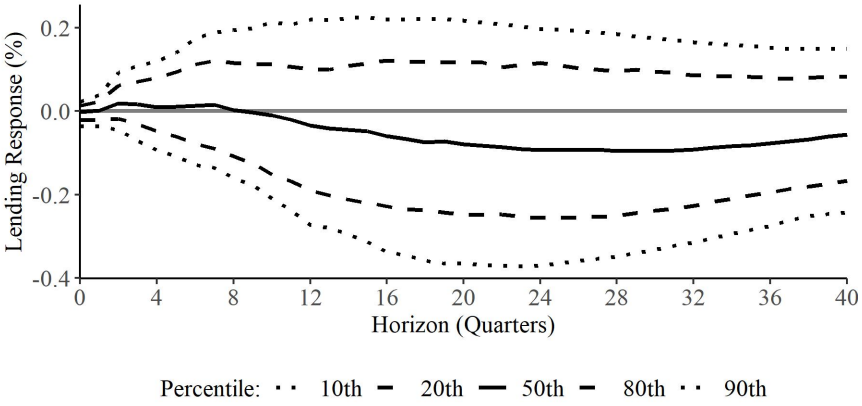

(a) Distribution of community bank lending volume responses

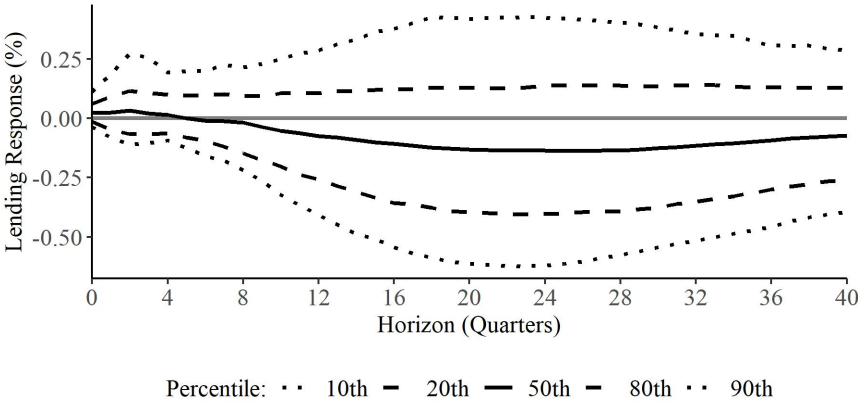

(b) Distribution of noncommunity bank lending volume responses

Figure A.12. Bank-specific responses in loan quantity to a one standard deviation positive (contractionary) monetary policy shock.

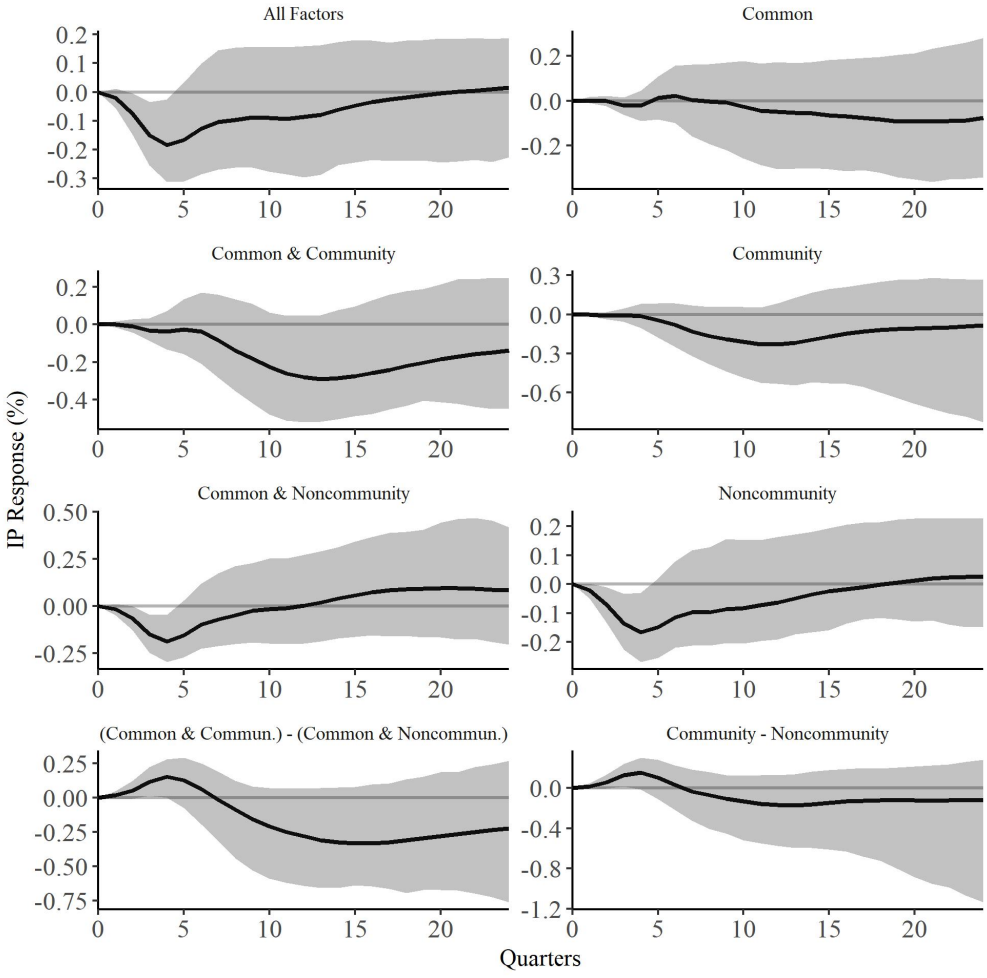

Figure A.13. PT-IRs of IP in response to a one standard deviation positive (contractionary) monetary policy shock via all relevant combinations of bank lending factors. Solid black lines represent point estimates. Gray bands represent 90% confidence intervals generated using the wild bootstrap with 1,000 runs.

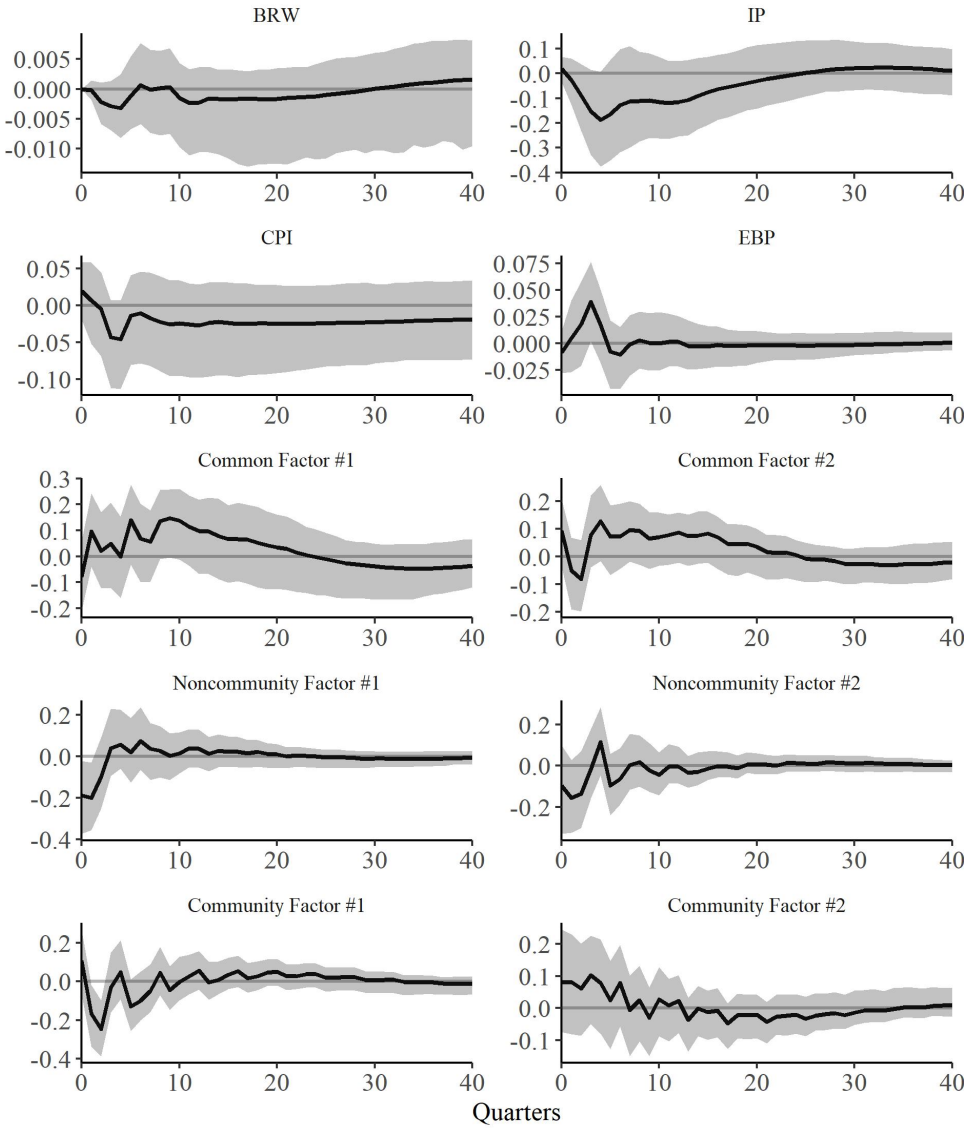

Figure A.14. PT-IRs of all variables in the VAR to a one standard deviation positive (contractionary) monetary policy shock via all bank lending factors. Solid black lines represent point estimates. Gray bands represent 90% confidence intervals generated using the wild bootstrap with 1,000 runs.

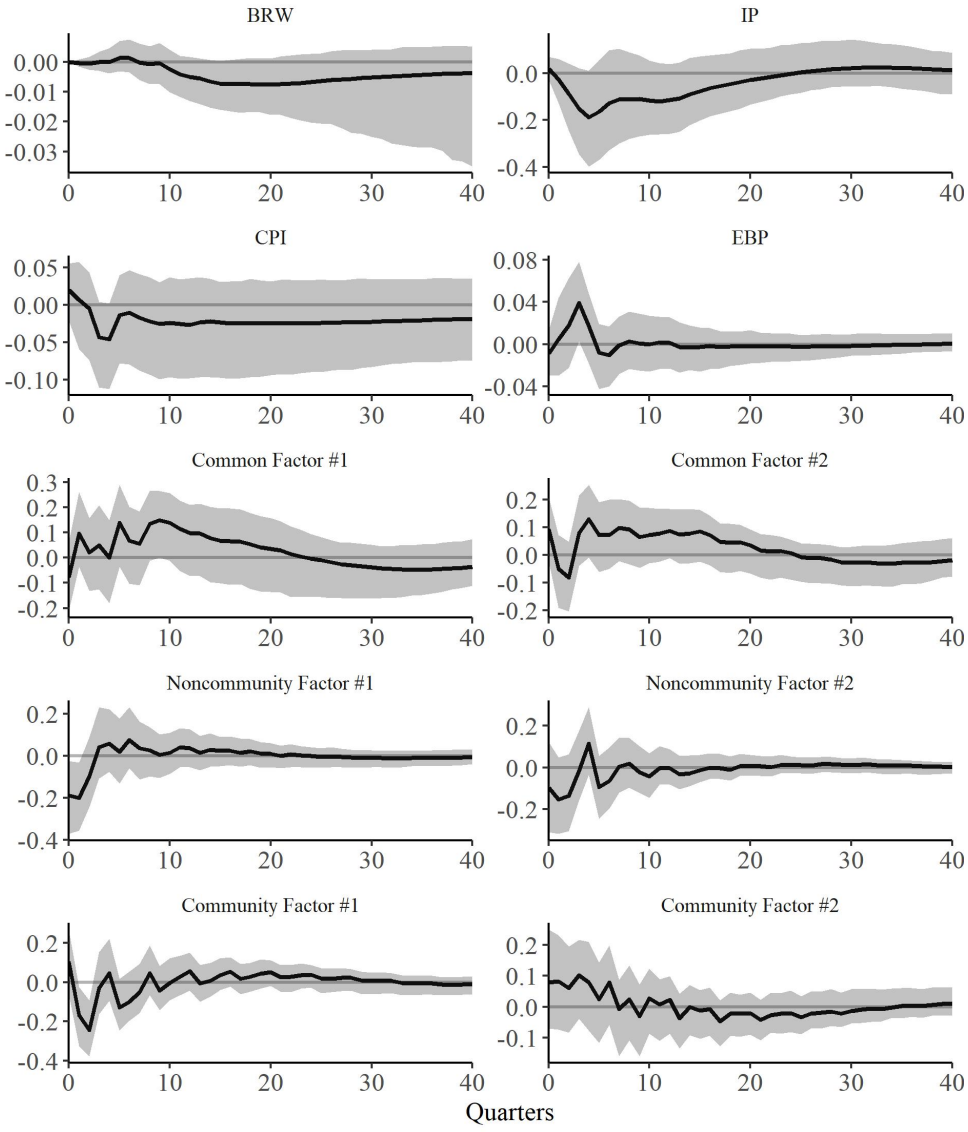

Figure A.15. PT-IRs of all variables in the VAR to a one standard deviation positive (contractionary) monetary policy shock via common and community bank lending factors. Solid black lines represent point estimates. Gray bands represent 90% confidence intervals generated using the wild bootstrap with 1,000 runs.

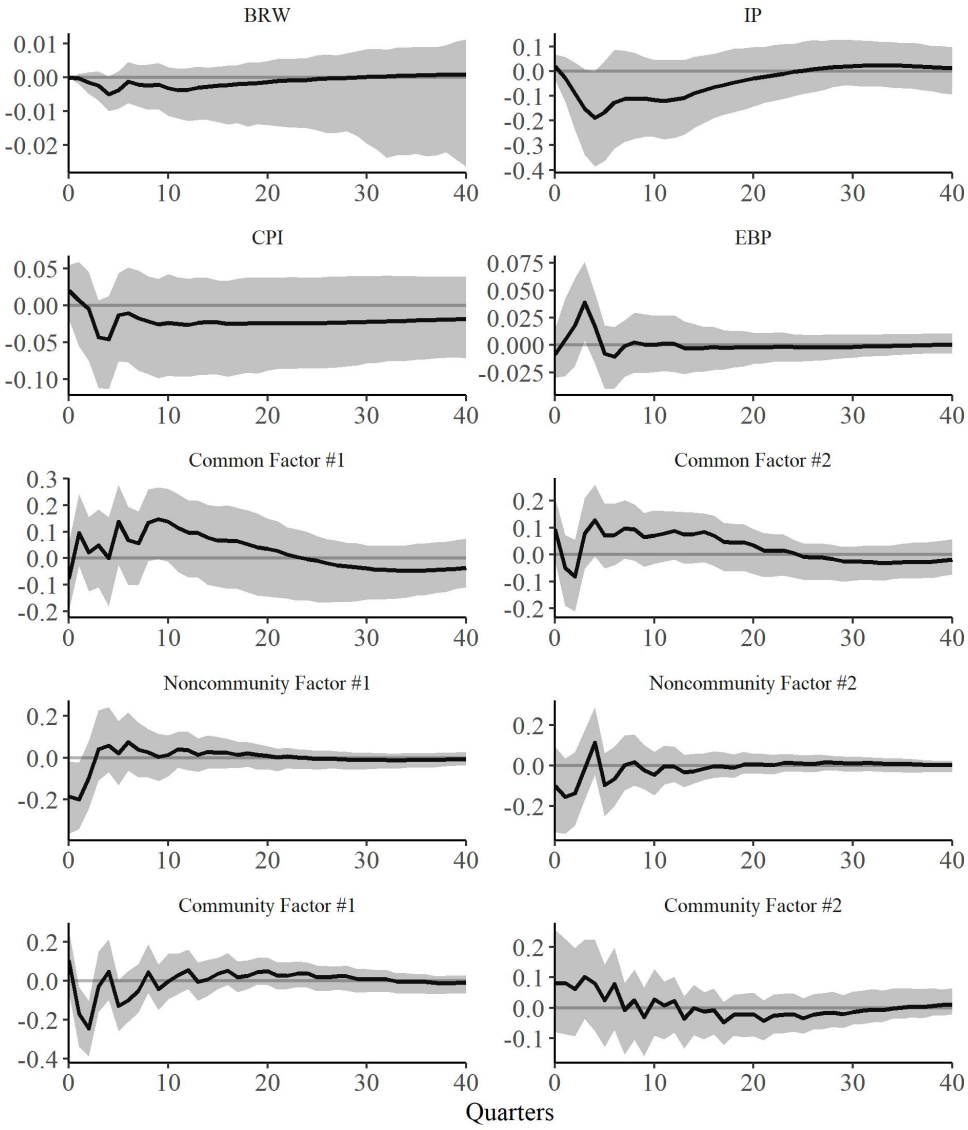

Figure A.16. PT-IRs of all variables in the VAR to a one standard deviation positive (contractionary) monetary policy shock via common and noncommunity bank lending factors. Solid black lines represent point estimates. Gray bands represent 90% confidence intervals generated using the wild bootstrap with 1,000 runs.

A.4 Robustness: Alternative Monetary Policy Shock

The alternative model is expressed as

$$X_t = \alpha + \Gamma F_t + \Lambda^N F_t^N + \Lambda^C F_t^C + u_t \,,\; u_t \sim N(0, \Sigma_u) \,,$$

$$Z_t = \gamma + \Psi(L) Z_{t-1} + B v_t \,,\; v_t \sim N(0, I) \,,$$

where X_t is the data matrix containing all bank loan growth rate series and

$$Z_t \equiv \begin{bmatrix} \text{JK}_t \\ \log(\text{GDP}_t) \\ \log(\text{GDPD}_t) \\ \text{EBP}_t \\ F_t \\ F_t^{\text{N}} \\ F_t^{\text{C}} \end{bmatrix} ,$$

such that JK, GDP, GDPD, and EBP denote the *raw* cumulative JK shock series, gross domestic product, GDP deflator, and excess bond premium, respectively; F^N represents the vector of noncommunity bank lending factors; F^C represents the vector of community bank lending factors; $\Psi(L)$ is a lag matrix polynomial; $v \sim N(0, I)$ is a vector of structural shocks; and B is a recursively identified contemporanous impact matrix.

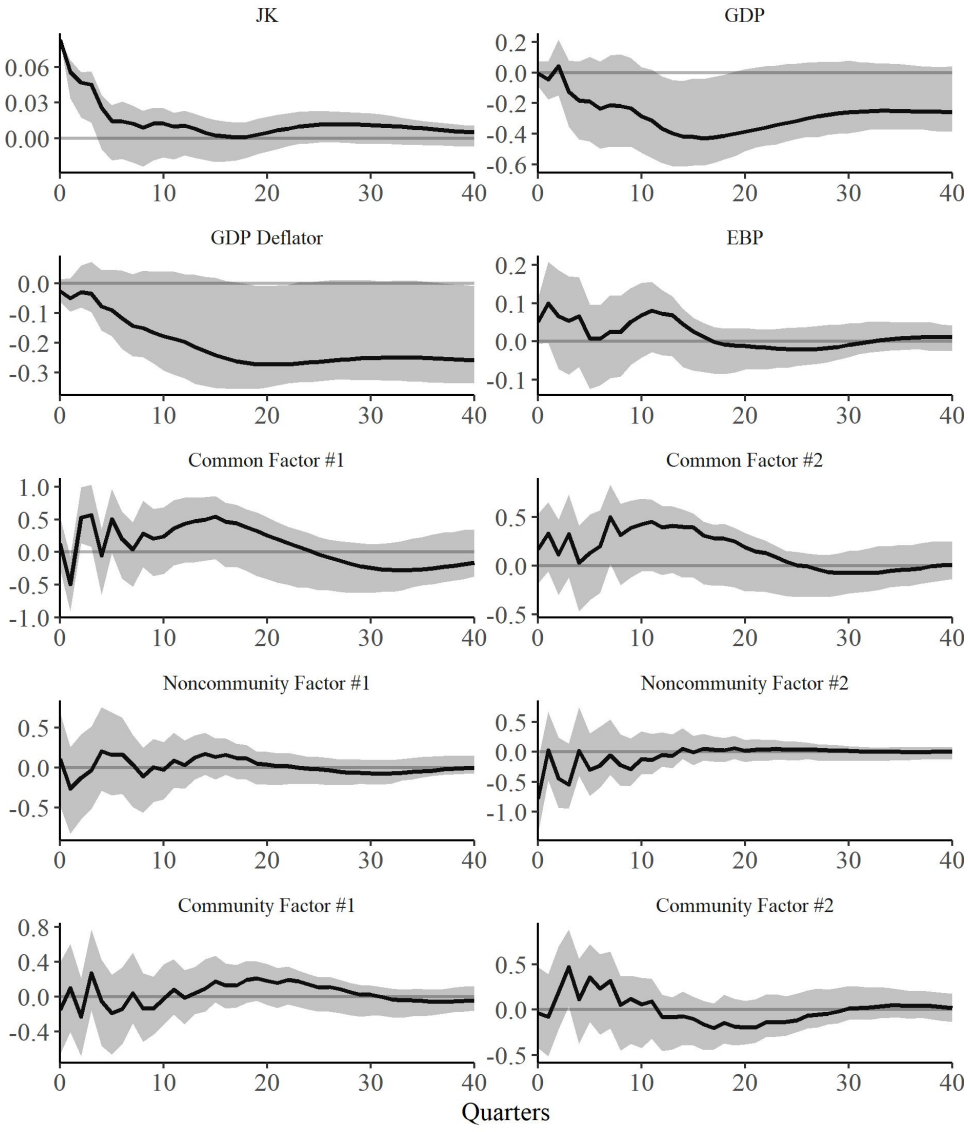

Figure A.17. Impulse responses of all variables in the VAR to a one standard deviation positive (contractionary) monetary policy shock via bank lending. Solid black lines represent point estimates. Gray bands represent 90% confidence intervals generated using the wild bootstrap with 1,000 runs.

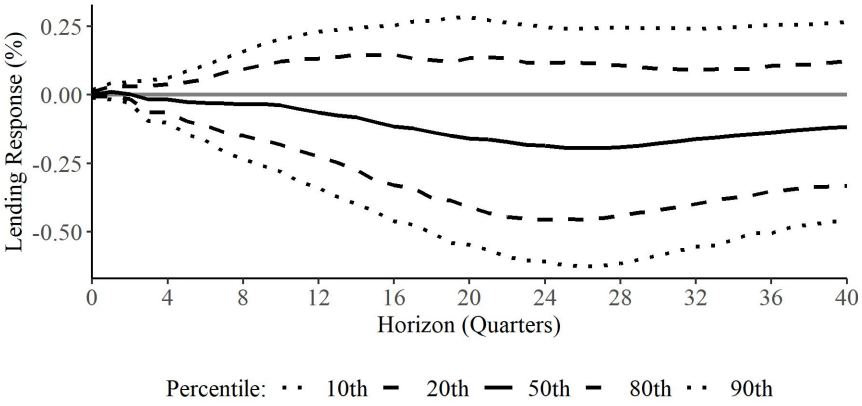

(a) Distribution of community bank lending volume responses

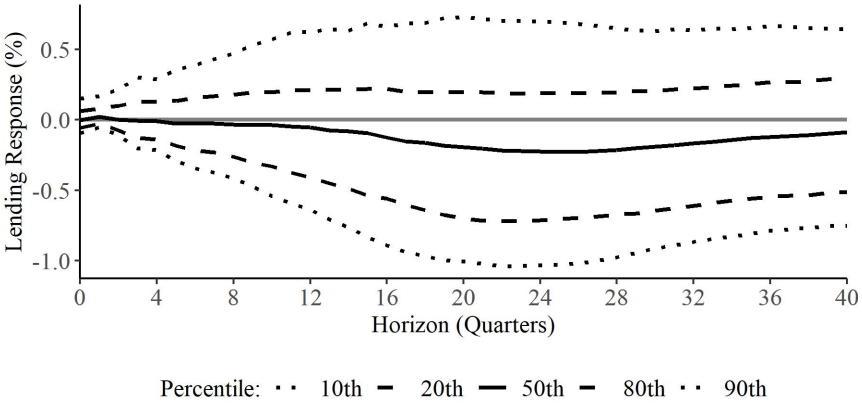

(b) Distribution of noncommunity bank lending volume responses

Figure A.18. Bank-specific responses in loan quantity to a one standard deviation positive (contractionary) monetary policy shock.

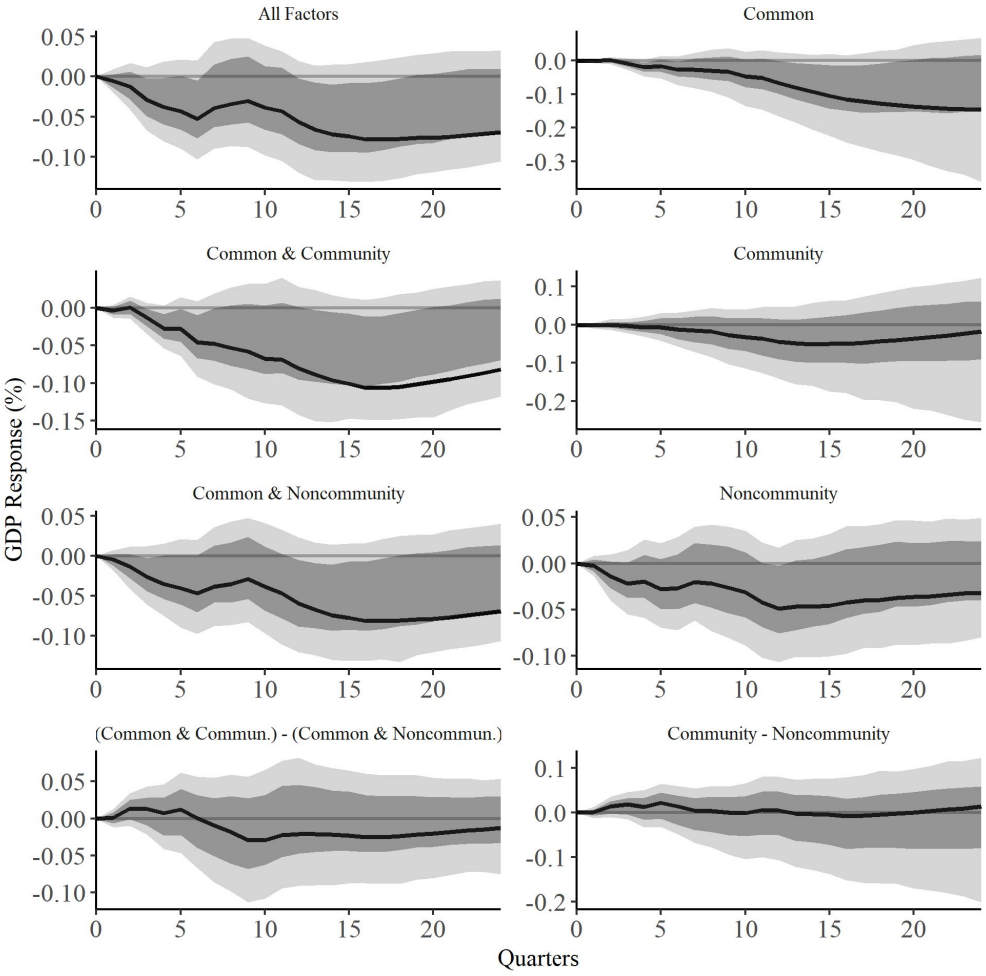

Figure A.19. PT-IRs of IP in response to a one standard deviation positive (contractionary) monetary policy shock via all relevant combinations of bank lending factors. Solid black lines represent point estimates. Gray bands represent 90% confidence intervals generated using the wild bootstrap with 1,000 runs.

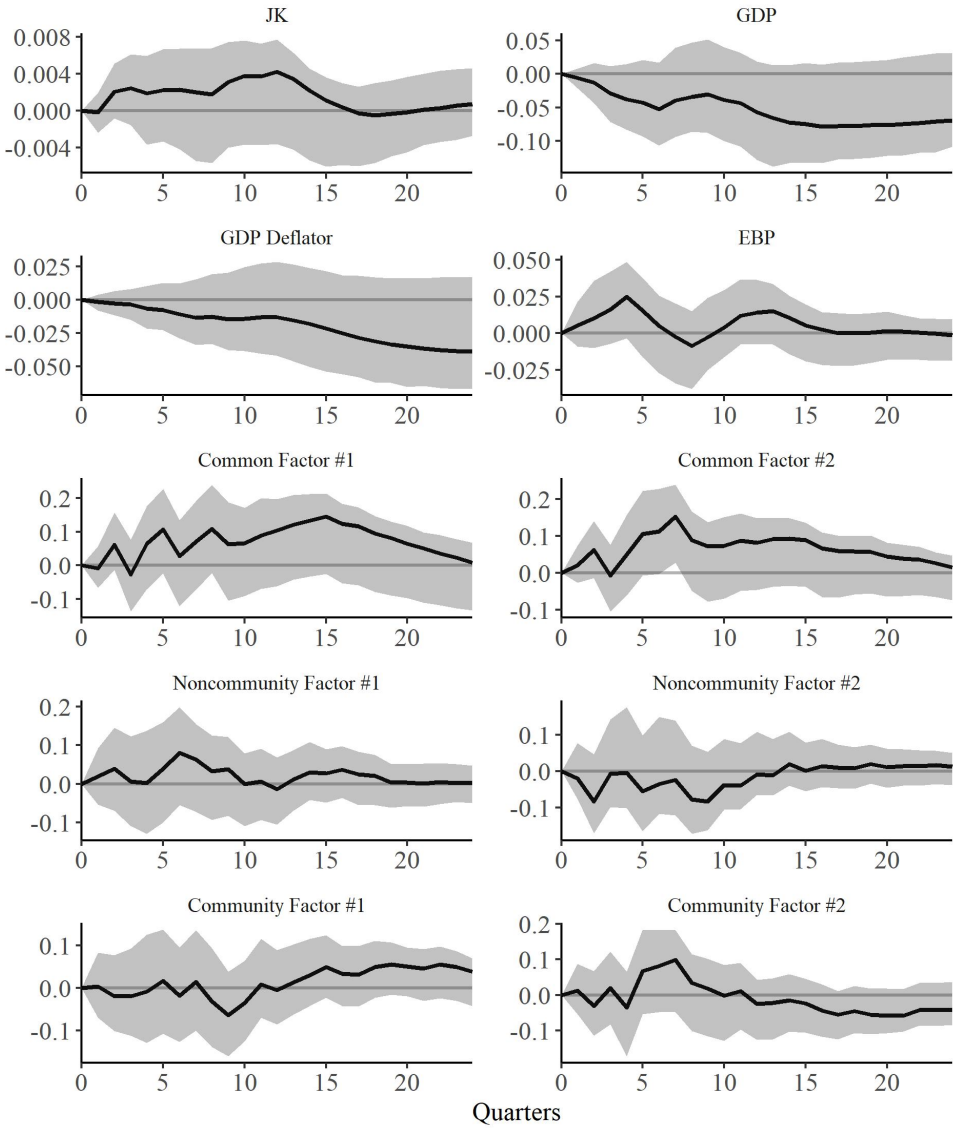

Figure A.20. PT-IRs of all variables in the VAR to a one standard deviation positive (contractionary) monetary policy shock via all bank lending factors. Solid black lines represent point estimates. Gray bands represent 90% confidence intervals generated using the wild bootstrap with 1,000 runs.

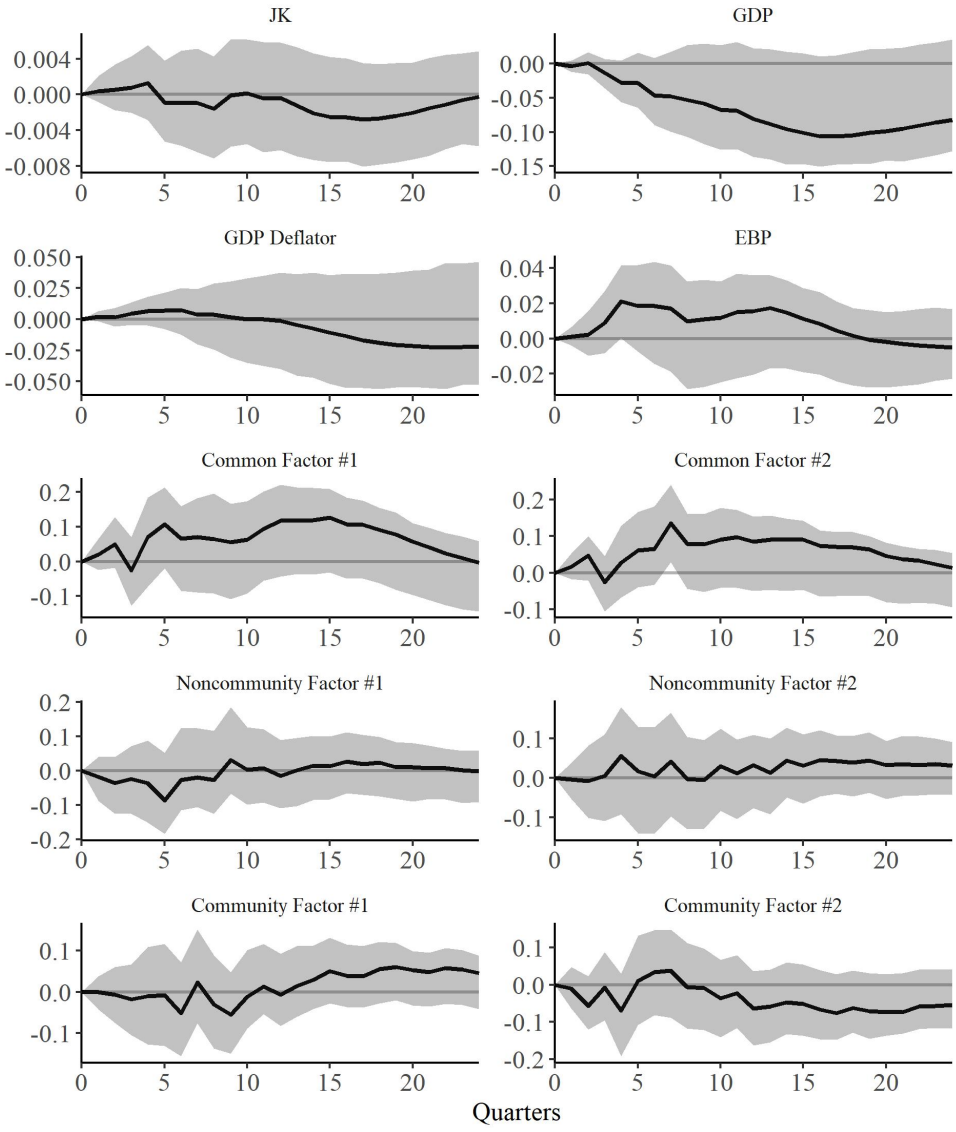

Figure A.21. PT-IRs of all variables in the VAR to a one standard deviation positive (contractionary) monetary policy shock via common and community bank lending factors. Solid black lines represent point estimates. Gray bands represent 90% confidence intervals generated using the wild bootstrap with 1,000 runs.

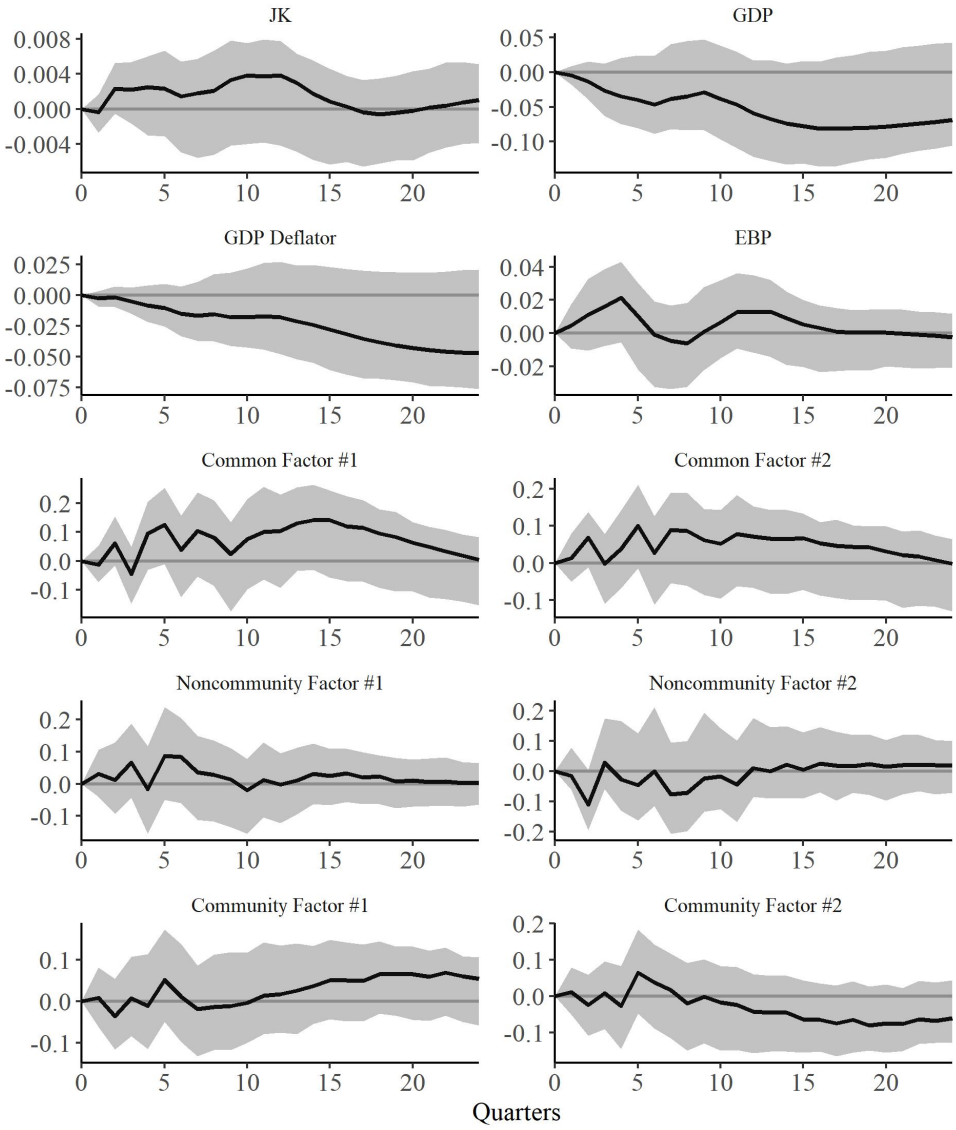

Figure A.22. PT-IRs of all variables in the VAR to a one standard deviation positive (contractionary) monetary policy shock via common and noncommunity bank lending factors. Solid black lines represent point estimates. Gray bands represent 90% confidence intervals generated using the wild bootstrap with 1,000 runs.

APPENDIX B

CHAPTER IV APPENDIX

B.1 Estimation Methodology

The HDFM hyperparameters and latent factors are estimated by iteratively drawing samples from their respective conditional posterior distributions using the following sampling procedure:

1. Initialize the latent factors, $(f^{US})^0$ and $(f^r)^0$ for $r = 1, \ldots, R$, by computing them using the PCA approach discussed in L. Jackson et al. (2015), and initialize hyperparameters by setting all regression coefficients to 0 and innovation variances to 1;

2. Draw β^j from $p(\beta \mid \phi^{j-1}, (\sigma^2)^{j-1}, \text{factors}^{j-1})$ for each i-th observable series;

3. Draw ϕ^j from $p(\phi \mid \beta^j, (\sigma^2)^{j-1}, \text{factors}^{j-1})$ for each i-th observable series;

4. Draw $(\sigma^2)^j$ from $p(\sigma^2 \mid \beta^j, \phi^j, \text{factors}^{j-1})$ for each i-th observable series;

5. Draw $(f^{US})^j$ from $p(f^{US} \mid \beta^j, \phi^j, (\sigma^2)^j, \text{regional factors}^{j-1})$;

6. Draw $(f^r)^j$ for $r = 1, \ldots, R$ from $p(f^{US} \mid \beta^j, \phi^j, (\sigma^2)^j, (f^{US})^j)$.

7. Repeat until $j = J = 5,000$, and discard the first $M = 1,000$ draws to guarantee convergence to a stationary distribution.[1]

[1]The choice of sample size and number of burn-in periods is the result of experimenting with the given data and estimator, rather than being a function of rigorous convergence criteria. I have visually observed the convergence properties of all parameter and factor distributions conditional on a set of different initialization conditions, and in all cases the MCMC seems to converge in under 100 periods. Initializing the factors using PCA seems to be most efficient in achieving convergence. Therefore, the choice of 1000 burn-in periods guarantees convergence in the context of this study.

Once the above Markov Chain Monte Carlo (MCMC) procedure is executed, the outcome will yield large samples of the unconditional posterior distributions of model hyperparameters and latent factors that may then be used for inference. The following subsections describe the specifics of how the above-mentioned posterior conditional distributions are constructed and utilized.

B.1.1 Drawing Hyperparameters. To draw the model hyperparameters, I refer to the methodology developed by Chib (1993), and subsequently applied in a context similar to that of this study by C.-J. Kim and Nelson (1999). We begin by expressing Eqs. (4.1) and (4.4) for any given $i \in \{1, \ldots, I\}$ in stacked form as

$$Y = X\beta + e\,, \tag{B.1}$$

and

$$e = E\phi + u\,, \tag{B.2}$$

respectively, such that the columns of X represent an intercept and observations of relevant latent factors. Let $e^* = Y - X\beta$, so that

$$e^* = E^*\phi + u\,. \tag{B.3}$$

Furthermore, let $Y^* = \Phi(L)\,Y$ and $X^* = \Phi(L)\,X$ be quasi-differenced versions of Y and X with respect to the lag polynomial corresponding to that of the autoregressive disturbance process, so that

$$Y^* = X^*\beta + u\,, \tag{B.4}$$

The constructed objects e^*, E^*, Y^*, and X^* are later used to construct conditional posterior distributions for the model hyperparameters used in the Gibbs sampler.

We begin by constructing the conditional posterior distribution for the β coefficients given the ϕ and σ^2 parameters. The coefficient prior may be expressed

as

$$\beta \,|\, \phi, \sigma^2 \sim N(b_0, A_0)\,, \tag{B.5}$$

where b_0 and A_0 are observed moment priors. It follows that the coefficient posterior may be expressed in the following manner:

$$\beta \,|\, \phi, \sigma^2, Y \sim N(b_1, A_1)\,, \tag{B.6}$$

where

$$b_1 = \left(A_0^{-1} + \sigma^{-2} X^{*'} X^*\right)^{-1} \left(A_0^{-1} b_0 + \sigma^{-2} X^{*'} Y^*\right)\,, \tag{B.7}$$

and

$$A_1 = \left(A_0^{-1} + \sigma^{-2} X^{*'} X^*\right)^{-1}\,. \tag{B.8}$$

At each iteration of the sampler, a new β is drawn for each series $i = 1, \ldots, I$ conditional on previous draws of ϕ and σ^2. If the direction restrictions on the national and regional factor loadings do not satisfy the restrictions imposed on the model (described in Section 3.2), then a given draw is discarded and a new one draw is made. If the direction restrictions are persistently violated, then after 100 such unsatisfactory draws the corresponding factor observations are mirrored around 0, and the above process is repeated until all restrictions are satisfied.

Next, we construct the conditional posterior distribution for ϕ given observations of the β and σ^2 parameters. The idiosyncratic disturbance autoregressive coefficient prior may be expressed as

$$\phi \,|\, \beta, \sigma^2 \sim N(c_0, B_0)\,, \tag{B.9}$$

where c_0 and B_0 represent our prior beliefs about the first two moments of ϕ. Therefore, the conditional posterior of σ^2 may be expressed in the following

manner:

$$\phi \,|\, \beta, \sigma^2, Y \sim N(c_1, B_1)_{I[s(\phi)]}\,, \tag{B.10}$$

where

$$c_1 = \left(B_0^{-1} + \sigma^{-2} E^{*'} E^*\right)^{-1} \left(B_0^{-1} c_0 + \sigma^{-2} E^{*'} e^*\right)\,, \tag{B.11}$$

and

$$B_1 = \left(B_0^{-1} + \sigma^{-2} E^{*'} E^*\right)^{-1}\,. \tag{B.12}$$

The indicator function $I[s(\phi)]$ keeps only those draws of ϕ that represent covariance-stationary autoregressive processes (roots of the lag polynomial $\phi(L)$ are outside of the unit circle). In the computational implementation of the estimator, ϕ is drawn repeatedly at each iteration of the sampler until desired stationary is achieved.

Lastly, I construct the conditional posterior distribution for σ^2 given observations of the β and ϕ parameters. The innovation variance prior may be expressed as

$$\sigma^2 \,|\, \beta \sim IG\left(\frac{\upsilon_0}{2}, \frac{\delta_0}{2}\right)\,, \tag{B.13}$$

where υ_0 and δ_0 are observed and represent our beliefs about the distribution of σ^2. The innovation variance conditional posterior distribution corresponding to any given observed series $i \in \{1, \ldots, I\}$ may be expressed in the following manner:

$$\sigma^2 \,|\, \beta, Y \sim IG\left(\frac{\upsilon_1}{2}, \frac{\delta_1}{2}\right)\,, \tag{B.14}$$

where

$$\upsilon_1 = \upsilon_0 + T \tag{B.15}$$

and

$$\delta_1 = \delta_0 + (Y^* - X^*\beta)'(Y^* - X^*\beta) \ . \tag{B.16}$$

Since there are no restrictions on the innovation variance parameters, a draw from the above posterior distribution is accepted by default.

B.1.2 Drawing Level-1 (National) Factor. The estimation of the national factor must be based on the variation in the data without the influence of the regional factors. For this reason, we define z_{it} as being the variation in the i-th observable series attributable only to the national factor and the idiosyncratic disturbance term:

$$z_{it} \equiv y_{it} - \beta_{2i} f_t^{r_i} \ . \tag{B.17}$$

We are able to partial out the variation in $f_t^{r_i}$ in z_{it} due to the fact that we are conditioning on the regional factors and model hyperparameters to generate the posterior conditional distribution of the national factor, and may therefore treat all else as observed. Once $z_t = (z_{1t}, \ldots, z_{It})$ is computed, we may apply the Kalman filter to it to generate the posterior conditional distribution described by

$$\beta_T \,|\, \widetilde{z}_T \sim N\left(\beta_{T\,|\,T}\,,\, P_{T\,|\,T}\right) \tag{B.18}$$

and

$$\beta_t \,|\, \widetilde{z}_t\,,\, \beta_{t+1} \sim N\left(\beta_{t\,|\,t,\beta_{t+1}}\,,\, P_{t\,|\,t,\beta_{t+1}}\right) \ , \tag{B.19}$$

for $t = T-1, T-2, \ldots, 1$, where

$$\beta_{T\,|\,T} = E(\beta_T \,|\, \widetilde{z}_T)\,, \tag{B.20}$$

$$P_{T\,|\,T} = Cov(\beta_T \,|\, \widetilde{z}_T)\,, \tag{B.21}$$

$$\beta_{t\,|\,t,\beta_{t+1}} = E(\beta_t \,|\, \widetilde{z}_t, \beta_{t+1} = E(\beta_t \,|\, \beta_{t\,|\,t}, \beta_{t+1})\,, \tag{B.22}$$

$$P_{t\,|\,t,\beta_{t+1}} = Cov(\beta_t \,|\, \widetilde{z}_t, \beta_{t+1}) = Cov(\beta_t \,|\, \beta_{t\,|\,t}, \beta_{t+1})\,, \tag{B.23}$$

such that $\tilde{z}_t$ represents the history of z up until period t. Note that the state-space formulation of the model used for the Kalman filter here is a more parsimonious one than, and nested in, the specification given in Section 3.2. More specifically, the given state-space formulation used in the generation of the conditional posterior distribution for the national factor need not contain any regional factor-related components due to the regional factors being treated as observed.

B.1.3 Drawing Level-2 (Regional) Factors. The regional factors are treated similarly to the national factor. First, we must partial out the variation attributable to the national factor from all of the series corresponding to a given regional factor. Then, we express the subset of the HDFM specifying the random DGP determining the variation in the given series in state-space form, such that all components related to all other series and the national factor are excluded due to being treated as observed. Lastly, we input the Kalman filter-generated objects into the same posterior distribution specified in Section 4.2 in order to make draws of each of the regional factors.

B.2 Figures

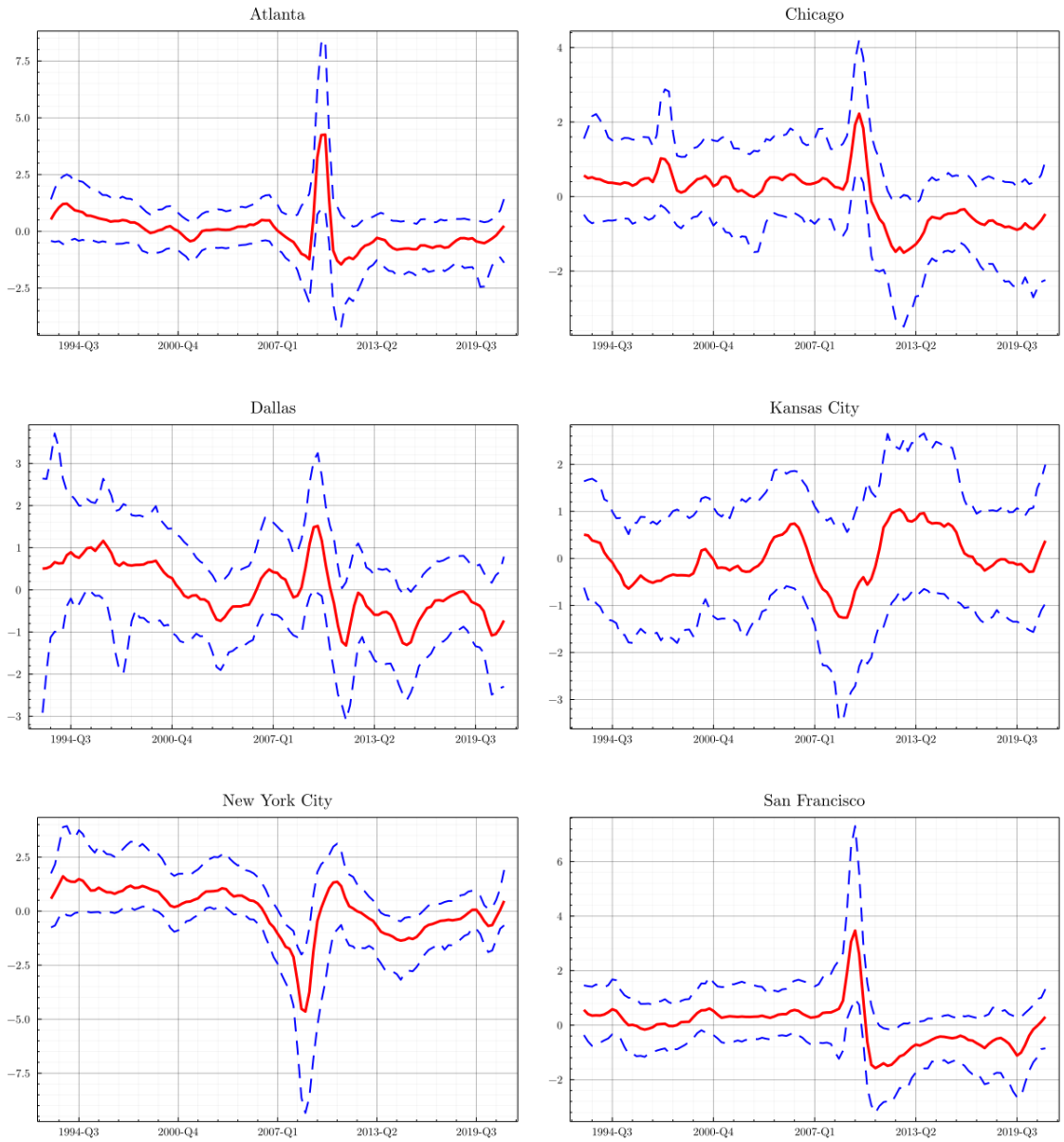

Figure B.1. Each of the facets in the given graph presents a timeplot of the estimated unconditional distribution of the corresponding regional latent dynamic factor over the full sample period. The solid red line represents the median of the distribution at each given point in time, while the dashed blue lines represent the 5th and 95th percentiles of the distribution – in other words, the dashed blue lines represent 90% confidence bands around the median.

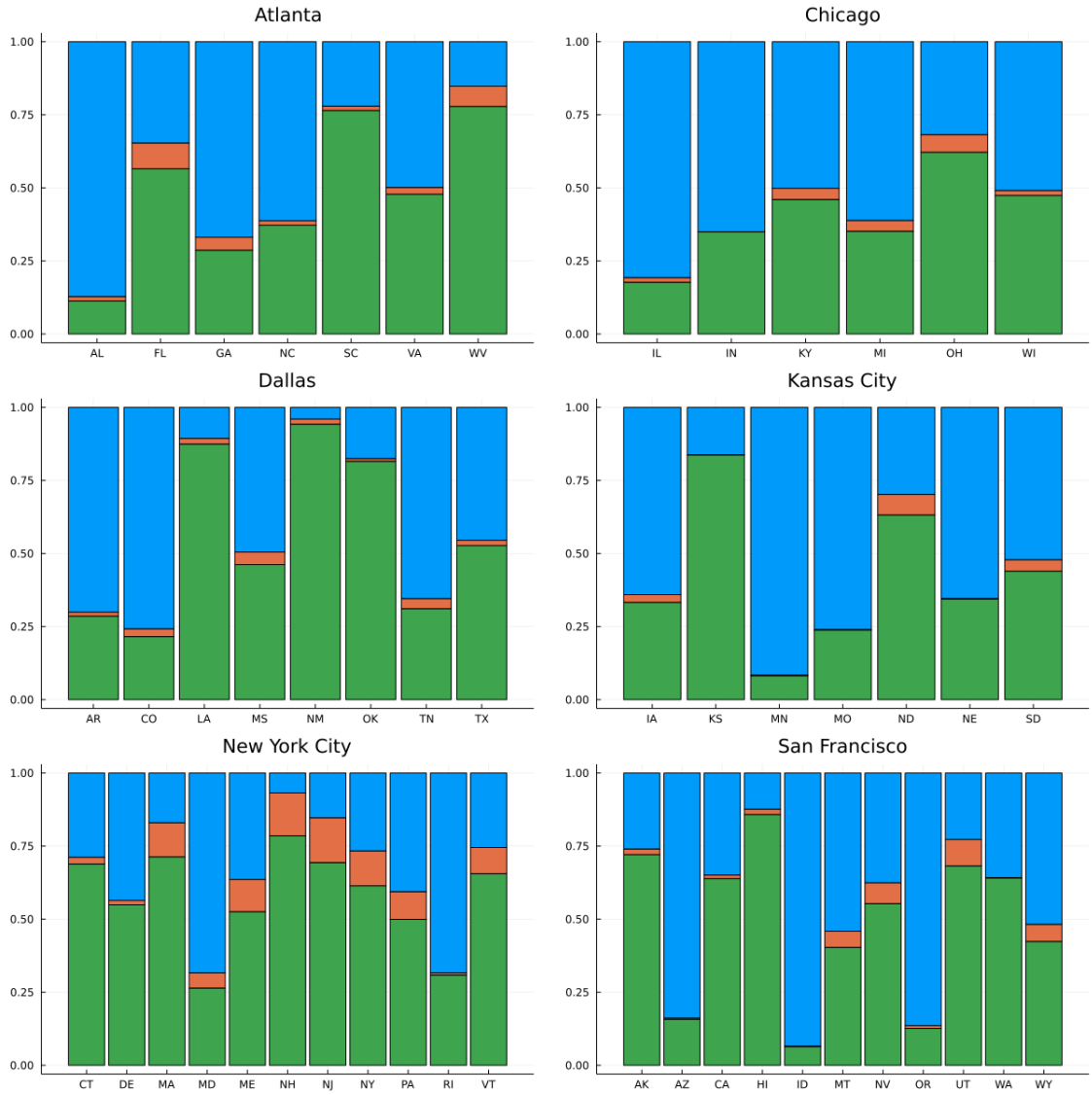

Figure B.2. Each of the facets in the given graph presents the variance decomposition of each of the state-average ROE series for a given region with respect to the three non-intercept independent variables: (1) the national factor (in blue), (2) a corresponding regional factor (in orange), and (3) the corresponding state-specific idiosyncratic disturbance process (in green). In other words, the graph shows the percentage of the total variance of each observable series in each region that may be attributed to each of its possible contributing drivers.

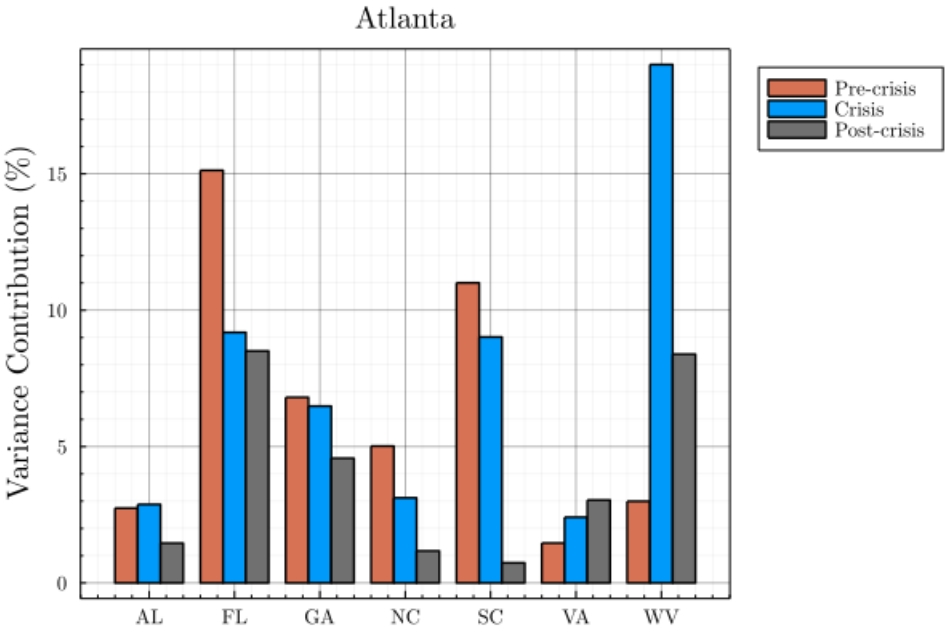

Figure B.3. This graph plots the percent variance contribution made by the Atlanta regional factor toward each of the state-average ROE series in the Atlanta region across the pre-, intra-, and post-crisis subsample periods.

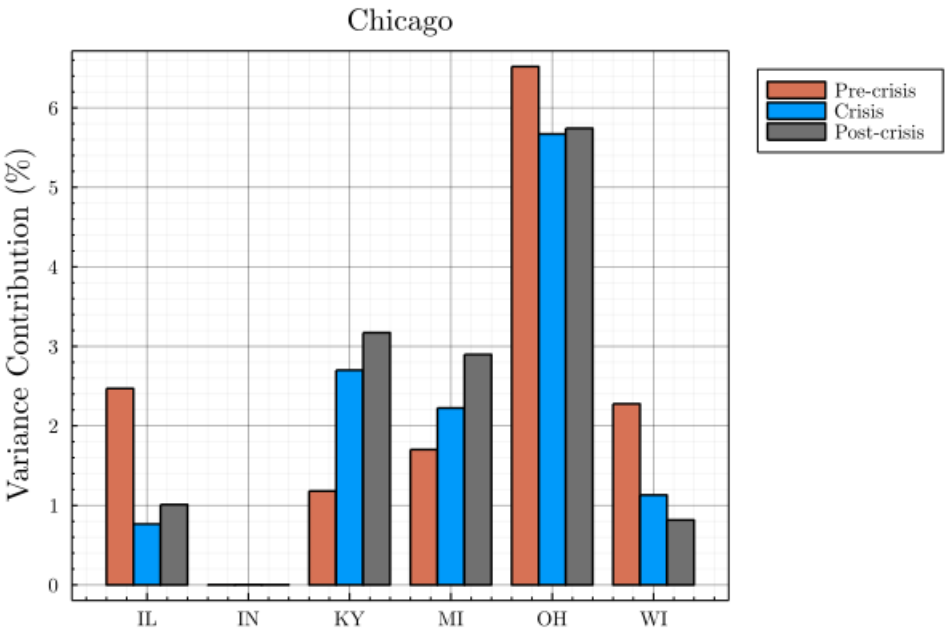

Figure B.4. This graph plots the percent variance contribution made by the Chicago regional factor toward each of the state-average ROE series in the Chicago region across the pre-, intra-, and post-crisis subsample periods.

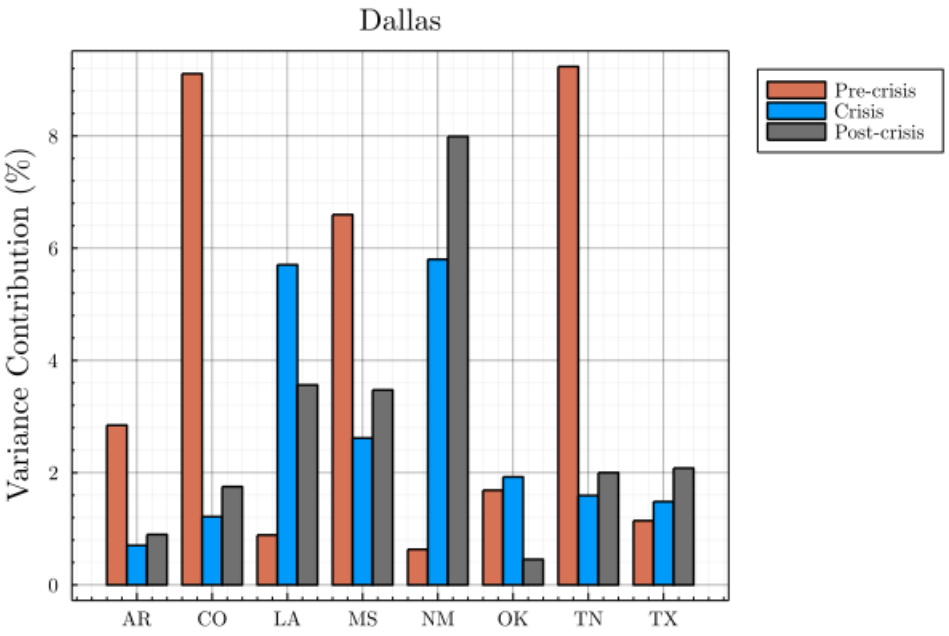

Figure B.5. This graph plots the percent variance contribution made by the Dallas regional factor toward each of the state-average ROE series in the Dallas region across the pre-, intra-, and post-crisis subsample periods.

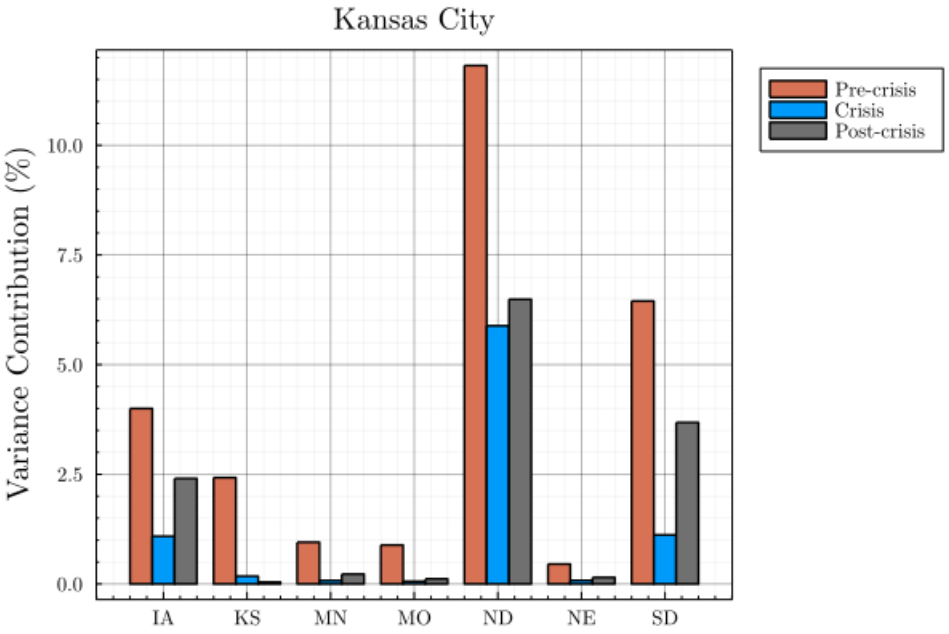

Figure B.6. This graph plots the percent variance contribution made by the Kansas City regional factor toward each of the state-average ROE series in the Kansas City region across the pre-, intra-, and post-crisis subsample periods.

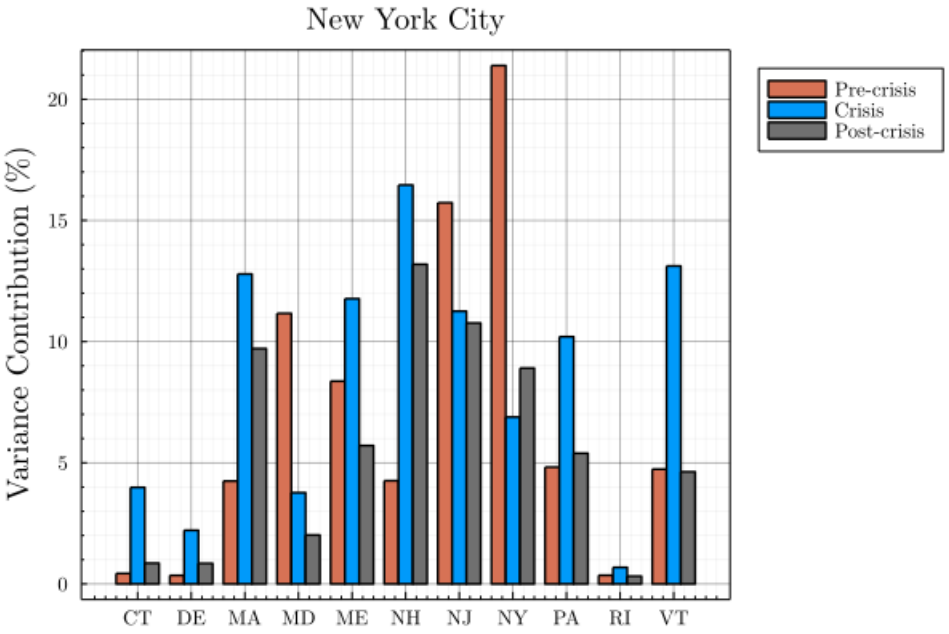

Figure B.7. This graph plots the percent variance contribution made by the New York City regional factor toward each of the state-average ROE series in the New York City region across the pre-, intra-, and post-crisis subsample periods.

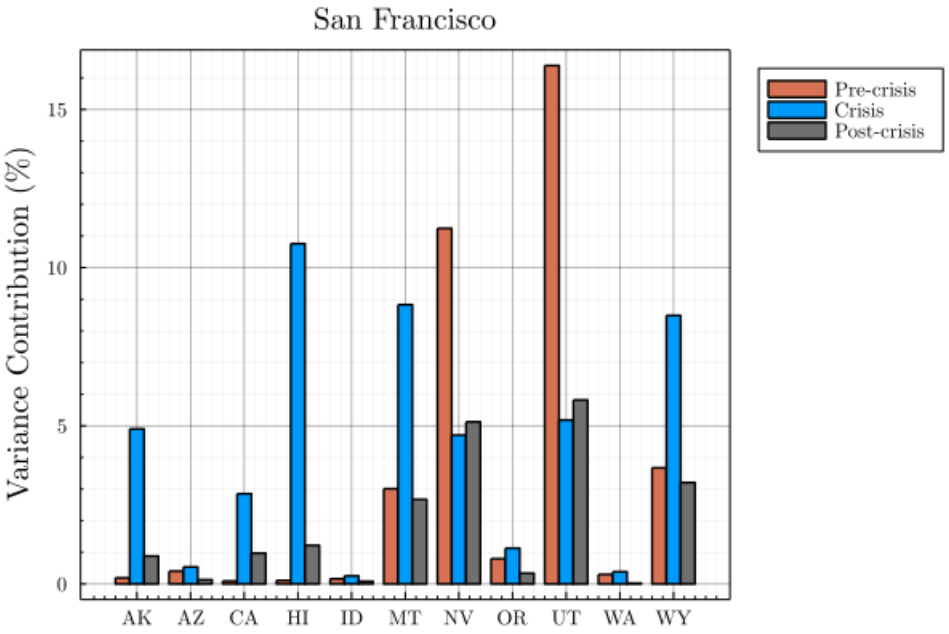

Figure B.8. This graph plots the percent variance contribution made by the San Francisco regional factor toward each of the state-average ROE series in the San Francisco region across the pre-, intra-, and post-crisis subsample periods.

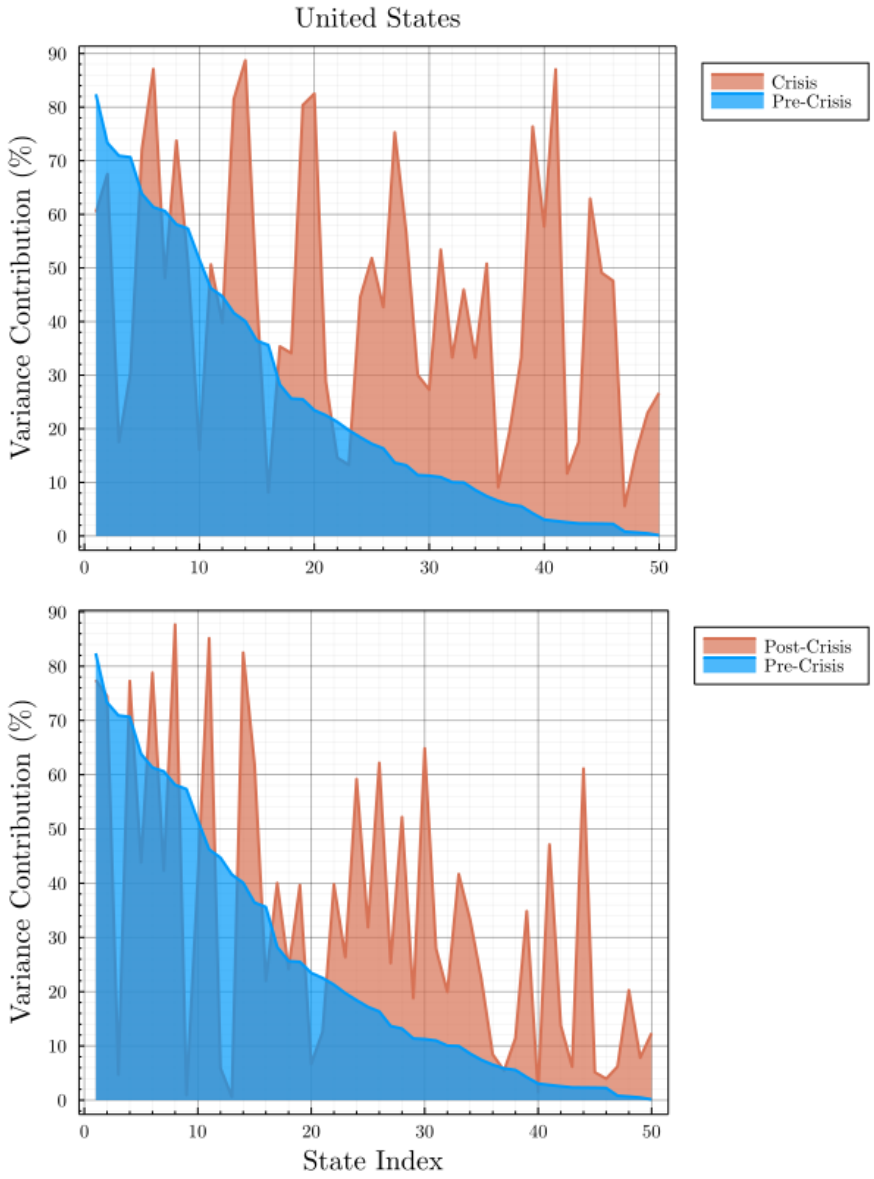

Figure B.9. This graph plots the percent variance contribution made by the US national factor toward each of the state-average ROE series in the dataset. In other words, the graph shows the percentage of the total variance of each observable series that may be attributed to the US national factor. The first facet compares the variance contributions made by the national factor during the pre- vs. intra-crisis periods, while the second facet compares that of pre- vs. post-crisis periods. The state index orders states by their pre-crisis national factor contribution in decreasing order.

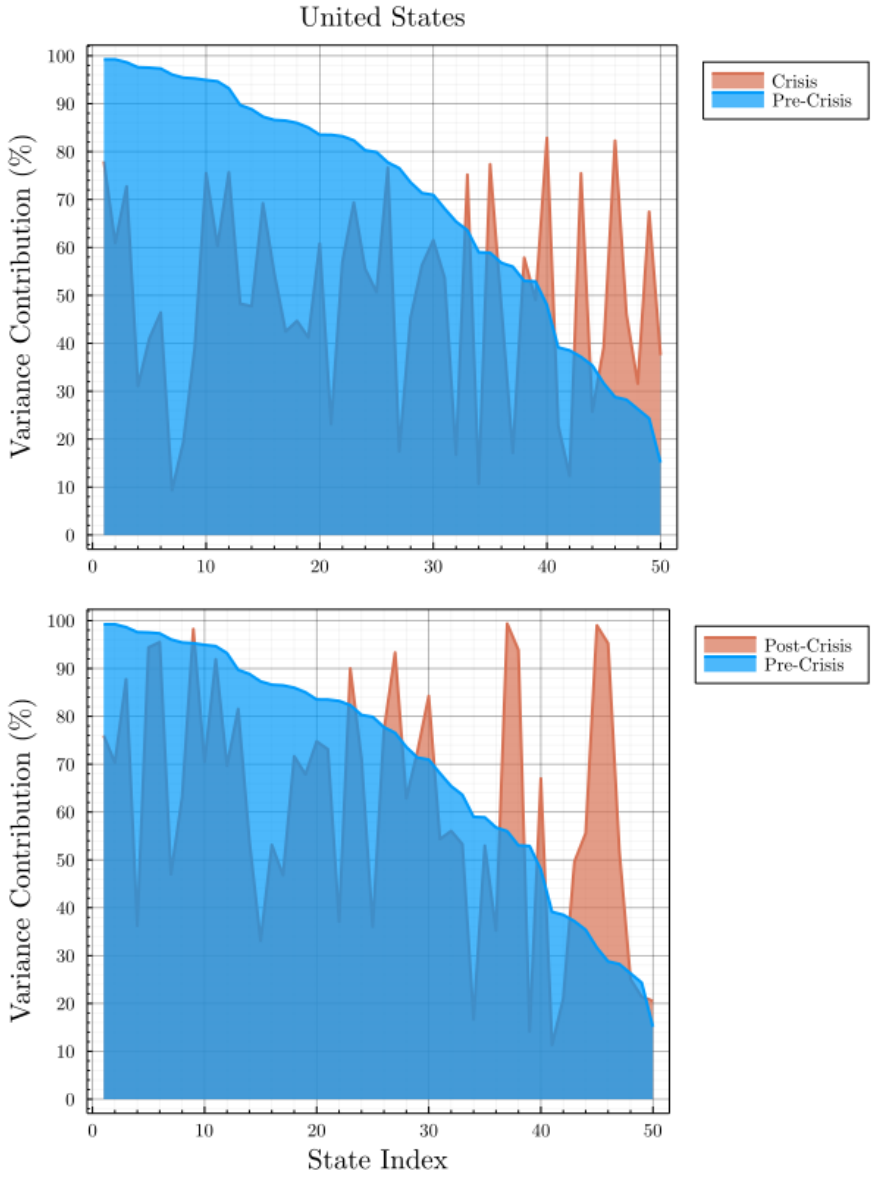

Figure B.10. This graph plots the percent variance contribution made toward each of the state-average ROE series in the dataset by their respective idiosyncratic disturbance processes. In other words, the graph shows the percentage of the total variance of each observable series that may be attributed to their corresponding idiosyncratic disturbance processes. The first facet compares the variance contributions during the pre- vs. intra-crisis periods, while the second facet compares that of pre- vs. post-crisis periods. The state index orders states by their pre-crisis national factor contribution in decreasing order.

REFERENCES CITED

Acemoglu, D., Ozdaglar, A., & Tahbaz-salehi, A. (2015). American Economic Association Systemic Risk and Stability in Financial Networks. *American Economic Review*, *105*(v), 564–608. Retrieved from http://dx.doi.org/10.1257/aer.20130456 doi: 10.1257/aer.20130456

Altavilla, C., Canova, F., & Ciccarelli, M. (2020). Mending the broken link: Heterogeneous bank lending rates and monetary policy pass-through. *Journal of Monetary Economics*, *110*, 81-98. Retrieved from https://doi.org/10.1016/j.jmoneco.2019.01.001 doi: 10.1016/j.jmoneco.2019.01.001

Ashcraft, A. (2006). New Evidence on the Lending Channel. *Journal of Money, Credit and Banking*, *38*(3), 751–775. Retrieved from https://www.jstor.org/stable/3839090

Auerbach, A., & Gorodnichenko, Y. (2012, May). Measuring the output responses to fiscal policy. *American Economic Journal: Economic Policy*, *4*(2), 1-27. Retrieved from https://doi.org/10.1257/pol.4.2.1 doi: 10.1257/pol.4.2.1

Bachmann, R., & Sims, E. (2012). Confidence and the transmission of government spending shocks. *Journal of Monetary Economics*, *59*(3), 235-249. Retrieved from https://www.sciencedirect.com/science/article/pii/S0304393212000323 doi: 10.1016/j.jmoneco.2012.02.005

Bai, J., & Wang, P. (2012). Identification and Bayesian Estimation of Dynamic Factor Models. *Journal of Business and Economic Statistics*, *33*(2), 221–240. Retrieved from https://doi.org/10.1080/07350015.2014.941467

Bernanke, B., & Blinder, A. (1988, March). *Credit, money, and aggregate demand* (Working Paper No. 2534). National Bureau of Economic Research. Retrieved from http://www.nber.org/papers/w2534 doi: 10.3386/w2534

Bernanke, B., & Blinder, A. (1992). The Federal Funds Rate and the Channels of Monetary Transmission. *The American Economic Review*, *82*(4), 901–921. Retrieved from https://www.jstor.org/stable/2117350

Bernanke, B., & Gertler, M. (1995). Inside the Black Box: The Credit Channel of Monetary Policy Transmission. *Journal of Economic Perspectives*, *9*(4), 27–48. Retrieved from https://www.aeaweb.org/articles?id=10.1257/jep.9.4.27 doi: 10.1257/jep.9.4.27

Bernanke, B., Gertler, M., & Watson, M. (1997). Systematic monetary policy and the effects of oil price shocks. *Brookings Papers on Economic Activity*, *28*(1), 91-157. Retrieved from https://EconPapers.repec.org/RePEc:bin:bpeajo:v:28:y:1997:i:1997-1:p:91-157

Black, L., & Rosen, R. (2007). How the Credit Channel Works: Differentiating the Bank Lending Channel and the Balance Sheet Channel;. *Federal Reserve Bank of Chicago*, *WP 2007-13*. Retrieved from https://ideas.repec.org/p/fip/fedhwp/wp-07-13.html

Bluedorn, J., Bowdler, C., & Koch, C. (2017). Heterogeneous bank lending responses to monetary policy: New evidence from a real-time identification. *International Journal of Central Banking*, *13*(1), 95–149. Retrieved from https://www.ijcb.org/journal/ijcb17q0a3.htm doi: 10.5089/9781484356760.001

Boivin, J., Giannoni, M., & Mihov, I. (2009, March). Sticky prices and monetary policy: Evidence from disaggregated us data. *American Economic Review*, *99*(1), 350-84. Retrieved from https://www.aeaweb.org/articles?id=10.1257/aer.99.1.350 doi: 10.1257/aer.99.1.350

Bu, C., Rogers, J., & Wu, W. (2021). A unified measure of Fed monetary policy shocks. *Journal of Monetary Economics*, *118*, 331–349. Retrieved from https://doi.org/10.1016/j.jmoneco.2020.11.002 doi: 10.1016/j.jmoneco.2020.11.002

Caccioli, F., Shrestha, M., Moore, C., & Farmer, D. (2014). Stability analysis of financial contagion due to overlapping portfolios. *Journal of Banking and Finance*, *46*(1), 233–245. Retrieved from http://dx.doi.org/10.1016/j.jbankfin.2014.05.021 doi: 10.1016/j.jbankfin.2014.05.021

Caldara, D., & Herbst, E. (2019, January). Monetary policy, real activity, and credit spreads: Evidence from bayesian proxy svars. *American Economic Journal: Macroeconomics*, *11*(1), 157-92. Retrieved from https://doi.org/10.1257/mac.20170294 doi: 10.1257/mac.20170294

Carter, C. K., & Kohn, R. (1994). On Gibbs sampling for state space models. *Biometrika*, *81*(3), 541–553. Retrieved from https://doi.org/10.2307/2337125 doi: 10.1093/biomet/81.3.541

Chib, S. (1993). Bayes Regression with Autoregressive Errors. *Journal of Econometrics*, *58*, 275–294. Retrieved from https://doi.org/10.1016/0304-4076(93)90046-8

Cleveland, R., Cleveland, W., McRae, J., & Terpenning, I. (1990). Stl: A seasonal-trend decomposition procedure based on loess (with discussion). *Journal of Official Statistics*, *6*, 3–73. Retrieved from https://www.proquest.com/scholarly-journals/stl-seasonal-trend-decomposition-procedure-based/docview/1266805989/se-2?accountid=14698

Dave, C., Dressler, S., & Zhang, L. (2013). The Bank Lending Channel: A FAVAR Analysis. *Journal of Money, Credit and Banking*, *45*(8), 1705–1720. Retrieved from https://www.jstor.org/stable/42920090 doi: 10.1111/jmcb.12067

Del Negro, M., & Otrok, C. M. (2011). *Dynamic Factor Models with Time-Varying Parameters: Measuring Changes in International Business Cycles* (No. 326). Retrieved from https://ideas.repec.org/p/fip/fednsr/326.html doi: 10.2139/ssrn.1136163

den Haan, W., Sumner, S., & Yamashiro, G. (2007). Bank loan portfolios and the monetary transmission mechanism. *Journal of Monetary Economics*, *54*(3), 904–924. Retrieved from https://doi.org/10.1016/j.jmoneco.2006.01.008 doi: 10.1016/j.jmoneco.2006.01.008

DePrince, A., Ford, W., & Morris, P. (2011). Some causes of interstate differences in community bank performance. *Journal of Economics and Finance*, *35*(1), 22–40. Retrieved from https://doi.org/10.1007/s12197-009-9105-3 doi: 10.1007/s12197-009-9105-3

Disyatat, P. (2011). The bank lending channel revisited. *Journal of Money, Credit and Banking*, *43*(4), 711-734. Retrieved from https://doi.org/10.1111/j.1538-4616.2011.00394.x doi: 10.1111/j.1538-4616.2011.00394.x

Doz, C., & Fuleky, P. (2020). Dynamic Factor Models. *Advanced Studies in Theoretical and Applied Econometrics*, *52*, 27–64. Retrieved from https://doi.org/10.1007/978-3-030-31150-6_2 doi: 10.1007/978-3-030-31150-6_2

Drechsler, I., Savov, A., & Schnabl, P. (2017, 05). The Deposits Channel of Monetary Policy*. *The Quarterly Journal of Economics*, *132*(4), 1819-1876. Retrieved from https://doi.org/10.1093/qje/qjx019 doi: 10.1093/qje/qjx019

Driscoll, J. (2004). Does bank lending affect output? Evidence from the U.S. states. *Journal of Monetary Economics*, *51*(3), 451–471. Retrieved from https://10.1016/j.jmoneco.2004.01.001 doi: 10.1016/j.jmoneco.2004.01.001

Duffie, D. (2018). Financial Regulatory Reform After the Crisis: An Assessment. *Management Science*, *64*(10), 4835–4857. Retrieved from https://doi.org/10.1287/mnsc.2017.2768 doi: 10.1287/mnsc.2017.2768

Eisenberg, L., & Noe, T. (2001). Sytemic Risk in Financial Systems. *Management Science*, *47*(2), 236–249. Retrieved from https://www.jstor.org/stable/2661572

Elsadek Mahmoudi, S. (2021). The Propagation of Local Credit Shocks: Evidence from Hurricane Katrina. *SSRN Electronic Journal*. Retrieved from https://doi.org/10.2139/ssrn.3751526 doi: 10.2139/ssrn.3751526

Emmons, W., Gilbert, A., & Yeager, T. (2004). Reducing the risk at small community banks: Is it size or geographic diversification that matters? *Journal of Financial Services Research*, *25*(2-3), 283–289. Retrieved from https://doi.org/10.1023/b:fina.0000020666.77879.20 doi: 10.1023/b:fina.0000020666.77879.20

Estes, K. (2014). Diversification and Community Bank Performance. *International Journal of Finance and Banking Studies*, *3*(4), 1–40. Retrieved from https://ideas.repec.org/a/rbs/ijfbss/v3y2014i4p01-40.html

Fang, C., & Yeager, T. (2020). A historical loss approach to community bank stress testing. *Journal of Banking and Finance*, *118*, 105831. Retrieved from https://doi.org/10.1016/j.jbankfin.2020.105831 doi: 10.1016/j.jbankfin.2020.105831

FDIC. (2020). *Community banking study.* Retrieved from https://www.fdic.gov/resources/community-banking/cbi-study.html

Feng, G., & Zhang, X. (2012). Productivity and efficiency at large and community banks in the US: A Bayesian true random effects stochastic distance frontier analysis. *Journal of Banking and Finance*, *36*(7), 1883–1895. Retrieved from http://dx.doi.org/10.1016/j.jbankfin.2012.02.008 doi: 10.1016/j.jbankfin.2012.02.008

Fields, P., Fraser, D., Berry, T., & Byers, S. (2006). Do bank loan relationships still matter? *Journal of Money, Credit and Banking*, *38*(5), 1195–1209. Retrieved 2023-03-17, from http://www.jstor.org/stable/3839004

Gai, P., Haldane, A., & Kapadia, S. (2011). Complexity, concentration and contagion. *Journal of Monetary Economics*, *58*(5), 453–470. Retrieved from http://dx.doi.org/10.1016/j.jmoneco.2011.05.005 doi: 10.1016/j.jmoneco.2011.05.005

Gilchrist, S., & Zakrajšek, E. (2012). Credit spreads and business cycle fluctuations. *American Economic Review*, *102*(4), 1692–1720. Retrieved from https://doi.org/10.1257/aer.102.4.1692 doi: 10.1257/aer.102.4.1692

Gonçalves, S., & Kilian, L. (2004). Bootstrapping autoregressions with conditional heteroskedasticity of unknown form. *Journal of Econometrics*, *123*(1), 89-120. Retrieved from https://doi.org/10.1016/j.jeconom.2003.10.030 doi: 10.1016/j.jeconom.2003.10.030

Gonçalves, S., & Kilian, L. (2007). Asymptotic and bootstrap inference for ar(infinity) processes with conditional heteroskedasticity. *Econometric Reviews*, *26*(6), 609-641. Retrieved from https://doi.org/10.1080/07474930701624462 doi: 10.1080/07474930701624462

Gospodinov, N., Herrera, A. M., & Pesavento, E. (2013, December). Unit roots, cointegration, and pretesting in var models. In *VAR models in macroeconomics – new developments and applications: Essays in honor of christopher a. sims* (pp. 81–115). Emerald Group Publishing Limited. Retrieved from https://doi.org/10.1108/s0731-9053(2013)0000031003 doi: 10.1108/s0731-9053(2013)0000031003

Görtz, C., Tsoukalas, J., & Zanetti, F. (2022, October). News shocks under financial frictions. *American Economic Journal: Macroeconomics*, *14*(4), 210-43. Retrieved from https://www.aeaweb.org/articles?id=10.1257/mac.20170066 doi: 10.1257/mac.20170066

Hanauer, M., Lytle, B., Summers, C., & Ziadeh, S. (2021). Community Banks' Ongoing Role in the U.S. Economy. *The Federal Reserve Bank of Kansas City Economic Review*, 37–81. Retrieved from https://doi.org/10.18651/er/v106n2hanauerlytlesummersziadeh doi: 10.18651/er/v106n2hanauerlytlesummersziadeh

Hassan, K., Karim, S., Lawrence, S., & Risfandy, T. (2022). Weathering the COVID-19 storm: The case of community banks. *Research in International Business and Finance*, *60*(December 2021), 101608. Retrieved from https://doi.org/10.1016/j.ribaf.2021.101608 doi: 10.1016/j.ribaf.2021.101608

Ivashina, V., & Scharfstein, D. (2010). Bank lending during the financial crisis of 2008. *Journal of Financial Economics*, *97*(3), 319-338. Retrieved from https://doi.org/10.1016/j.jfineco.2009.12.001 (The 2007-8 financial crisis: Lessons from corporate finance) doi: 10.1016/j.jfineco.2009.12.001

Jackson, L., Kose, A., & Owyang, M. (2015). *Specification and Estimation of Bayesian Dynamic Factor Models: A Monte Carlo Analysis with an Application to Global House Price Comovement*. Retrieved from https://doi.org/10.20955/wp.2015.031

Jackson, M., & Pernoud, A. (2021). Systemic Risk in Financial Networks: A Survey. *Annual Review of Economics*, *13*(December), 171–202. Retrieved from https://doi.org/10.1146/annurev-economics-083120-111540 doi: 10.1146/annurev-economics-083120-111540

Jarociński, M., & Karadi, P. (2020, April). Deconstructing monetary policy surprises—the role of information shocks. *American Economic Journal: Macroeconomics*, *12*(2), 1-43. Retrieved from https://www.aeaweb.org/articles?id=10.1257/mac.20180090 doi: 10.1257/mac.20180090

Jordà, O. (2005, March). Estimation and inference of impulse responses by local projections. *American Economic Review*, *95*(1), 161-182. Retrieved from https://www.aeaweb.org/articles?id=10.1257/0002828053828518 doi: 10.1257/0002828053828518

Kapinos, P., Kishor, K., & Ma, J. (2020). Dynamic comovement among banks, systemic risk, and the macroeconomy. *Journal of Banking and Finance*. Retrieved from https://doi.org/10.1016/j.jbankfin.2020.105894 doi: 10.1016/j.jbankfin.2020.105894

Kashyap, A., Rajan, R., & Stein, J. (2002). Banks as liquidity providers: An explanation for the coexistence of lending and deposit-taking. *Journal of Finance*, *57*(1), 33–73. Retrieved from https://doi.org/10.1111/1540-6261.00415 doi: 10.1111/1540-6261.00415

Kashyap, A., & Stein, J. (1994). Monetary Policy and Bank Lending. In *Monetary policy* (pp. 221–261). The University of Chicago Press. Retrieved from https://doi.org/10.1016/s0378-4266(02)00200-5 doi: 10.1016/s0378-4266(02)00200-5

Kashyap, A., & Stein, J. (1995). The impact of monetary policy on bank balance sheets. *Carnegie-Rochester Confer. Series on Public Policy*, *42*(C), 151–195. Retrieved from https://doi.org/10.1016/0167-2231(95)00032-U doi: 10.1016/0167-2231(95)00032-U

Kashyap, A., & Stein, J. (2000). What Do a Million Observations on Banks Say About the Transmission of Monetary Policy? *American Economic Review*, *90*(3), 407–428. Retrieved from https://doi.org/10.1257/aer.90.3.407 doi: 10.1257/aer.90.3.407

Kilian, L. (2009, June). Not all oil price shocks are alike: Disentangling demand and supply shocks in the crude oil market. *American Economic Review*, *99*(3), 1053-69. Retrieved from https://www.aeaweb.org/articles?id=10.1257/aer.99.3.1053 doi: 10.1257/aer.99.3.1053

Kilian, L., & Lewis, L. (2011). Does the fed respond to oil price shocks?*. *The Economic Journal*, *121*(555), 1047-1072. Retrieved from https://onlinelibrary.wiley.com/doi/abs/10.1111/j.1468-0297.2011.02437.x doi: 10.1111/j.1468-0297.2011.02437.x

Kilian, L., & Lütkepohl, H. (2017). Vector autoregressive models. In *Structural vector autoregressive analysis* (p. 19–74). Cambridge University Press. Retrieved from https://doi.org/10.1017/9781108164818.003 doi: 10.1017/9781108164818.003

Kim, C.-j., & Nelson, C. (1998). Factor Model With Regime Switching. *The Review of Economics and Statistics*, 188–201.

Kim, C.-J., & Nelson, C. (1999). *State-space models with regime switching: Classical and gibbs-sampling approaches with applications* (1st ed., Vol. 1). The MIT Press. Retrieved from https://EconPapers.repec.org/RePEc:mtp:titles:0262112388

Kim, H., Batten, J., & Ryu, D. (2020). Financial crisis, bank diversification, and financial stability: OECD countries. *International Review of Economics and Finance*, *65*(September 2019), 94–104. Retrieved from https://doi.org/10.1016/j.iref.2019.08.009 doi: 10.1016/j.iref.2019.08.009

Kishan, R., & Opiela, T. (2000). Bank Size , Bank Capital , and the Bank Lending Channel. *Journal of Money, Credit and Banking*, *32*(1), 121–141. Retrieved from https://doi.org/10.2307/2601095

Kose, A., Otrok, C., & Whiteman, C. (2003, September). International business cycles: World, region, and country-specific factors. *American Economic Review*, *93*(4), 1216-1239. Retrieved from https://www.aeaweb.org/articles?id=10.1257/000282803769206278 doi: 10.1257/000282803769206278

Kose, A., Otrok, C., & Whiteman, C. (2008). Understanding the evolution of world business cycles. *Journal of International Economics*, *75*(1), 110–130. Retrieved from https://doi.org/10.1016/j.jinteco.2007.10.002 doi: 10.1016/j.jinteco.2007.10.002

Kress, J., & Turk, M. (2020). Too many to fail: Against community bank deregulation. *Northwestern University Law Review*, *115*(3), 647–716. Retrieved from https://doi.org/10.2139/ssrn.3503692 doi: 10.2139/ssrn.3503692

Lux, M., & Greene, R. (2015). The State and Fate of Community Banking. *Working Paper*(37). Retrieved from www.hks.harvard.edu/mrcbg

McKay, A., & Wolf, C. (2023, February). *What Can Time-Series Regressions Tell Us About Policy Counterfactuals?* (Staff Report No. 642). Federal Reserve Bank of Minneapolis. Retrieved from https://ideas.repec.org/p/fip/fedmsr/95599.html doi: 10.21034/sr.642

Meslier, C., Morgan, D., Samolyk, K., & Tarazi, A. (2016). The benefits and costs of geographic diversification in banking. *Journal of International Money and Finance*, *69*, 287–317. Retrieved from http://dx.doi.org/10.1016/j.jimonfin.2016.07.007 doi: 10.1016/j.jimonfin.2016.07.007

Moench, E., Ng, S., & Potter, S. (2013, 12). Dynamic Hierarchical Factor Models. *The Review of Economics and Statistics*, *95*(5), 1811-1817. Retrieved from https://doi.org/10.1162/REST_a_00359 doi: 10.1162/REST_a_00359

Montiel Olea, J. L., & Plagborg-Møller, M. (2019). Simultaneous confidence bands: Theory, implementation, and an application to svars. *Journal of Applied Econometrics*, *34*(1), 1-17. Retrieved from https://onlinelibrary.wiley.com/doi/abs/10.1002/jae.2656 doi: 10.1002/jae.2656

Montiel Olea, J. L., & Plagborg-Møller, M. (2021). Local projection inference is simpler and more robust than you think. *Econometrica*, *89*(4), 1789-1823. Retrieved from https://onlinelibrary.wiley.com/doi/abs/10.3982/ECTA18756 doi: 10.3982/ECTA18756

Nakamura, E., & Steinsson, J. (2018). High-frequency identification of monetary non-neutrality: The information effect. *Quarterly Journal of Economics*, *133*(3), 1283–1330. Retrieved from https://doi.org/10.1093/QJE/QJY004 doi: 10.1093/QJE/QJY004

Nguyen, N. T., & Barth, J. (2020). Community Banks vs. Non-Community Banks: Where is the Advantage in Local Small Business Funding? *Atlantic Economic Journal*, *48*(2), 161–174. Retrieved from https://doi.org/10.1007/s11293-020-09671-5 doi: 10.1007/s11293-020-09671-5

Otrok, C., & Whiteman, C. (1998). Bayesian Leading Indicators : Measuring and Predicting Economic Conditions in Iowa. *International Economic Review*, *39*(4), 997–1014. Retrieved from https://doi.org/10.2307/2527349 doi: 10.2307/2527349

Paul, P. (2020, 10). The Time-Varying Effect of Monetary Policy on Asset Prices. *The Review of Economics and Statistics*, *102*(4), 690-704. Retrieved from https://doi.org/10.1162/rest_a_00840 doi: 10.1162/rest_a_00840

Peek, J., & Rosengren, E. (2000). Collateral damage: Effects of the japanese bank crisis on real activity in the united states. *The American Economic Review*, *90*(1), 30–45. Retrieved 2023-03-17, from http://www.jstor.org/stable/117280

Peek, J., Rosengren, E., & Tootell, G. (2003). Identifying the macroeconomic effect of loan supply shocks. *Journal of Money, Credit and Banking*, *35*(6), 931-46. Retrieved from https://EconPapers.repec.org/RePEc:mcb:jmoncb:v:35:y:2003:i:6:p:931-46

Peirce, H., Robinson, I., & Stratmann, T. (2014). *How Are Small Banks Faring Under Dodd-Frank?* Retrieved from https://www.mercatus.org/students/research/working-papers/how-are-small-banks-faring-under-dodd-frank#:~:text=Small%20banks%20report%20having%20eliminated,and%20services%20to%20be%20cut. (Working Paper)

Petach, L., Weiler, S., & Conroy, T. (2021). It's a wonderful loan: local financial composition, community banks, and economic resilience. *Journal of Banking and Finance*, *126*, 106077. Retrieved from https://doi.org/10.1016/j.jbankfin.2021.106077 doi: 10.1016/j.jbankfin.2021.106077

Plagborg-Møller, M., & Wolf, C. (2021). Local projections and vars estimate the same impulse responses. *Econometrica*, *89*(2), 955-980. Retrieved from https://doi.org/10.3982/ECTA17813 doi: 10.3982/ECTA17813

Ramey, V. A. (2016). *Macroeconomic Shocks and Their Propagation* (1st ed., Vol. 2). Elsevier B.V. Retrieved from http://dx.doi.org/10.1016/bs.hesmac.2016.03.003 doi: 10.1016/bs.hesmac.2016.03.003

Rice, T., & Rose, J. (2016). When good investments go bad: The contraction in community bank lending after the 2008 GSE takeover. *Journal of Financial Intermediation*, *27*, 68–88. Retrieved from http://dx.doi.org/10.1016/j.jfi.2016.02.001 doi: 10.1016/j.jfi.2016.02.001

Romer, C., & Romer, D. (1990). New evidence on the monetary transmission mechanism. *Brookings Papers on Economic Activity*, *21*(1), 149-214. Retrieved from https://EconPapers.repec.org/RePEc:bin:bpeajo:v:21:y:1990:i:1990-1:p:149-214

Romer, C., & Romer, D. (2004). A New Measure of Monetary Shocks: Derivation and Implications. *American Economic Review*, *94*(4), 1055–1084. Retrieved from https://doi.org/10.1257/0002828042002651 doi: 10.1257/0002828042002651

Sargent, T., & Sims, C. (1977). *Business Cycle Modeling Without Pretending to Have Too Much A Priori Economic Theory* (Vol. 1). Retrieved from https://EconPapers.repec.org/RePEc:fip:fedmwp:55

Sims, C., & Zha, T. (2006). Does monetary policy generate recessions? *Macroeconomic Dynamics*, *10*(2), 231-272. Retrieved from https://EconPapers.repec.org/RePEc:cup:macdyn:v:10:y:2006:i:02:p:231-272_05

Stock, J., & Watson, M. (2001, December). Vector autoregressions. *Journal of Economic Perspectives*, *15*(4), 101-115. Retrieved from https://www.aeaweb.org/articles?id=10.1257/jep.15.4.101 doi: 10.1257/jep.15.4.101

Stock, J., & Watson, M. (2018). Identification and estimation of dynamic causal effects in macroeconomics using external instruments. *The Economic Journal*, *128*(610), 917-948. Retrieved from https://doi.org/10.1111/ecoj.12593 doi: 10.1111/ecoj.12593

Stock, J. H., & Watson, M. W. (2016). *Dynamic Factor Models, Factor-Augmented Vector Autoregressions, and Structural Vector Autoregressions in Macroeconomics* (1st ed., Vol. 2). Elsevier B.V. Retrieved from http://dx.doi.org/10.1016/bs.hesmac.2016.04.002 doi: 10.1016/bs.hesmac.2016.04.002

Swanson, A., & Zanzalari, D. (2021). Do local labor market conditions impact bank profitability? *Review of Financial Economics*, *39*(3), 314-333. Retrieved from https://onlinelibrary.wiley.com/doi/abs/10.1002/rfe.1130 doi: https://doi.org/10.1002/rfe.1130

Sykes, J. (2018). *Regulatory reform 10 years after the financial crisis: Systemic risk regulation of non-bank financial institutions.*

U.S. Treasury Department. (2017). *A Financial System That Creates Economic Opportunities: Banks and Credit Unions* (No. Executive Order 13772). Retrieved from https://home.treasury.gov/system/files/136/archive-documents/A-Financial-System.pdf

Yeager, T. (2004). The demise of community banks? Local economic shocks are not to blame. *Journal of Banking and Finance*, *28*(9), 2135–2153. Retrieved from https://doi.org/10.1016/j.jbankfin.2003.08.004 doi: 10.1016/j.jbankfin.2003.08.004

Yellen, J. L. (2013). *Interconnectedness and Systemic Risk: Lessons from the Financial Crisis and Policy Implications Remarks* (No. January). Retrieved from https://fraser.stlouisfed.org/title/930/item/36153?start_page=2